Technical Report Documentation Page

1. Report No.	2. Government Accession No.	3. Recipient's Catalog No.

4. Title and Subtitle	5. Report Date
The Performance of Pile Driving Systems Main Report, Volume I	December 1985
	6. Performing Organization Code
	8. Performing Organization Report No.
7. Author(s) Rausche, F., Likins, G.E., Goble, G.G., and Miner, R.	
9. Performing Organization Name and Address Goble Rausche Likins and Associates, Inc. 4535 Emery Industrial Parkway Cleveland, Ohio 44128	10. Work Unit No. (TRAIS)
	11. Contract or Grant No. DTFH61-82-C-00059
	13. Type of Report and Period Covered Final Report
12. Sponsoring Agency Name and Address U.S. Department of Transportation Federal Highway Administration Offices of Research and Development Washington, D.C. 20590	14. Sponsoring Agency Code
15. Supplementary Notes	

16. Abstract

A study was undertaken on the performance of pile driving systems. First, analytical methods available for routine pile design and installation analysis were summarized (Main Report, V.I). Next, the existing technology for the measurement of performance parameters was reviewed (Main Report, V.II). Third, new measurement systems were evaluated and, finally, recommendations for the development of a new measurement were made (Main Report, V.III). Another facet of the project investigated the actual behavior of pile driving systems based on existing measurements. Depending on hammer type, average wave equation efficiencies were calculated and summarized (Main Report, V.IV).

The third group of results was an inspection manual for pile driving systems, i.e. for impact hammers as well as cushions, helmets, leads, etc. This inspection manual was illustrated by a tape slide show in five parts as a teaching aid for pile driving inspectors. A Saximeter was also delivered as an inspection tool.

This is the First Volume of the Main Report which comprises four volumes. An Inspection Manual, the narrative of the Tape Slide Show, and a Summary Report were also issued.

17. Key Words	18. Distribution Statement
analysis, construction, design, diesel hammer, external combustion hammer, foundations, hammer efficiency, piles, pile driving	

19. Security Classif. (of this report)	20. Security Classif. (of this page)	21. No. of Pages	22. Price
		175	

Form DOT F 1700.7 (8-72) Reproduction of completed page authorized

PREFACE

The art of pile driving has undergone major changes, primarily because of developments in hammer technology. Since installation method and both analysis and design of piling are closely related, foundation engineers must continuously update their knowledge about these new machines.

It is therefore greatly appreciated that the manufacturers and their representatives made available to the authors not only time and experience but also, in several instances, their test stand facilities and financial means for hammer and/or cushion material testing.

Hammer testing was financially supported by the following firms and individuals (in chronological order of support).

(a)	Messrs. Alan McKinnon F. Koltermann	The Foundation Equipment Corporation Dover, OH
(b)	Messrs. William and Patrick Bermingham	Berminghammer Corporation Ltd. Hamilton, Ontario, Canada
(c)	Messrs. Otto Kammerer Fritz Kuemmel	Pilceco/Delmag Houston, TX
(d)	Mr. Tony Last	International Construction Equipment Matthews, NC

In addition to supporting hammer testing, the manufacturers were also contacted on several occasions for general information, experience and data. The authors gratefully acknowledge this support to the following firms and individuals (in alphabetic order) in addition to those mentioned earlier.

(a)	Mr. George Wendell	Conmaco Kansas City, KS
(b)	Messrs. Streffkerk and Stam	Hera Hammers Holland
(c)	Messrs. Robert Compton George Korelko	MKT Geotechnical Systems Dover, NJ
(d)	Mr. Pieter van Luipen	Menck West Germany
(e)	Mr. Don Warrington	Vulcan Iron Works, Inc. Chattanooga, TN

It is hoped that the results of the present study will aid the profession in the understanding of the pile driving process. With this improved knowledge it will be possible to provide safer pile foundations at a reduced cost. At the same time it is hoped that the number of requests for information to the manufacturers can be reduced.

VOLUME I

TABLE OF CONTENTS

APPENDIX B: MATHEMATICAL MODELS

LIST OF TABLES

LIST OF FIGURES

1. INTRODUCTION

Pile driving involves the rapid loading of a long slender rod with momentary, but high loads. These loads are generated by an impacting mass whose weight is small compared to the dynamic loads which it generates. The smaller the impacting mass, the more economical the pile driving process, provided that a reasonable pile penetration rate is maintained. Decreasing the mass should be compensated for by increasing the impact velocity of that mass. For this reason, hammer development in recent decades has seen increased fall heights (strokes). Furthermore, for improved productivity, it was found desirable to increase the blow rate (number of blows per unit time), a goal that was achieved by use of double-acting hammers. Increasing use of longer piles with higher capacity led to the development of pile driving hammers with more power. Because of these hammer developments, a variety of different hammer types exists today. As a consequence, it is often difficult for geotechnical and structural engineers, as well as for field inspection personnel, to understand the operating principles of each hammer type, and their relative advantages and shortcomings.

Another important development that took place during the past century was the increased use of steel and concrete for piling. Before the advent of steel and concrete piles, the driving of timber piles for moderate loads (say up to 30 tons) was relatively simple. With today's high capacity steel piling, overstressing problems may occur during driving. The driving of concrete piles may also be complex, due to the limited tensile strength of concrete. The development of variable-stroke hammers addressed some of these pile stress problems, but required new engineering analysis techniques.

The rate of penetration (e.g. blows per foot) of a pile is important to the economy of installation; it is also an obvious measure of the pile's load carrying capacity. However, this method of capacity determination cannot be relied upon, as soil strength changes, variations in hammer performance, or pile damage can all be responsible for unexpected pile penetration rates. Thus, pile bearing capacity predictions that are based on rate of penetration

must also include an evaluation of hammer performance. As a result, electronic measurement techniques which evaluate actual hammer energy have been used with increasing frequency during the past 20 years. Important contributions to this measurement technology were made by the Michigan State Highway Commission (1965, Ref.1) and at Case Institute of Technology (Goble, et al. 1967, 1968, 1970, 1975, 1977, Ref's. 2-6).

Historically, methods for calculating pile bearing capacity from blow count were based on a hammer's energy potential, computed as the product of the ram weight times the fall height. These methods often included energy losses in hammer, pile and soil, but only in a very simplistic manner. Great improvements in the dynamic analysis of pile driving were made when Smith (1960, Ref. 7) introduced the wave equation approach, which provided a more rational method for calculating bearing capacity and pile stresses. Nevertheless, hammer performance often remained a significant uncertainty. Further work on the wave equation approach was directed at refining the hammer model, particularly for diesel hammers, Goble and Rausche (1976, Ref. 8), Rempe (1977, Ref. 9); at developing a more representative soil model, Holloway, et. al. (1978, Ref. 10) and Matlock (1980, Ref. 11); and at examining alternative pile models, Fischer (1960, Ref. 12). However, even after incorporation of these improved analytical concepts into the wave equation, large differences between prediction and performance were sometimes observed. The primary source of these differences was the lack of a realistic prediction of a hammer performance and/or inadequate hammer inspection.

The use of electronic equipment to monitor pile driving gradually became more accepted. With progressive developments in transducer technology and signal conditioning and processing, dynamic testing of piles using the Pile Driving Analyzer™, which is based on the Case Method, became common in the early 1970's. (See Goble, et al, 1975, Ref. 5). By inputing the records of pile top force and velocity measured during these tests into the CAPWAP programs, the need for an accurate hammer model was obviated. (Goble, et al 1980, Ref. 13). This method, however, does <u>not</u> predict hammer-pile-soil behavior.

As previously mentioned, the use of steel and concrete piles, sometimes with complex geometries, and driven to high capacities, necessitates the accurate prediction of hammer energy output. As confirmed by many field tests performed to date, prediction by wave equation methods of pile stresses and bearing capacities using observations of the rate of penetration may be possible if hammer performance conforms to the hammer's specifications or its test stand performance. However, this field testing also revealed that transferred energies can be as much as 50% less than normal, depending on the hammer as well as on driving system components, such as the hammer and pile cushions. The Michigan State Highway Commission research and field tests, and results based on the Case Method, indicated surprisingly low hammer energy transfers to the pile. Typically, 60% or less of the hammer's rated energy was transmitted below the pile top. The percentage of transferred energy was even lower for hammers with high energy ratings that were based upon high design impact velocities or double acting principles. In conclusion, the objective determination of capacities and stresses requires that measurements be made.

The following study has three goals:

(a) to provide the engineer or field inspector with a comprehensive treatment of the analyses of piles and hammers

(b) to document existing measurement techniques used for hammer performance evaluations

(c) to make recommendations for the use of a simple and accurate electronic device for measurements of hammer energy output.

Furthermore, as part of this investigation, data from a large number of construction sites was analyzed and summarized, yielding hammer and driving system efficiencies. Also, the experience of hammer manufacturers regarding

hammer performance was documented after visiting their plants. Finally, their recommendations for improved hammer maintenance and inspection were compiled.

The results of this study are presented in four volumes:

Volume I: An Analytical and Experimental Treatment of Impact Pile Driving

Volume II: Performance of Available Measurement Systems

Volume III: Improved Measurement Concepts

Volume IV: Impact Pile Driving Hammers: Measured Performance and Recommended Usage

It is hoped that the broad range of topics and results contained in this study will be of interest to readers of varying backgrounds and occupations. For example, a field inspector may be most interested in the portions of the report dealing with hammer performance measurements and manufacturer's recommendations for hammer maintenance and inspection. On the other hand, an engineer involved in wave equation work may find useful information in all four volumes.

2. THE MECHANICS OF PILE DRIVING

2.1 Introduction

The developments in wave equation analysis and in related measurement equipment and techniques have made it possible to rationally explain the processes occurring during the impact driving of piles. This explanation is rooted in one dimensional wave mechanics. However, it can be approached from a physical description of what happens during impact pile driving.

Packaged computer programs which perform wave equation analyses have been available for several years. With these programs it has been possible, to calculate the response of a pile being driven into a soil, if everything has been realistically modeled. The programs produce large volumes of quantitative information, but are not conducive to physical visualization. Large amounts of computer time are often expended in performing parametric studies to learn the effect of modifications of driving system elements. In many cases, a basic understanding of one dimensional wave mechanics would make it possible to reach the same conclusions intuitively. An understanding of the more simplistic dynamic formulae is also helpful.

2.2 The Dynamic Formulae

Prior to the introduction of the wave equation approach, the analysis of pile driving was based on a host of theoretically derived "dynamic formulae." These formulae were all based on energy analysis, which was used to produce a relationship between hammer energy and pile penetration. All of them assumed that the soil resistance could be represented by a constant force. The simplest of these formulae assumed that both ram and pile were rigid bodies, whereas the more complex formulae attempted to account for pile elasticity. As many of these refinements resulted from questionable assumptions, the more complex formulae often did not give better results than the simple formulae.

The model common to all the simple dynamic formulae is represented in Figure 2.1. If the potential energy in the initial condition is equated to the work done by the pile during vertical advance, while it experiences a constant soil resistance, R, then

$$Wh = Rs \tag{2.1a}$$

or

$$R = Wh/s \tag{2.1b}$$

where W is the weight of the ram, h is the ram stroke, and s is the pile set. Now consider a particular relationship, the Engineering News formula. R is defined as the safe load and is given in kips. A safety factor of 6 is introduced, as is a "loss" term, e, (considered to be lost set), and appropriate conversion factors are introduced.

$$R = (1/6)\ Wh/(s+e)/12 \tag{2.2}$$

or

$$R = 2Wh/(s+e)$$

In this equation the stroke is expressed in feet and both set and loss terms are expressed in inches. To calibrate the formula, test results have been compared with capacties predicted by the formula, and various values of e have been selected which give the best possible agreement. Usually, e is related to by the hammer type used. Extensive literature (Chellis, Ref. 14), has been produced over the past century that reported attempts to modify the formula or to produce more accurate constants. Other authors have shown that all of the various formulae give unreliable results. The subject of dynamic formulae accuracy hardly needs further review.

If a dynamic formula is selected and a plot is made of capacity, R, versus blow count (the inverse of set), a curve of the characteristic shape shown in Figure 2.2 is obtained. While this curve may not produce results that agree with actual load test data, it does give a representation of the relationship between capacity and blow count which is in qualitative agreement with what is observed in the field. In general, this relationship is non-linear, with increases in blow count producing ever smaller increases in

$$Wh = Rs$$

$$R = \frac{Wh}{s}$$

R = SOIL RESISTANCE

W = HAMMER WEIGHT

h = HAMMER STROKE

s = PERMANENT SET

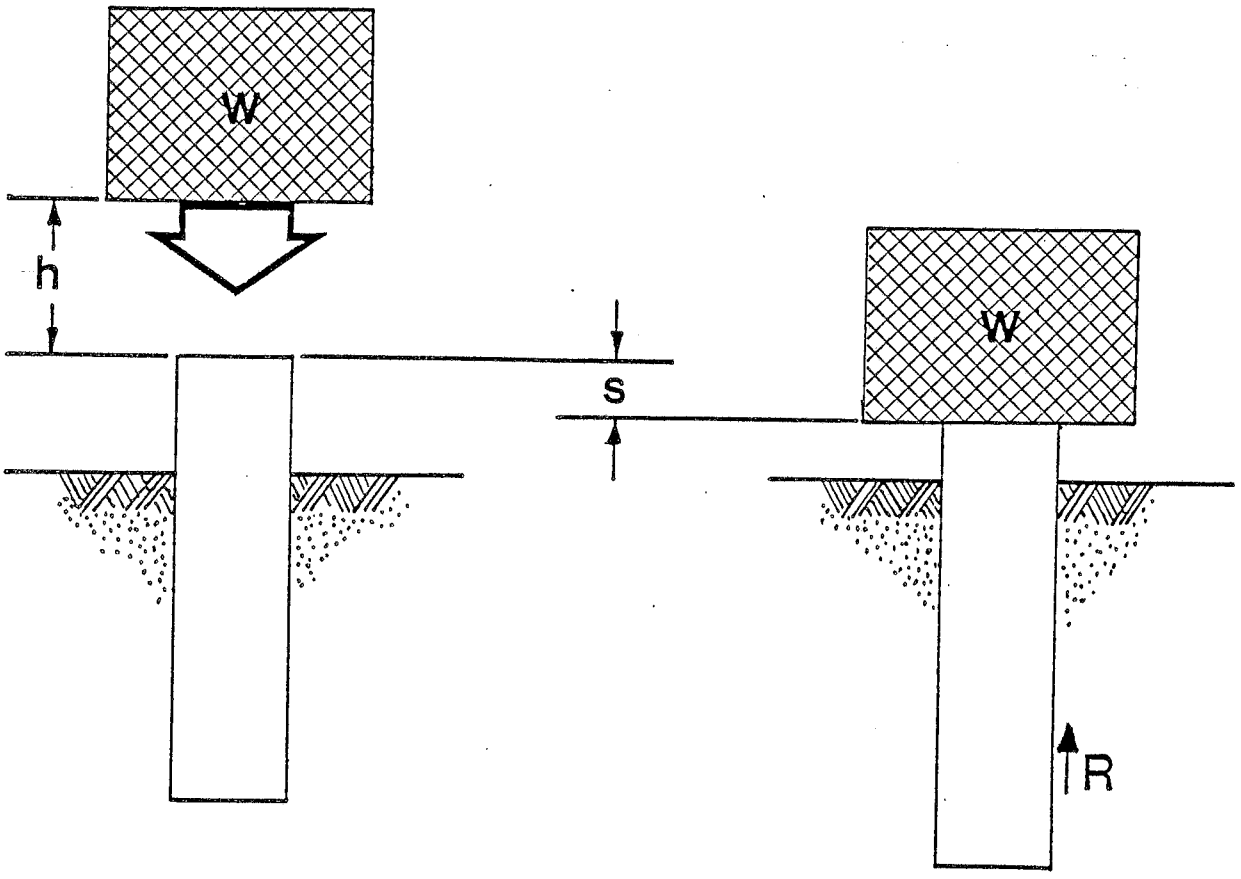

Figure 2.1: Physical Representation of the Basic Dynamic Formula

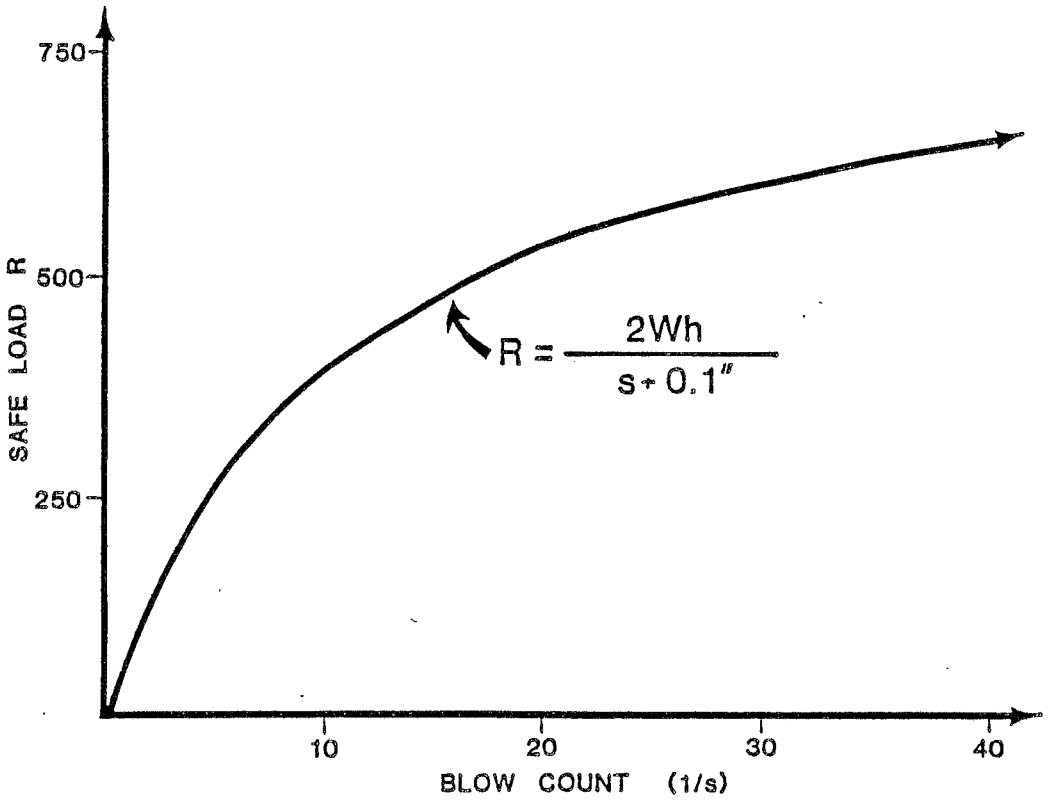

Figure 2.2: Typical Engineering News Formula Bearing Graph
1 inch = 25.4mm

capacity until a limiting resistance is reached. A plot of resistance versus set, as shown in Figure 2.3, clearly demonstrates this limiting capacity.

Reliance on such a qualitatively correct representation may lead to incorrect conclusions. It is common in pile driving to observe a pile penetrating easily to a depth where a dramatic increase in blow count occurs. It is often assumed that this increase is due to the penetration of a very strong layer. In fact, a point may have been reached on the bearing graph where a rather small increase in capacity (or a small decrease in hammer efficiency) produces a very large increase in blow count, and thus a particularly strong layer does not really exist. It is apparent, therefore, that a quantitative relationship between blow count and capacity is a fundamental requirement.

In order to ascertain such a quantitative relationship based on dynamic formulae, the following approach has been successfully adopted. A pile is driven according to a dynamic formula, and it is then statically load tested to failure (of the soil). The constants in the dynamic formula are then adjusted to produce agreement with the load test. The adjusted dynamic formula is then used to select a new a driving criteria. This procedure is illustrated in Figure 2.4.

2.3 Wave Mechanics

The dynamic formulae exemplify theories of the mechanics of pile penetration that are based on several gross assumptions. Many of these assumptions are eliminated in the one dimensional wave mechanics approach to pile driving. This approach is similar to wave equation analysis, but cannot readily produce quantitive results. However, it does provide a good visualization of elastic pile penetration under the action of real hammer systems.

Several important relationships must be developed to proceed with this approach. These are developed in Appendix A1. However, a summary follows.

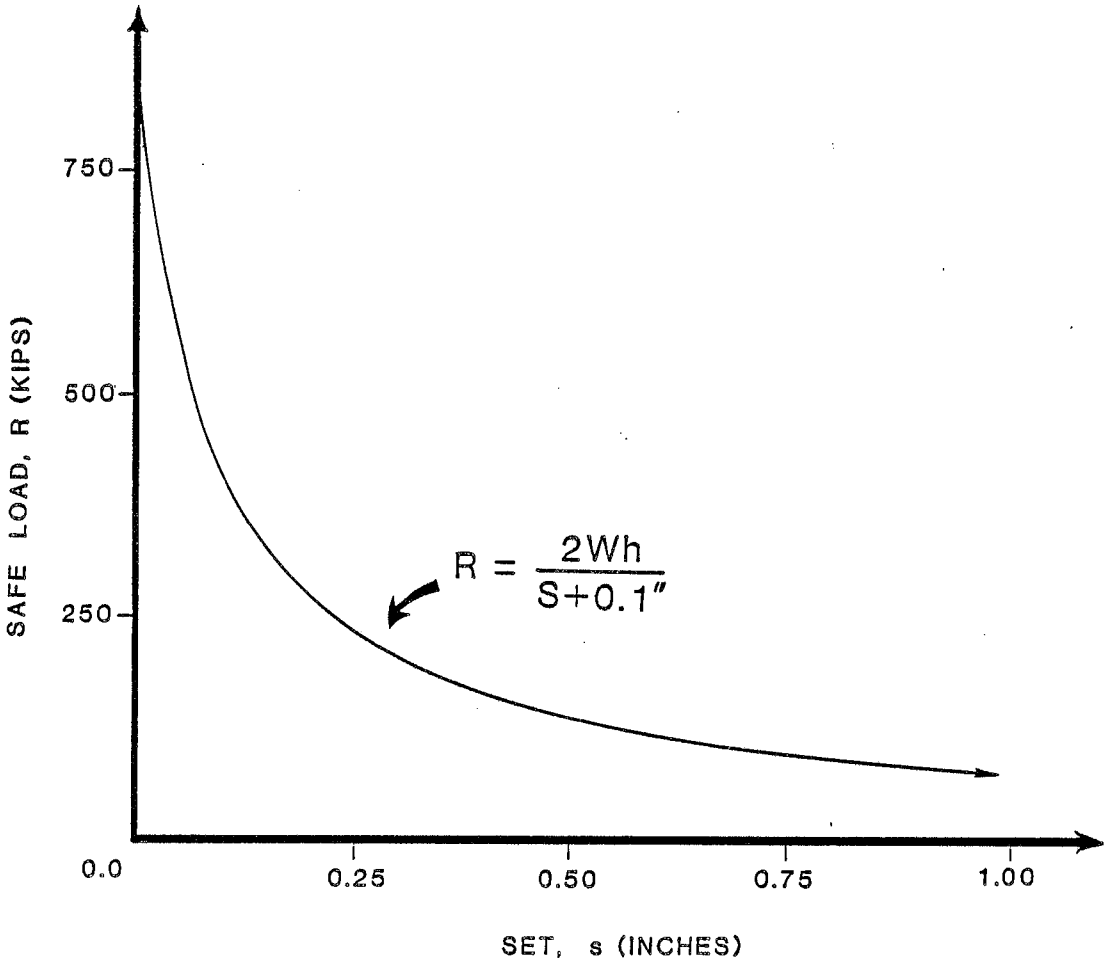

Figure 2.3: Safe Load vs. Set from Engineering News Formula

1 kip = 4.5 KN
1 inch = 25.4 mm

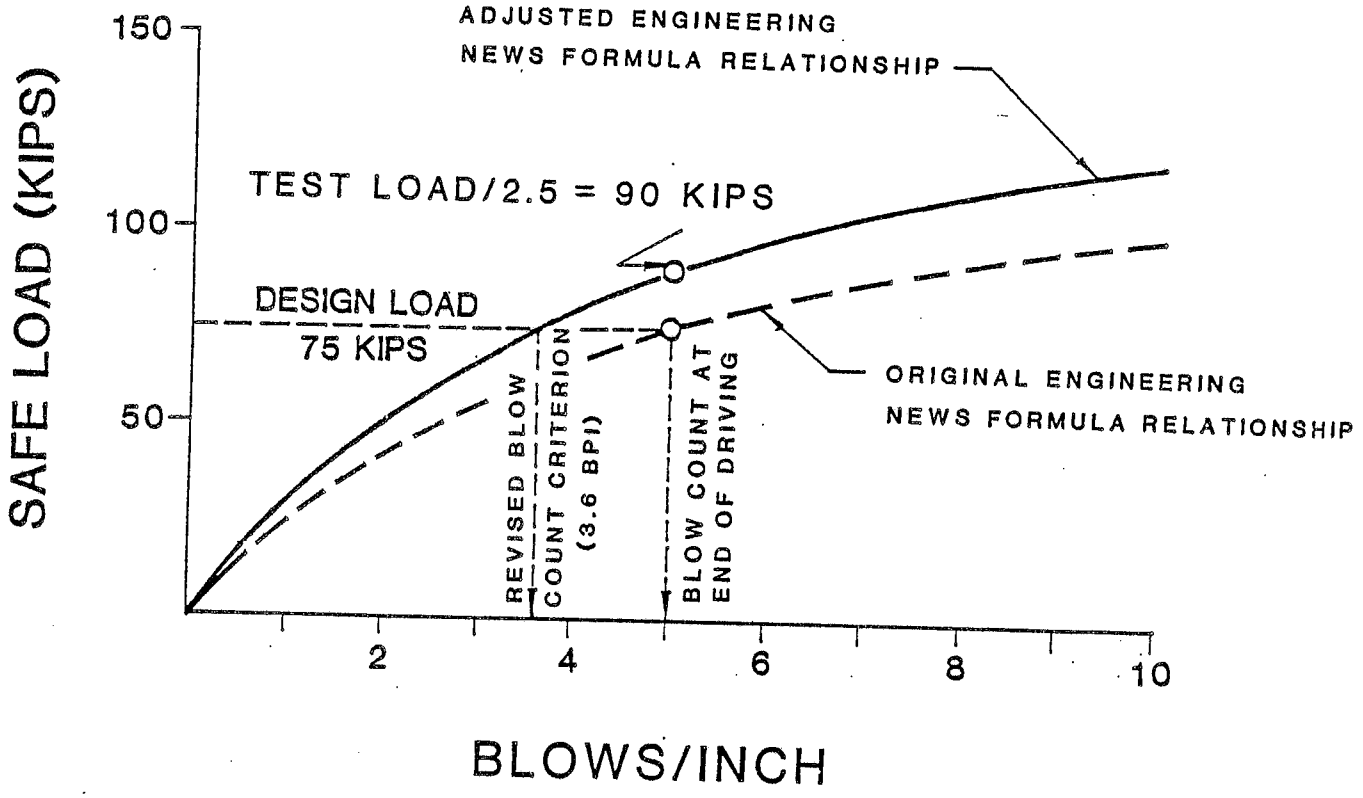

TEST DETAILS

Hammer: Vulcan 01 (Wh = 15 kip ft)
Ultimate Static Test Load: 225 kips
Factor of Safety: 2.5

Original E.N. formula for site: $R = \frac{2Wh}{(s+0.2)}$

Adjusted E.N. formula for site: $R = \frac{2.4Wh}{(s+0.2)}$

Original Driving Criterion: 5 blows per inch
Revised Driving Criterion: 3.6 blows per inch (BPI)

1 kip = 4.5 KN
1 foot = .3048 m
1 inch = 25.4 mm

Figure 2.4: Determination of Blow Count Criterion from Engineering News Formula and Static Load Test

2.3.1 The One-Dimensional Wave Equation

One dimensional wave transmission in a slender elastic rod is governed by the differential equation

$$a = c^2 u_{xx} \tag{2.3}$$

This linear, second order, partial differential equation relates the axial displacement along the rod, u, to two variables, namely, the position, x, and time, t. In the above equation, a and u_{xx} are the second partial derivatives of rod displacement with respect to time and pile length, respectively. The constant c^2 equals E/rho, where E is the elastic modulus of the rod material (e.g. 30,000 ksi or 210,000 MN/m^2 for steel) and rho is the rod's specific weight.

The solution of Equation 2.3 reveals that

a) Waves can propagate in either direction in the rod.
b) Waves propagate with a velocity c.
c) As the waves propagate, they are unchanged in amplitude.

It should be noted that the velocity of wave propagation is a material property and is unrelated to the manner in which the wave is generated.

The velocity of wave propagation in steel is 16,800 ft/s (5,120 m/s). In both concrete and timber, this velocity is approximately 12,500 ft/s (3,800 m/s), but varies considerably from case to case, depending upon material properties. In concrete, this velocity is a function of both density and strength (since the concrete modulus is related to strength). The situation is similar for timber, where again the velocity is dependent upon density the and modulus.

2.3.2 The Force-Velocity Proportionality

A relationship exists between the stress, f, at a point in a rod due to a single stress wave propagating in one direction, and the velocity of motion of a particle, v, at the same location. This relationship is

$$f = Ev/c \tag{2.4}$$

Typical maximum values for v during pile driving are approximately 10 ft/s (3m/s), and are dependent upon the ram impact velocity. Thus, for a steel pile, the stress induced by a typical air/steam hammer will be

$$f = 30{,}000\ (10)/16{,}800 = 17.9\ \text{ksi}$$

or

$$f = 210{,}000\ (3)/5{,}120 = 123\ \text{MN/m}^2$$

This implies that in a typical case the maximum driving stress induced in a steel pile will be about 18 ksi (120 MN/m^2). This example will be discussed further at a later point in this report. Other useful expressions that can be easily obtained from Eq. 2.4 include a relationship between strain and velocity

$$eps = v/c \tag{2.5}$$

where eps is strain
and between force and velocity

$$F = (EA/c)v \tag{2.6}$$

where A = pile cross-sectional area

This latter relationship is one that appears with great frequency in pile dynamics literature. The quantity EA/c, a pile material and cross sectional property, is commonly called the pile IMPEDANCE.

2.3.3 Reflections - The Fixed End Rod

Consider a semi-infinite rod with an applied compression wave traveling as shown in Figure 2.5. Assume that the end of the rod is fixed. When the induced stress wave reaches the fixed end, it is reflected as a compression wave traveling in the opposite direction. The particle velocity is shown together with the force representation in Figure 2.5. It can be seen that in the process of reflecting from the fixed end, the force doubles, while the velocity goes to zero in the reflection region. The velocity is then reflected back to the free end of the rod, but now the velocity has the opposite sign.

2.3.4 Reflections - The Free End Rod

Consider the same stress wave as in Figure 2.5 traveling in a rod having a free end (Figure 2.6). In this case, the stress reflects with the opposite sign, so in the immediate vicinity of the free end, the arriving and reflecting forces superimpose and sum to zero, satisfying the boundary condition. The particle velocity, in this case, will reflect with the same sign and will therefore double in magnitude at the free end.

2.3.5 Load Application at an Intermediate Location

If a force is suddenly applied at some point along an infinite rod, as shown in Figure 2.7, then two stress waves are initiated. They travel in opposite directions from the point of application of the force. One wave will be a compression wave, and the other will be a tension wave. If the rod is of uniform section, the force in each wave will be one-half of the applied force.

2.3.6 Applications to Pile Driving

Now consider a case that begins to resemble pile driving. Figure 2.8 shows an elastic rod with a fixed end being impacted by a rigid mass. At the instant of contact between the mass and the rod, it is assumed that the im-

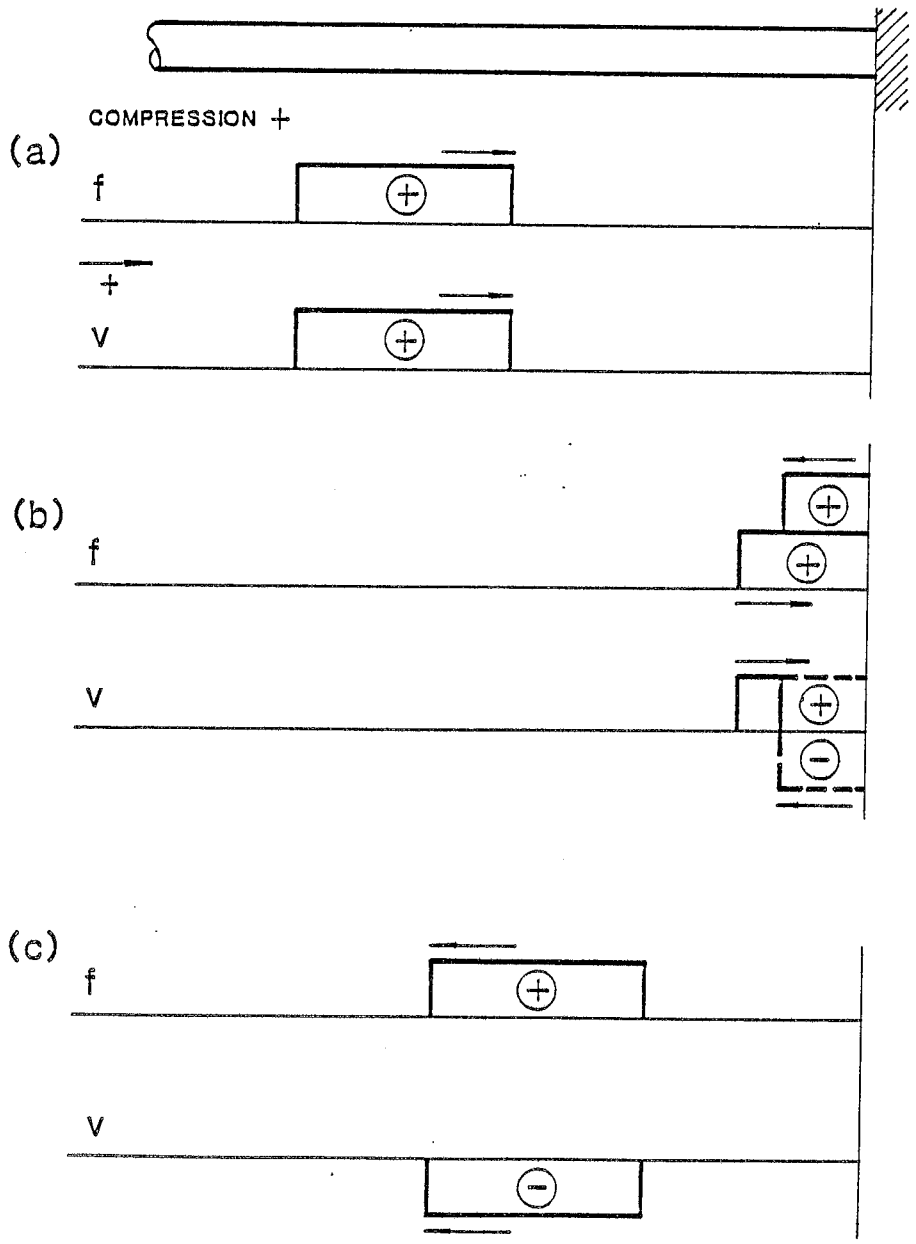

Figure 2.5: Stress, f, and Velocity, V, in a Semi-infinitely Long Rod, Fixed at Its End.

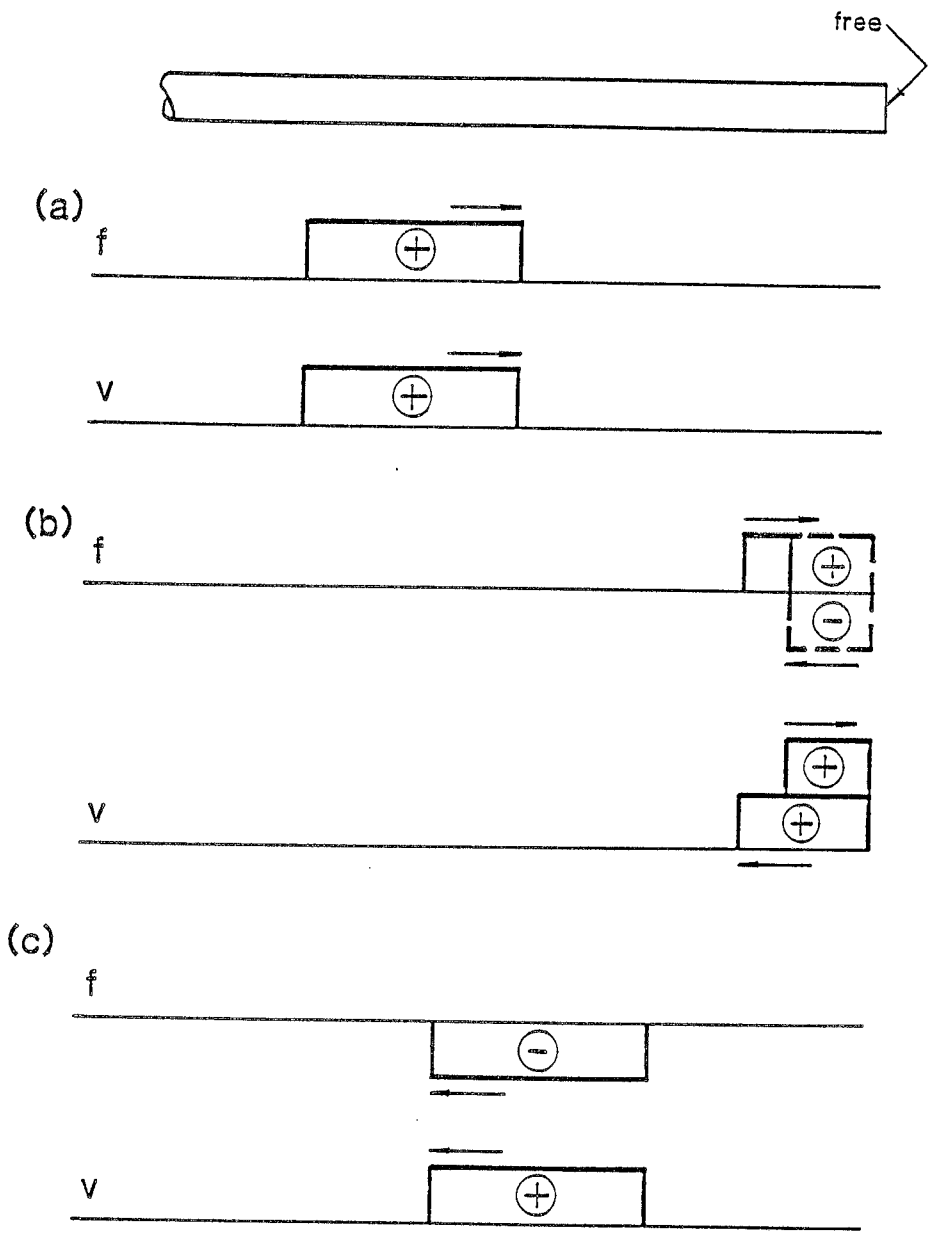

Figure 2.6: Stress, f, and Velocity, V, in a Semi-infinitely Long Rod, Free at Its End.

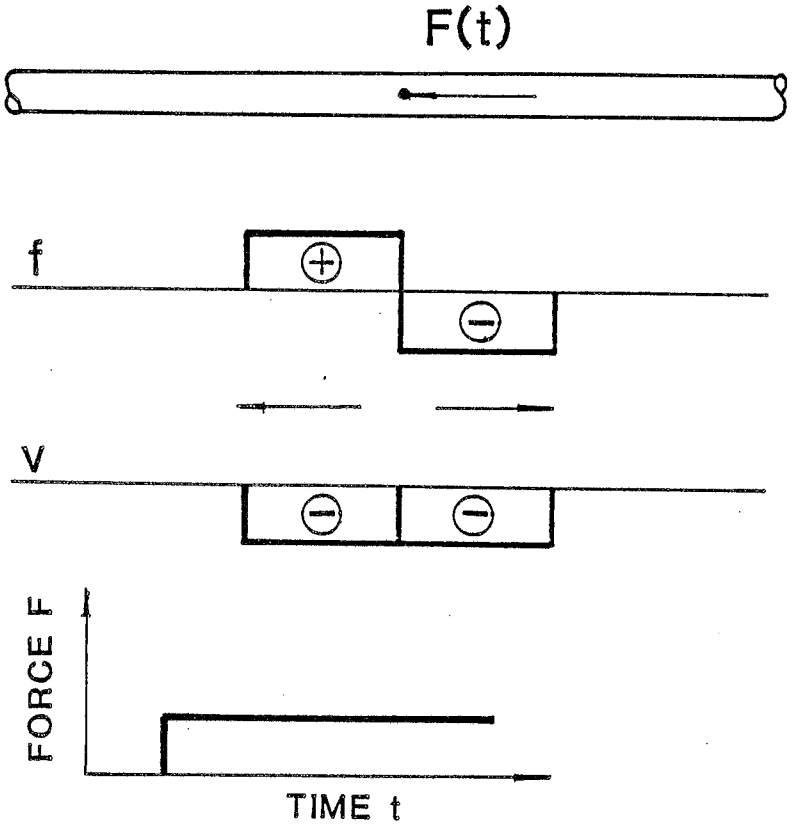

FORCE, F, VS TIME t

Figure 2.7: Waves Due to Force Application at an Intermediate Pile Location.

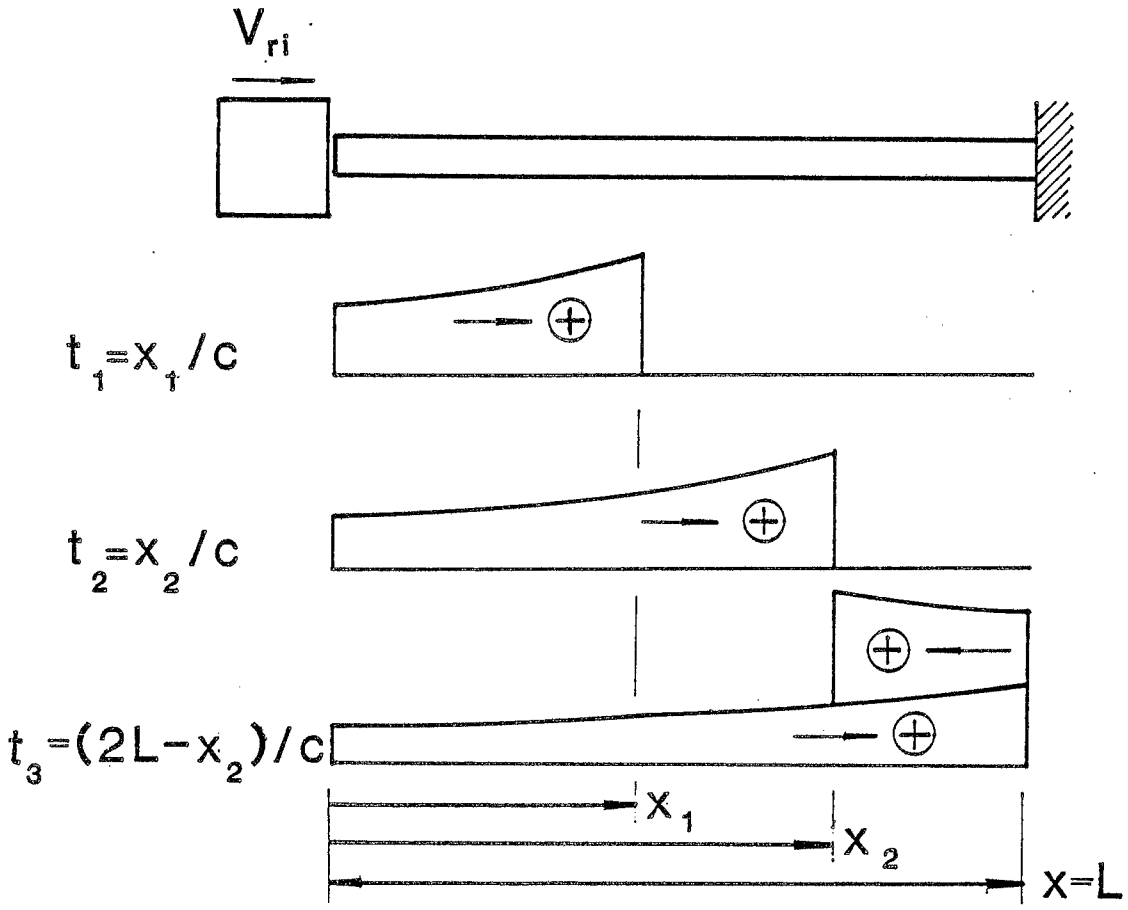

Figure 2.8: Stress Distribution in a Pile With Fixed End at Various Times.

pacted surface of the rod adopts the velocity of the ram over its entire cross section, and that this condition continues until the force between the rod and the ram becomes zero, at which time they separate. Imagine what is happening during the impact. Since particle motion is generated in the rod upon impact, a force is also generated, related to the velocity by the impedance of the rod, (Eq. 2.6). This force acts to impede the motion of the ram. As the ram velocity reduces, so does the induced force in the rod. The stress in the rod's top end as a function of time can be determined from the following relationship:

$$f = Ev_{ri}\, e^{[(-EA/c)(t/m_r)]} \tag{2.7}$$

where v_{ri} is the ram impact velocity, m_r is the mass of the ram, and e is the base of the natural Logarithms. This relationship is plotted as a function of time in Figure 2.8. The velocity is also shown at the impacted end.

In the case of a rod with a fixed end, the force reflects in compression, and is superimposed on the incoming compression wave. When it returns to the impacted end, it is again reflected as a compression force. This causes a dramatic increase in the force acting against the impacting mass, causing it to decelerate more rapidly, and then to accelerate in rebound. When the force becomes zero, separation occurs. The ram has regained some of its initial kinetic energy, although its velocity is now directed in the opposite direction.

The pile top stress is plotted as a function of time in Figure 2.9 for several ram/pile weight ratios. Velocities at the impacted end are also plotted in Figure 2.9. It should be noted that the force-velocity proportionality holds, in this case, over the first 2L/c time interval. It is possible to calculate the energy in the rod as a function of time from the relationship

$$E(t) = \int_0^t F(t^*)v(t^*)dt^* \tag{2.8}$$

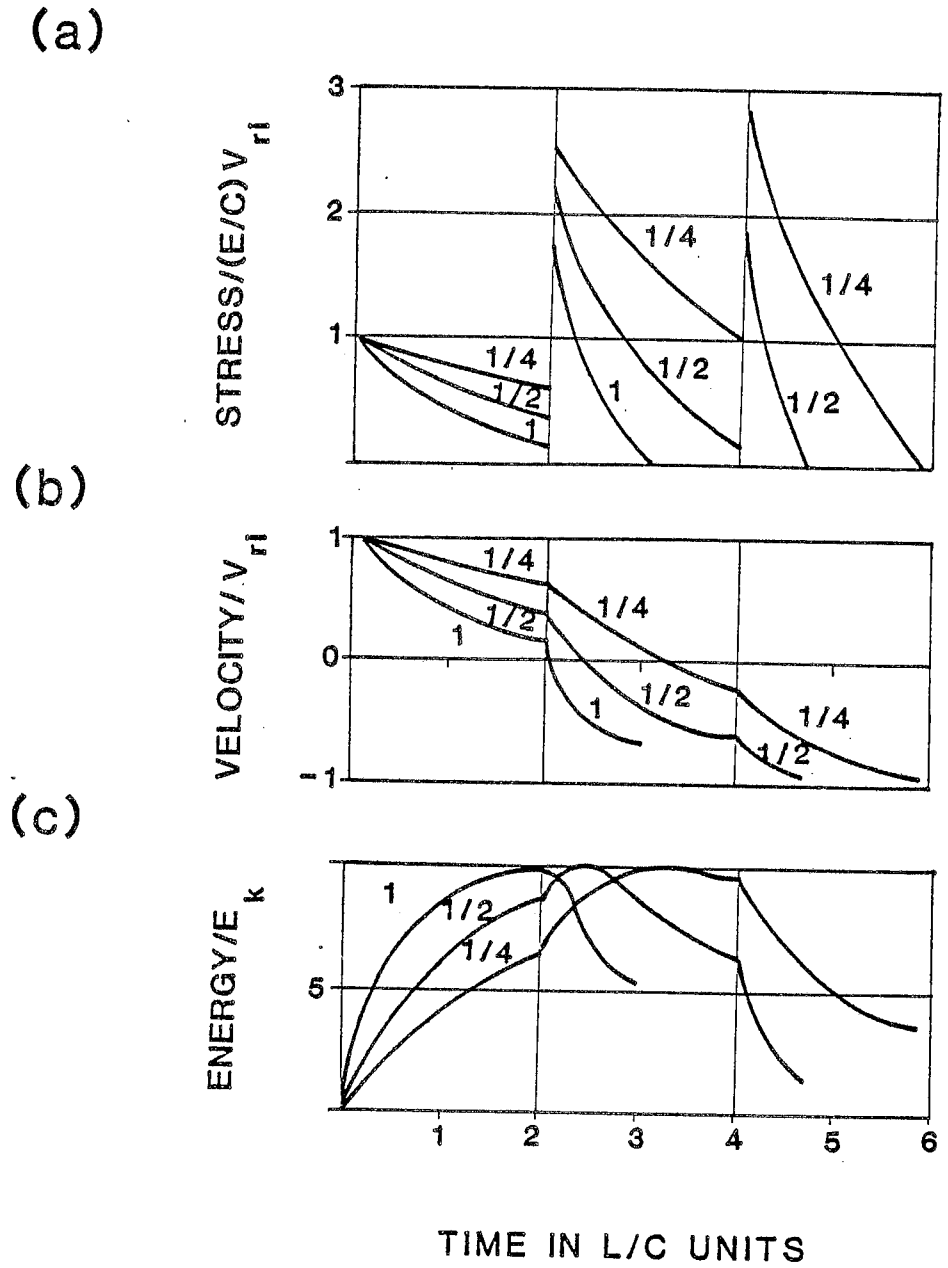

L = Pile Length
E_k = Ram Kinetic Energy

C = Wave Speed
V_{ri} = Ram Impact Velocity

Figure 2.9: Nondimensionalized Pile Top Stress, Pile Top Velocity, and Pile Top Transferred Energy as a Function of Time for Three Pile/Ram Weight Ratios

The energy is given as a function of time in Figure 2.9 for several ram/pile weight ratios.

It has been considered an attractive alternative by many to avoid the measurement of velocity by referring to the force-velocity relationship as shown in Eq. 2.6. If this equation is substituted in Eq. 2.8, the result is

$$E(t) = c/EA\int_0^t F(t^*)^2 dt^* \tag{2.9}$$

However, this relationship is only true if the force and velocity are always proportional. There must be no reflected forces returning to the impacted end of the rod before separation from the impacting mass. This condition is basically satisfied only when the pile is very long, is of uniform cross section and has little skin friction. These stringent conditions preclude the use of Eq. 2.9 in favor of the more general Eq. 2.8 for the vast majority of piles driven.

3. THE ANALYSIS OF PILE DRIVING

3.1 Introduction

This chapter is intended to provide the reader with mathematical and physical details of pile driving analysis. It is divided into two sections, (a) the description of components of a hammer-pile-soil system, and (b) an introduction to the commonly employed mathematical models and their use. Major reference is made to Appendix B.

There are two techniques of investigating pile driving behavior. The first one is a Prediction, the second one an In-Situ Test. Prediction methods require that an accurate static soil analysis is performed and that the effects of pile driving on the soil are estimated. Predictions may be done by either "The Formula", (i.e. any one of the several hundred dynamic formulae developed through the past hundred years), or the "The Wave Equation".

In-situ tests require measurements of a pile's response to a hammer blow. The most basic of these measurements is the permanent set or blow count; interpretation of capacity is then made by either Formula or Wave Equation. In-situ tests may also be done using measurements of force and motion of the pile near its top. Calculation of pile capacity from measurements may be accomplished by a simple formula (e.g. Case Method), or by numerical analysis (e.g. CAPWAP). Both Case Method and CAPWAP are based upon one dimensional wave mechanics.

Pile top measurements using the Case Method, are increasingly used for hammer and driving system performance investigations. A few other data interpretation techniques which use only force measurements have also been developed, and are in use on a proprietary basis. These techniques are described later in Chapter 5 and in Volume II.

Figure 3.1 shows in block diagram form, the preconditions and results for the various techniques of predicting pile driving behavior and interpreting.

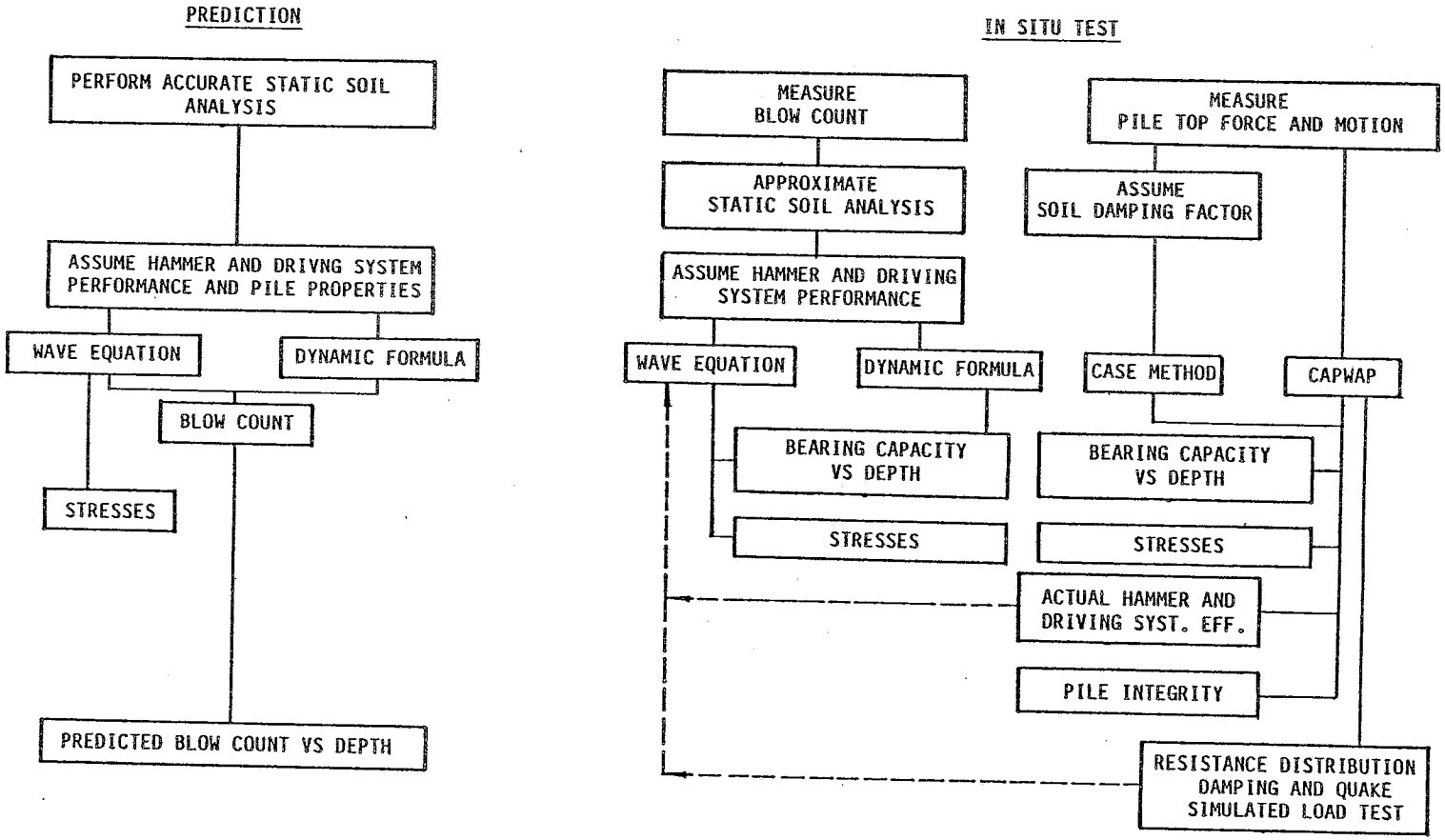

Figure 3.1: Dynamic Pile Analysis: Methods and Results

Obviously, quantity and quality of the results increase with the amount of engineering effort performed.

Using the concept of the simple dynamic formula, a prediction is usually obtained in the following manner.

(a) Step one is a static formula design; given a soil profile and soil strength parameters and certain pile design loads, a pile type is selected and the pile length is calculated.

(b) Step two is selection of a hammer based on experience.

(c) Step three is the computation of a blow count from hammer energy and soil resistance as inputs into the dynamic formula. Thus, for the design load, a required blow count is found, and the expected driving effort can be estimated.

After having performed the prediction, the in-situ test of measuring blow counts as the pile is driven is a natural extension which produces the following result:

(d) For any blow count, the current ultimate and/or pile design load may be calculated.

With the exception of step (b) the procedure outlined above is not very different when a wave equation analysis replaces the formula. Now, a hammer is selected not only based on experience, but by analysis, rejecting those units that either overstress the pile, or require too many blows to be economical. This selection process is also called a driveability study.

Both dynamic formula and wave equation can be used to produce a resistance vs. blow count curve commonly called a BEARING GRAPH. Actually, the wave equation is only a more accurate "formula" than the traditional ones. This increased accuracy results from the consideration of a variety of

parameters. For example, while the dynamic formula only deals with a single soil resistance paramter (the ultimate static pile capacity, the wave equation analysis considers

a) Skin friction magnitude and distribution,
b) Soil stiffness,
c) and Soil damping

In most formulae, properties of the pile are not an input parameter, and are therefore not considered. The wave equation, however, requires information on

d) Pile cross sectional area
e) Pile length
f) Pile material properties (modulus of elasticity, density)

The complexity of the wave equation input for the hammer and driving system varies with the hammer type analyzed. For example, diesel hammers analyzed by WEAP (Goble and Rausche, Ref. 8) are described with at least twelve (12) parameters while the typical formula contends with only two, the ram weight and stroke.

As a result of these detailed inputs and computations, more accurate results are obtained. However, the precision of the prediction cannot be improved if real and assumed parameters are in gross disagreement. Differences between hammer ratings and hammer performance are a major reason why wave equation results are sometimes inaccurate. Thus, wave equation accuracy improved when it became possible to measure actual hammer performance.

3.2 Dynamic Formulae Analysis

Dynamic formulae such as the basic formula given by Chellis (Ref 4) are discussed in Chapter 2 and little needs to be added here. Nevertheless, for comparison with other analysis types, it may be of interest to investigate the various inputs included in the formula presented by Chellis:

$$R_u = [(e_f W_r h)/s] \cdot (W_r + C_c^2 W_p)/(W_r + W_p) \qquad (3.1)$$

where R_u is the ultimate pile capacity, e_f is the hammer efficiency, W_r is the ram weight, and h is the ram stroke. The quality $e_f W_r h$ represents the energy available in the ram at impact. The coefficient of restitution, C_c^2, represents energy losses occurring due to the collision of the ram with the pile. W_p is the combined helmet and pile weight and Wr is the ram weight. The pile penetration under a blow is denoted by the set, s.

This formula includes losses in ram and driving system in a manner very similar to the wave equation, i.e. it includes a hammer efficiency and a coefficient of restitution. The primary shortcoming, however, is that losses in pile and soil are not considered. Other formulae include those losses with constants in the denominator of Eq. 3.1. Since these constants are only rough estimates of the actual energy losses, increased accuracy may or may not result through their use.

The formula can be demonstrated to be fundamentally deficiat by way of one basic example. If the pile area, and hence stiffness and weight (Wp), is increased, the formula predicts a decrease in ultimate capacity, Ru. Experience shows, however, that stiffer piles are driven more easily.

Other deficiencies of the formula are that

(a) common to all analysis methods which are not verfied by measurement, the efficiency, ef, is estimated.

(b) the formula accuracy decreases with increasing pile length, or non-uniformity of section.

Obviously, with an ultimate capacity determined from static analyses it is easy to compute s (prediction); thus with s determined in the field from measured blow count, R_u may be calculated. This R_u value must be divided by an appropriate safety factor to yield the pile's safe or design load.

3.3 Components of the Hammer-Pile-Soil System in Wave Equation Analysis

In modern pile driving practices, the following items (shown schematically in Figure 3.2) are needed for pile driving:

(a) A ram which strikes with a certain impact velocity.

(b) A leader and its carrier (e.g. crane) to guide the hammer assembly and ram; also called lead or leads.

(c) A power medium such as a rope and winch (drop hammer), compressed air or steam (air/steam hammer), pressurized hydraulic fluid (hydraulic hammer), or combustible fuel (diesel hammer).

(d) A cushion between ram and pile, also referred to as hammer cushion or capblock.

(e) A cushion container and load distributing device called the helmet.

(f) A gate which (together with the helmet) keeps the pile parallel to the leader.

(g) A cushion between helmet and pile (concrete piles only) simply referred to as the pile cushion.

(h) A pile, i.e. a long slender steel, concrete or timber rod.

(i) Soil

With the exception of leader, carrier and gate, all of these items must be included in a dynamic pile analysis. It is important, therefore, that the physical properties of each component be thoroughly understood before the wave equation analysis is explained in detail.

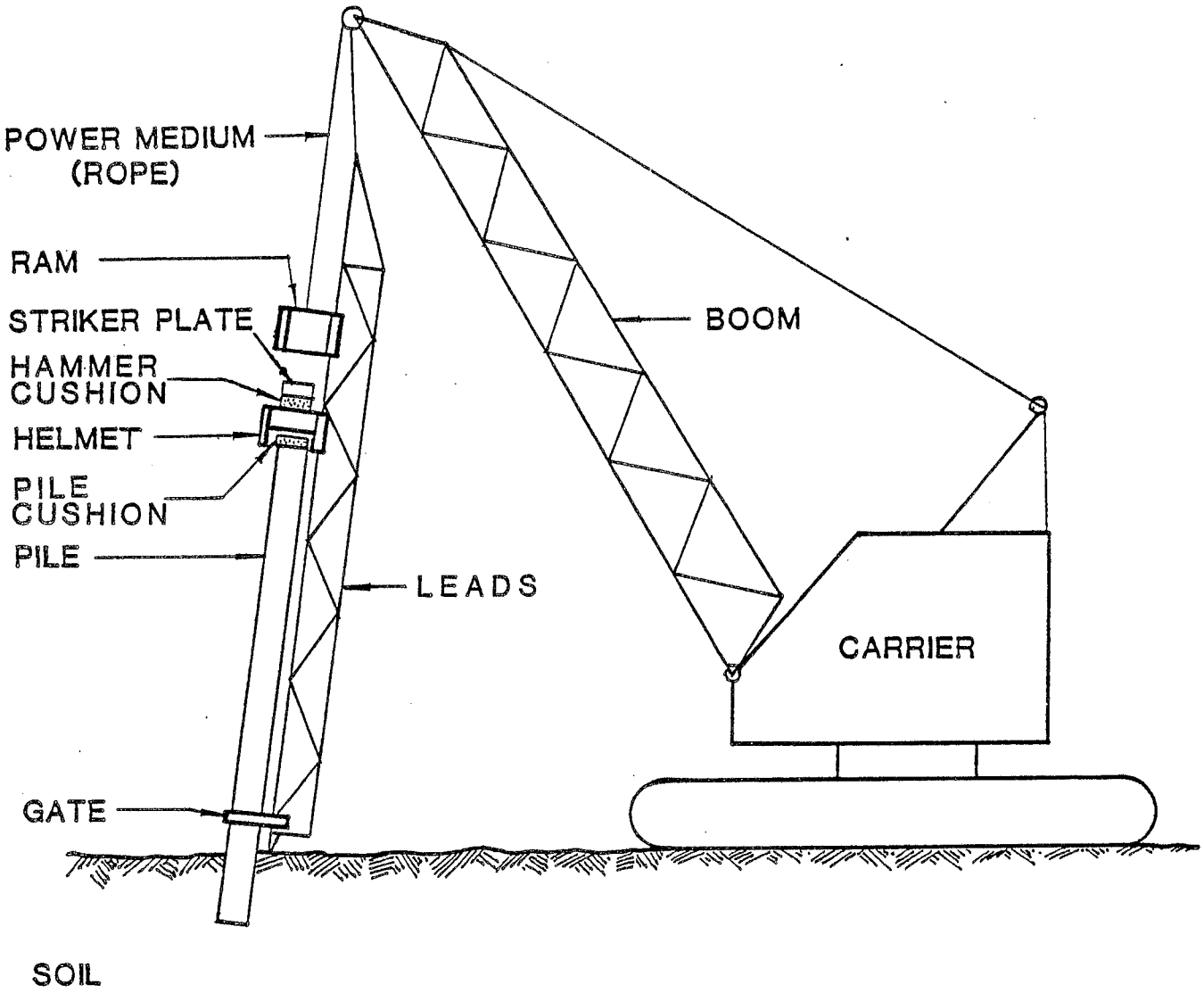

Figure 3.2: Schematic Representation of a Complete Pile Driving System.

3.3.1 Hammers

A great variety of pile driving hammers are used today. With the exception of drop hammers, hammer designs are complex and their interaction with the pile and soil is not easily modeled or predicted. A description of the most important hammer types is given in Appendix B1.

Drop hammers, as well as air/steam or hydraulically powered units (ASH) are schematically shown in Figure 3.3 (a). They may be represented by a simple mass. It is commonly assumed that the external power medium has no significant effect on the process of energy transfer. However, it is known that improper valve adjustments greatly affect the energy output of the hammer. In this regard, improvement of the hammer model and state of the art of wave equation analyses would be possible.

Diesel hammers (Figure 3.3b) generate by internal combustion the pressures which drive the ram upwards. For this reason, an impact block or anvil is needed; the upper surface of the impact block forms part of the combustion chamber. The WEAP program (Goble and Rausche, Ref. 8) models the entire thermodynamic cycle, i.e. the pressure-volume relationship, within the diesel hammer. Other programs, such as TTI, (Hirsch et., al. Ref. 15) treat the diesel hammer like a drop hammer and add an "explosive force" term.

3.3.2 Driving Systems

The term Driving System incoporates all elements between the bottom of the ram and the top of the pile, in addition to accessories like leaders or gates, which do not participate in the load transfer.

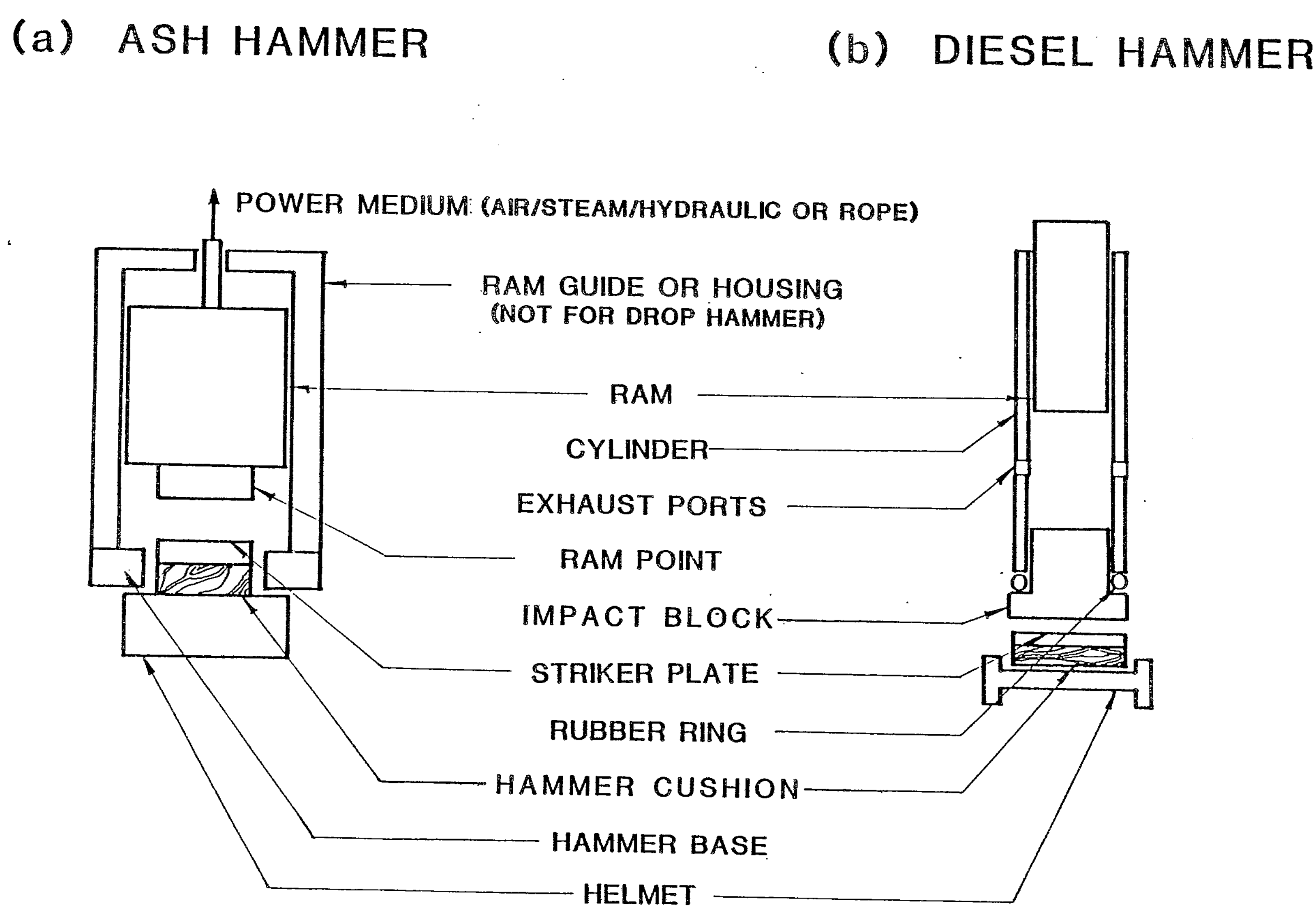

Figure 3.3: Principles of (a) Air/Steam Hydraulic and Drop Hammers (b) Diesel Hammers.

3.3.2.1 Leaders

The leaders maintain the aligment of hammer, helmet and pile. As this device does not participate in the load transfer, it is not included in the wave equation analysis, and will be excluded from further discussions relating to the driving system. It should be noted, however, that improper pile or hammer alignment and guidance way be the cause of large energy losses.

3.3.2.2 Hammer Cushion

A hammer cushion is usually inserted in the driving system below the impacting ram (ASH hammers) or below the impact block (diesel hammers), for protection of the hammer. Wood (e.g. oak, Bongossi etc.) is the traditional cushion material. Today, a variety of man-made materials such as Micarta, nylon and coiled steel cable. are encountered. Asbestos is no longer used as a cushioning material because it poses a health hazard.

Man-made cushion materials are relatively stiff, i.e. they have a high modulus of elasticity, E_c, do not quickly change their properties, and absorb relatively little energy as expressed by a high (near 1) coefficient of restitution, C_c. It seems to be a basic law of nature, that soft cushions temporarily store, and also dissipate, more energy than stiff cushions.

In wave equation analysis, E_c and C_c are used to completely describe the behavior of a cushion material. Errors are introduced with this description, because it assumes a bilinear, rather than a curved, force-deformation relationship (Figure 3.4a). An alternative non-linear model as used by WEAP is shown in Figure 3.4.b.

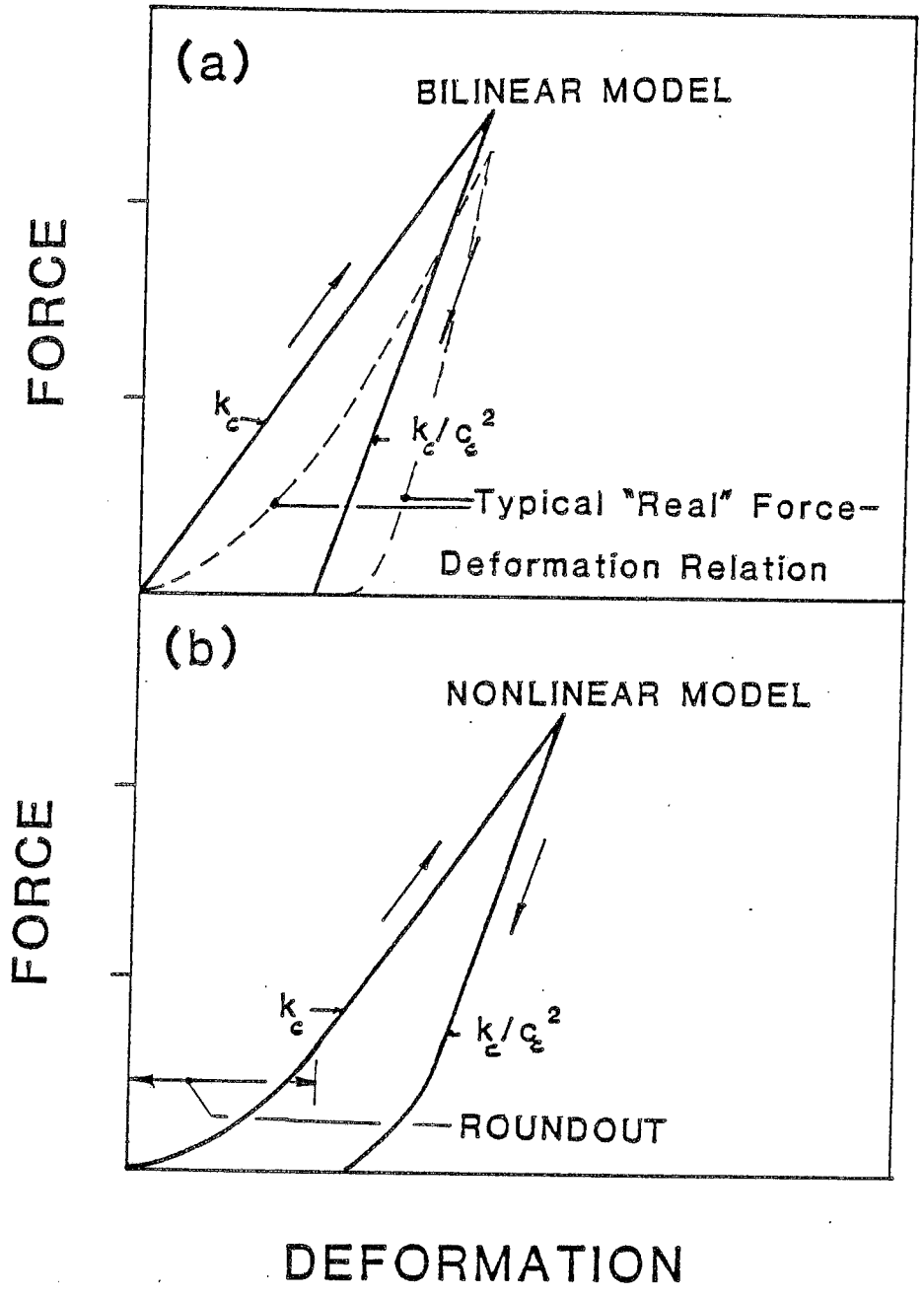

Figure 3.4: (a) Bilinear Wave Equation Model for Cushion Force Deformation Relation, Together With a Typical Real Behavior. (b) Modified Bilinear Model With Non-linear Portion.

3.3.2.3 Helmet

The helmet is a massive steel box which often includes inserts to adapt to a certain pile profiles. Little effort is expended to model the helmet, except that its weight is computed as accurately as possible. The helmet weight should include all the components between the hammer and pile, such as striker plates, cushions and adaptors.

It should be mentioned that a poorly fitting helmet is often a prime cause of poor hammer-pile-alignment and contributes to either pile damage or poor energy transfer. Similarly, non-flat impact surfaces of the helmet cause similar problems.

3.3.2.4 Pile Cushion

A pile cushion is normally used when driving concrete piles. Pile cushions in the U.S. are usually made of several plywood layers. Cushion thicknesses of three (3) to twelve (12) inches (75-300 mm) are common. The larger thicknesses are necessary where there is a danger of tension cracking. Plywood easily moulds to the pile top surface and, therefore, reduces the danger of local overstressing. A pile top cushion, like a hammer cushion, is modeled through use of a stiffness and a coefficient of restitution.

Further descriptions of all driving system components are contained in Appendix B2.

3.3.3 Piles

Piles are the simplest components of the total system to be analyzed. It is sufficient to know the cross sectional area and length of steel piles, as material properties do not vary. For timber or concrete piles, the elastic modulus and specific weight must also be known. In a prediction analysis, these quantities may be taken from specifications; for in-situ tests, wave

speed measurements are employed to more accurately assess these material properties.

Modeling complications may occur when the pile is spliced or if a heavy toe plate is added. The latter may be described as a cross sectional change of the pile. For the former it is necessary to know whether or not the splice allows for a forceless deformation called slack. In general, nearly rigid splices may be modeled as a continuous section with little loss of accuracy. Splices which allow the pile to separate more than a small fraction of an inch, must be identified.

A pile soil plug may occur when an open pile profile is driven into dense cohesionless materials. These situations are sometimes modeled as pile segments with increased mass over the bottom five (5) feet (1.5 m). It is important that the corresponding toe soil resistance parameters be included. In general, knowledge of dynamic soil plug behavior is limited; an improvement in the precision of prediction cannot be expected from plug modeling.

3.3.4 Soils

The dynamic behavior of soil is even more complex than static behavior. Research in both areas is still being conducted. A detailed representation is not warranted, simply because the appropriate values for the soil parameters would not be known. A simple model which produces a reasonably accurate representation has been used.

The basic and most important quantity of soil resistance is represented by the ultimate pile bearing capacity. This ultimate capacity is apportioned to skin friction and end bearing according to static analysis results (which are often based merely on guesses or standard penetration test results). A skin friction distribution is also determined according to static considerations.

The static soil deformation is considered proportional to the static soil

resistance up to an elastic limit deformation value (called "quake") (see Figure 3.5a). The soil is assumed to be linear elastic until the displacement reaches the quake deformation. When the pile penetration exceeds this quake, the soil resistance assumes the ultimate resistance and deforms plastically.

The dynamic component of soil resistance is defined by the damping factor. Damping factors vary with soil type, and are currently chosen on the basis of grain size analyses. Unless very detailed studies are done, a single skin damping factor is used to represent the average dynamic soil behavior, on the pile skin even in the presence of layered soils. A separate toe damping factor is also specified. The definition of the traditional Smith type damping factor assumes damping increases with both static resistance and pile velocity (Figure 3.5b).

3.4 Wave Equation Analysis

As far as the program-user is concerned, (manual calculations are uneconomical because of the large volume of repetitive calculations), use of the wave equation is not much more complicated than a formula. Unfortunately, the user cannot expect that the wave equation will solve his basic pile design problem.

A wave equation analysis can only predict a certain pile's behavior under a certain hammer for a certain soil condition. The wave equation gives a blow count for each soil resistance input; it does not give a resistance for a blow count. If a wave equation analysis is to be used in conjunction with an in-situ test, then a curve must be constructed that relates various ultimate resistance values to their blow counts (Bearing Graph).

After the soil conditions have been analyzed, the pile embedment for the desired ultimate capacity (design load times safety factor, e.g. 2.5) should be estimated. The skin friction percentage and distribution should also be determined. From the soil grain sizes or classification, damping factors and

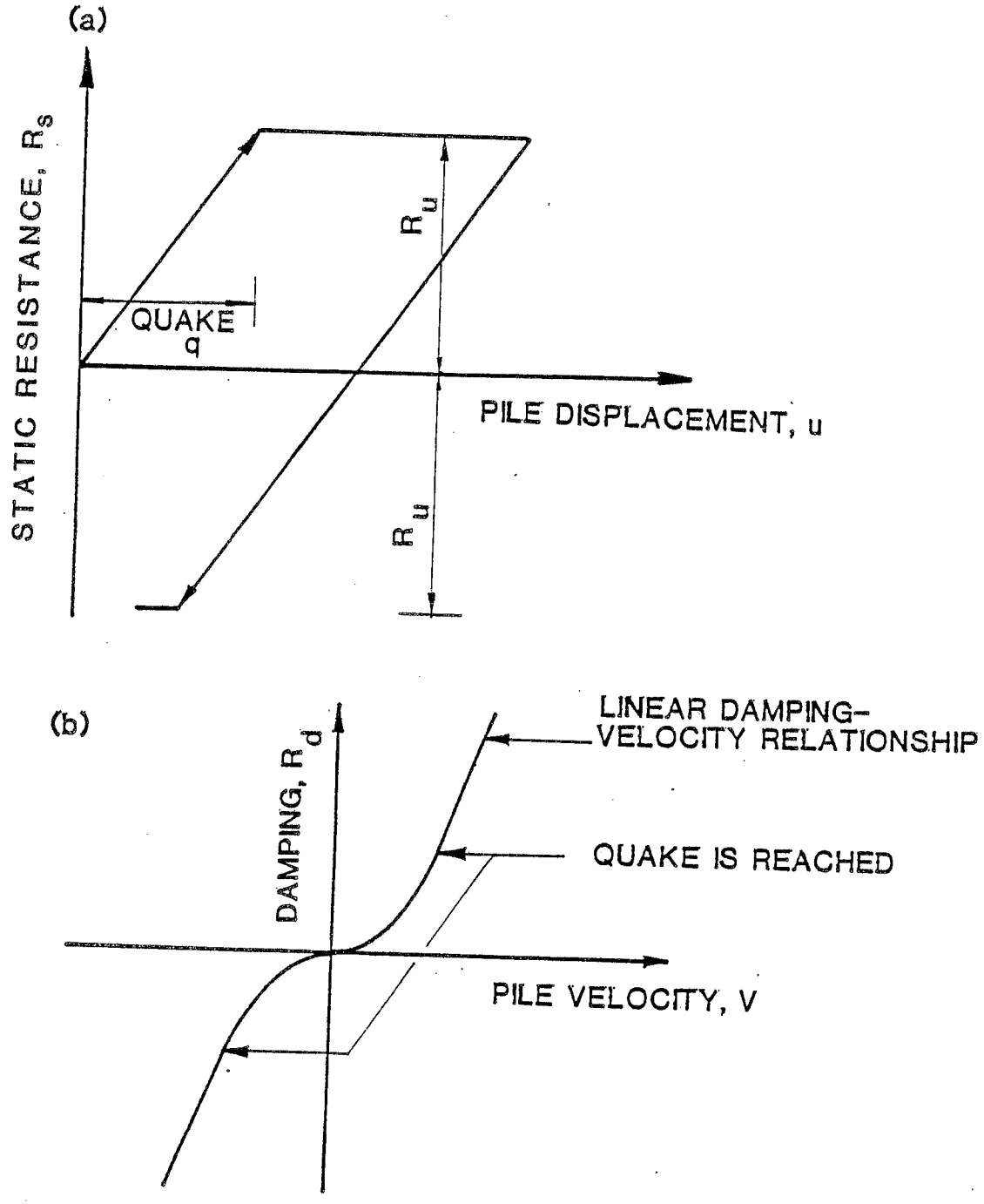

Figure 3.5: Soil Resistance Model after Smith (a) Static Portion $R_s = u(R_u/q)$, with $|R_s| < R_u$; (b) Damping $R_d = R_s\, j_s\, V$, j_s is the Smith Damping Factor.

quakes are selected from appropriate tables in the wave equation manuals.

Actually the wave equation models system elements with springs, dashpots, and masses. A detailed description of the mathematical formulations of the wave equation approach is given in Appendix B2. Depending on the wave equation program used, the model stiffnesses and masses may have to be computed by the user. The more sophisticated programs compute these quantities automatically from the pile and cushion data entered by the user. This "modeling" has to be done for hammer, driving system and pile.

The input data for most common hammers, is usually prepared and available in tables or on data file. However, the stiffnesses of cushions need to be computed from elastic modulus, E_c, cross sectional area, A_c, and thickness t_c. The individual stiffnesses are then calculated from

$$k_c = E_c A_c / t_c \tag{3.2}$$

Appropriate coefficients of restitution also need to be entered for all driving system elements.

The pile is modeled by dividing it into segments of approximately 5 feet (1.5 m) lengths . For each pile segment, an element stiffness is computed using Eq. 3.2 with t_c replaced by the pile segment length. E_c and A_c become the relevant pile modulus and cross-sectional area. For nonuniform piles, average quantities are used for each segment. The mass of each pile segment is computed from specific pile weight, cross sectional area and segment length.

This completes the modeling effort and an analysis can be run for a total ultimate capacity, R_u. Usually it is desirable to analyze several R_u values since the static soil capacity is not exactly known. It has become common practice to analyze five (5) or more capacities so that a complete bearing graph can be constructed. It is also usually recommended to produce several curves with different assumptions of hammer efficiency, damping or soil quake

to find upper and lower bounds to the solution.

In general, only stresses in the pile are sensitive to the skin resistance distribution. Thus, the blow count computed for the ultimate capacity at a certain embedment can be used for a different embedment, provided soil (damping) properties do not change.

Differences between wave equation predictions and actual static pile-soil performance can be attributed to either inaccurate soil, hammer, or driving system assumptions or time dependant setup/relaxation effects in the soil. The latter effects are particularly pronounced in fine-grained soils; these errors may be avoided in the "In-Situ Test" if the pile is restruck after a waiting period some time after installation.

3.5 Case Method Analysis

The measurement of pile top force and velocity forms the basis for the more extensive and accurate in-situ tests (see Fig. 3.1). The Case Method uses the pile top force and velocity records to determine the ultimate pile capacity.

As shown in Appendix B3, the Case Method formula was derived for evaluating the total resistance. A damping factor, J, which reflects the dynamic behavior of the soil, was introduced into the equation to allow separation of dynamic and static components of the total resistance. Of course, as for wave equation analysis, an assumption has to be made regarding the soil's dynamic behavior, and errors in prediction of the ultimate static resistance will result from use of inappropriate damping factors. Typically, the damping factor for a site is determined by comparing Case Method predictions of ultimate static capacity with the results of static load tests, or the more rigorous CAPWAP analysis (see section 3.6).

The Case Method also allows, with some restrictions, the determination of maximum tensile and compressive stresses at any location along the pile length

and assessment of pile integrity. Restrictions apply primarily to non-uniform piles. The hammer performance is also verfied by calculation of the energy that is transferred to the pile for each hammer blow. All the above quantities can be determined within a few milliseconds after each hammer blow using modern microprocessor technology.

3.6 CAPWAP

CAPWAP (CAse Pile Wave Analysis Program) combines measured force and motion data with a wave equation model of the pile and soil. The pile and soil models are similar to those used in wave equation analysis. Certain modifications are discussed in Appendix B4.

In CAPWAP, typically the measured velocity record is applied to the model to predict the force or velocity response, which is compared with the measured force. In general, these will not agree, and the experienced engineer iteratively alters the pile or soil model until a satisfactory match is obtained. The soil parameters are thus obtained independently of a static soil analysis. The force and velocity records themselves fully define the performance of the hammer, so that hammer modeling in CAPWAP is unnecessary.

Differences between computed and actual static pile performance can be caused by differences in soil behavior between the static and dynamic situation, however, most differences are caused by setup/relaxation effects which can be minimized by requiring that analyses be performed on measurements taken during restrike.

The CAPWAP process allows for an accurate assessment of the stress state of the entire pile length as a function of time. This stress assessment is superior to that of the Case Method or the wave equation, because CAPWAP determines and works with an accurate resistance distribution. In fact, it is even possible to use the CAPWAP results for estimating a pile's uplift capacity.

Use of CAPWAP is presently limited because CAPWAP requires substantial computer time and an experienced engineer as computer operator. Developement of more powerful microcomputers and automated matching routines will make it possible to train and equip more engineers with this capability.

4. SELECTION OF MINIMUM COST PILE

4.1 Introduction

The estimation of pile driving costs remains a very inexact activity not greatly changed over the past half century. To some extent, all of constuction cost estimation is inexact, but improvements have been made in other areas. Sophisticated analytical tools are available for job scheduling and planning, and a great deal of effort goes into the cost estimation of various job phases. In general, foundation work is more difficult to deal with, since subsurface information is not as reliable as other aspects of the job. Therefore, many piling contractors tend to limit their work to a particular geographical region, relying on equipment of a familiar type. When the job is estimated, the contractor will commonly depend more on previous experience than on anything revealed by normal subsurface investigations. It is common practice for the contractor to estimate productivity on a completely intuitive basis. Equipment selection is usually made on a subjective basis with emphasis placed on using driving systems owned by the contractor.

If difficulty occurs with piles that cannot be advanced at a rate consistent with the estimate, quarrels frequently result between the engineer responsible for construction and the contractor. A frequent result is large cost overruns and litigation. The quality of the job is not improved by this development.

To avoid these problems, engineers have sometimes resorted to a tighter job specification. However, it is possible to specify requirements that cannot be met. In such cases, the contractor is in an excellent position to obtain extra payment. For example, the engineer may specify the pile type, the blow count, the rated hammer energy and the pile capacity. If the contractor, then meets these requirements, but the pile fails the load test, the contractor may successfully argue that he can recover costs in unanticipated reduced productivity. A worse possibility is that the contractor may follow all of the requirements, and have serious problems with pile damage.

In the past twenty years, and particularly in the last decade, engineering techniques have become available that allow a scientific approach to cost estimating. It is possible to estimate pile driving time on a rational basis. These predictions, while still of limited reliability, are at least better than any other available approach.

Pile driving costs can be categorized into several general activities including:

1. Mobilization
2. System testing, modification and implementation
3. Production
    A. Hammer time
    B. Dead time
    C. Overhead

The effort that can be devoted to Items 1 and 2 will depend on the size of the job. For very large jobs, it may be worthwhile to spend a great deal of effort in developing the systems and procedures to produce high degrees of productivity. On small jobs, only modest field efforts can be made in improving productivity since the total costs will not be reduced extensive system testing and modification.

The procedures outlined here will emphasize the production phase of the job, and in particular, the hammer time. If decisions made during the study prior to going to the field work well, the time spent on Item 2 will be short. If the results are poor, then considerable effort may be devoted to system modification. It is unfortunate that the reliability of subsurface investigations and the translation of this information to driving analyses are so imprecise. Such is the current state-of-the-art. However, it is always advantageous to do the best possible analysis prior to going to the field in order to avoid as many problems as possible.

In the evaluation of pile driving production, it is common to divide the operation into hammer time and dead time. In this discussion, dead time is

defined as that time during driving operations when the hammer is not running. During this time, the hammer is removed from the previously driven piles. The cushion may be replaced, and the hammer is moved to the next location. The next pile is brought into place, lifted under the hammer, set into position and aligned. On many jobs this portion of the production operation may be the primary time consumer. Typically, driving may be through very soft material to a bearing layer. After only a few hammer blows, the pile reaches the bearing layer, and the next few hammer blows then mobilize the pile capacity to the strength of the bearing layer. In such cases, it is obvious that job productivity will depend on the reduction of dead time. Where predrilling or jetting is used to reduce the total number of blows or penetrate a particularly difficult soil layer, productivity will again be affected by activities other than pile driving.

The reduction of dead time is typical of the problems that a contractor usually faces. Material must be placed and handled efficiently and personnel must be used effectively. This discussion does not propose to add new ideas to the handling of this problem. It is recognized that, in many cases, this phase of the job may be greatly improved, resulting in large cost savings.

A procedure will be presented here for pile driving cost estimation. This procedure will be illustrated by a hypothetical example. Important aspects of hammer operation will be clearly illustrated. The purpose of this chapter however, is to present a procedure for cost estimation and no general conclusions about driving system efficiency should be drawn from the example presented.

4.2 Procedure

For the purpose of this illustration, all mobilization, system testing and modification costs will be neglected. This is clearly not realistic, but in dealing with a hypothetical case, it is difficult to do better in a realistic fashion. In addition, the effects of equipment ownership and previous partial or full depreciation will be ignored. The equipment costs used will

be straight rental costs. A more realistic analysis can be accomplished by modification of the procedures presented here when job particulars are known.

Since only daily cost and productivity are considered, only two of the cost categories will be present, hammer time and dead time. The latter category is clearly a very important one in controlling costs. Contractors should devote great effort to minimizing it. Also, overhead is an important cost that may be, to some extent, a function of the driving system. An analysis of this cost is outside the scope of this discussion.

The job operation should be carefully organized, for example, the piles should be placed near where they are to be driven, so that they can be quickly put under the hammer. Careful study of the operation from hammer shut-down to start-up by the contractor can usually produce time savings. For the example treated here, it is impossible to make a meaningful evaluation of this activity. It is probably quite independent of the hammer used, which is the basic question under examination. The assumption is made that only seven hours are available per shift and that a total of ten minutes elapse between each hammer shut-down and start-up.

Finally, the principal problems of relevance here, hammer time, must be estimated. The procedure used is as follows:

1. For the specified conditions, perform a static soils analysis. Check for subsurface conditions that may cause problems during driving.

2. Determine soil input data for wave equation analyses at several pile penetrations.

3. Select candidate hammer systems.

4. Perform wave equation analyses at each selected depth to determine blow count, and for diesel hammers, operating speed.

5. Determine rate of pile penetration at each selected depth.

6. Calculate total driving time and hence piles per day.

In order to perform a static soil analysis, subsurface data must be available. The primary result that comes from this effort is the static pile capacity as a function of pile penetration. The calculation of static pile capacity from subsurface investigation information is quite unreliable due to an imperfect understanding of the fundamental mechanisms controlling bearing capacity. A second factor is the lack of reliability of assumed soil strength parameters. The best possible solutions must be found but it must be understood that exact values will depend, to a considerable degree, on experience in evaluation. This evaluation will include both skin resistance and tip resistance as a function of depth so that pile capacity can be estimated for a variety of depths.

Wave equation representation of soils requires an estimate of three different parameters: static resistance, quake and damping. The ultimate static resistance value comes directly from the static soils analysis, and in combination with the quake, defines the soil stiffness. The quake is the displacement at which the soil resistance changes from linear elastic to plastic; traditionally, a value of 0.1 inches (2.54 mm) has been used for all quakes. However, it has recently been conclusively shown (Likins, Ref. 16) that quakes can vary over a large range and that tip quakes can be as large as one inch (25.4 mm). Unfortunately, these high quake cases cannot be identified from the subsurface investigation. At this stage, it is reasonable to recommend that quakes somewhat larger than 0.1 inch (2.54 mm) be used at the pile tip for displacement type piles larger than about 18 inches (457 mm) in diameter or for displacement piles driven into saturated soils, particularily if the soil is poorly drained.

The third quantity, damping, must be estimated from the soil classification. The current state-of-the-art relates a damping constant to soil type

(see Chapter 3). This quantity is very important in estimating driveability at high blow counts and current knowledge is clearly inadequate. This practice must be followed until basic research produces a better understanding.

Candidate hammer and driving systems can only be selected by experience or rule-of-thumb. A quick check by dynamic formula may assist the engineer in getting into the correct range, if his experience is inadequate. Some contractors may want to use only their own equipment and, thus, have only a limited selection.

Several wave equation programs are available in the public domain. In addition, further developments have included derivative programs of the basic original software. The most widely used program is WEAP, (Goble and Rausche, Ref. 17). This program offers several important advantages over others, particularly in analyzing diesel hammers. The total operating cycle of the diesel hammer, including precompression, combustion, expansion and stroke, has been modeled. Thus, stroke for single-acting hammers and bounce chamber pressure for double-acting hammers is obtained as an output. Proper impact velocities and operating speeds are also obtained. In addition, the program performance has been extensively checked against measurements made during the research project involved in the development of the Case Method (Goble et al, Ref. 5) and its ability to predict driving stresses has been extensively tested. This program is still based on the same soil model as other wave equation programs. As previously noted, this is a serious weakness.

A wave equation analysis is performed at several different penetrations, so that a "blow count versus depth" curve is generated. Since speed of operation is known for air/steam hammers, and is calculated for diesel hammers, the rate of pile penetration can be deduced at each depth analyzed. From this information, total hammer time can be estimated for each pile and, hence, the number of piles driven per day. If the various unit costs are known, then cost per pile can be determined.

4.3 Example Problems

An example was selected from available job experiences. The pile to be driven was a 12-3/4 inch (320 mm) diameter steel pipe with a wall thickness of 3/8 inches (9.5 mm). The specified design capacity was 100 tons (900 kN) with a factor of safety of 2.0. Thus, an ultimate capacity of 200 tons (1800 kN) was required. The design specification indicated that the piles would penetrate to a depth of 65 feet (20 m) and that a representative soil profile is as shown in Figure 4.1.

In the process of reviewing the job, a bearing capacity analysis showed that, at 65 feet (20 m) penetration, a capacity of 222 tons (2010 kN) should be reached. Therefore, the contractor should use care before bidding the job to ascertain whether the pile must be driven to full depth or to a specified resistance. All wave equation analyses were run for both cases: 200 and 222 tons (1800 and 2010 kN). It should be emphasized that a difference in two independently performed static analyses of only 10 percent represents very close agreement.

The performance of six driving systems was examined; they included three air/steam hammers and three open-end diesel hammers. The air/steam hammers selected were the Vulcan 06 (19.5 kip-ft or 27 kN-m), 08 (26.0 kip-ft or 36 kN-m) and the 010 (32.5 kip-ft or 45 kN-m). Diesel hammers used were the Delmag D-15 (27.1 kip-ft or 37 kN-m), D-22 (39.8 kip-ft or 55 kN-m) and D-30 (54.2 to 239 kip-ft or 75 to 333 kN-m, depending on hammer setting).

For the air/steam hammers, the first step in the analysis was to determine the depth that the piles would penetrate under their dead weight and the weight of the driving system (run). Static analyses were made at depths of 36, 48, 62.5 and 65 feet (11, 14.6, 19 and 20 m). Since a different capacity at final penetration was determined than the design engineer had found, wave equation analyses were performed at each depth using two static resistance values. The output of the wave equation analysis for each penetration and capacity was blow count for the air/steam hammer, which is shown as a function

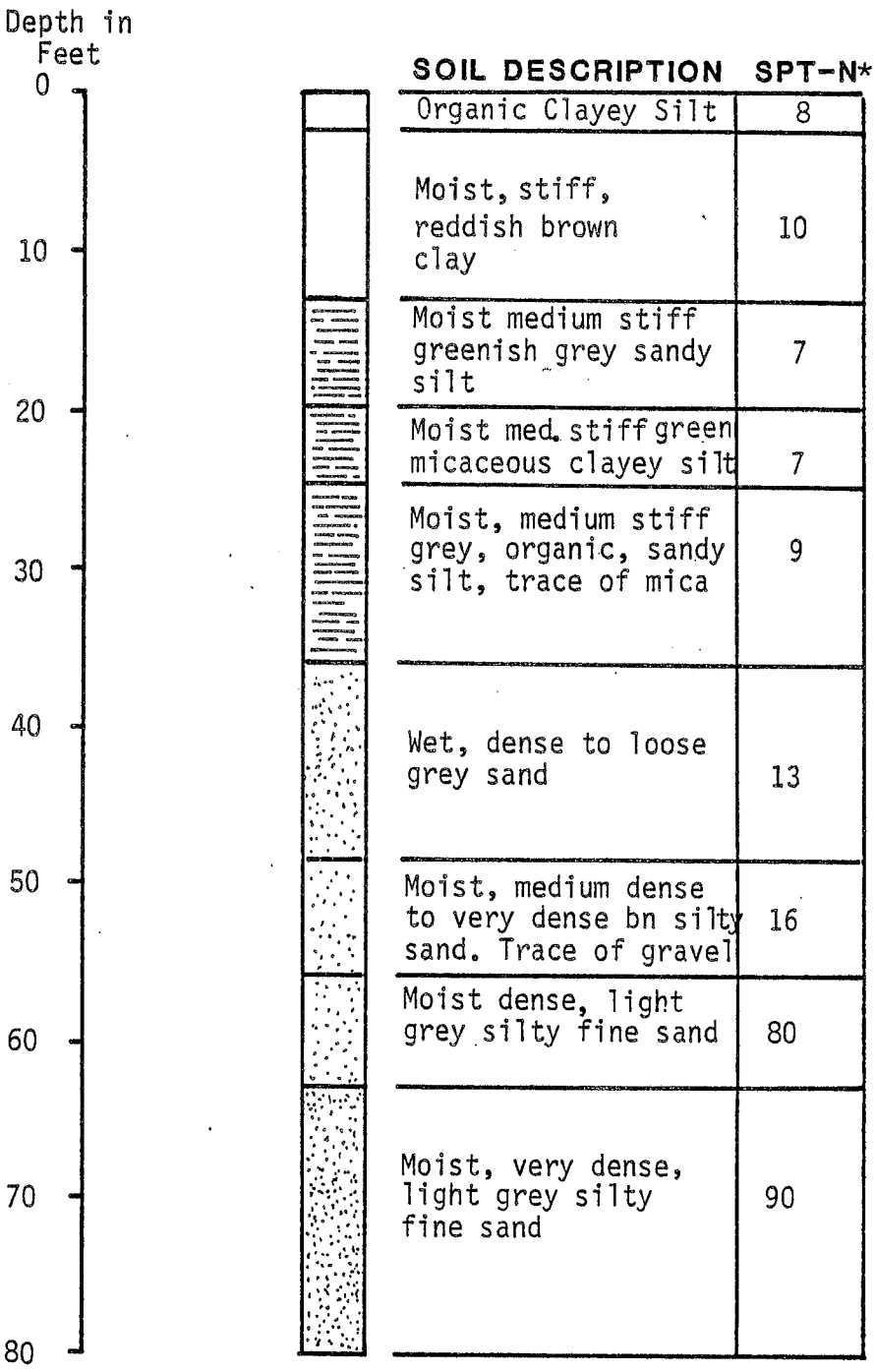

Figure 4.1: Soil Description and Standard Penetration Test Results

*Blow count "N" in Blows/foot

1 ft = .3048 m

of depth in Figure 4.2. Blow count and operating speed for the diesel hammer are both output by the WEAP wave equation program (Figure 4.4). Combining the predicted blow counts with the hammer operating speeds allowed the pile penetration rates for both hammer types to be computed (see Figures 4.3 and 4.5). It was assumed that air/steam hammers would operate at a steady 60 blows per minute, so that total driving time could be calculated. This is not exactly correct since they operate somewhat slower in easy driving. For diesel hammers, the WEAP program predicted the blow rate.

For the diesel hammers, an additional complication occurs since it is necessary to estimate the penetration at which the hammer will first operate. When the soil resistance is very low and the pile has a low mass (such as for this steel pile), the penetration per blow will be so large under the startup hammer blow that insufficient ram stroke will be generated to provide adequate scavenging. The hammer will not run continously and it is operated almost like a drop hammer. When adequate resistance is developed to produce a stroke of about 3.8 feet (1.15 m), the hammer will operate continuously.

In order to compute this resistance, wave equation analyses were performed using the WEAP program, and stroke was obtained in addition to blow count and driving stresses. Successive wave equation runs were made with increasing resistance until a stroke in excess of 3.8 feet (1.15 m) was achieved. In that portion of the driving record for which strokes of less than 3.8 feet (1.15 m) was predicted, it was assumed that the hammer would operate at a speed of six blows per minute as the crane has to lift the ram for each blow. When the predicted stroke exceeded 3.8 feet (1.15 m), the hammer was assumed to run and the operating speed was taken from the WEAP output.

This calculation is probably excessively conservative, since if the hammer fires once, more than a single blow will be achieved as the hammer "bounces down". The analysis presented here is at least a crude attempt to analyze this performance. The predicted productivity should be correlated with actual field performance.

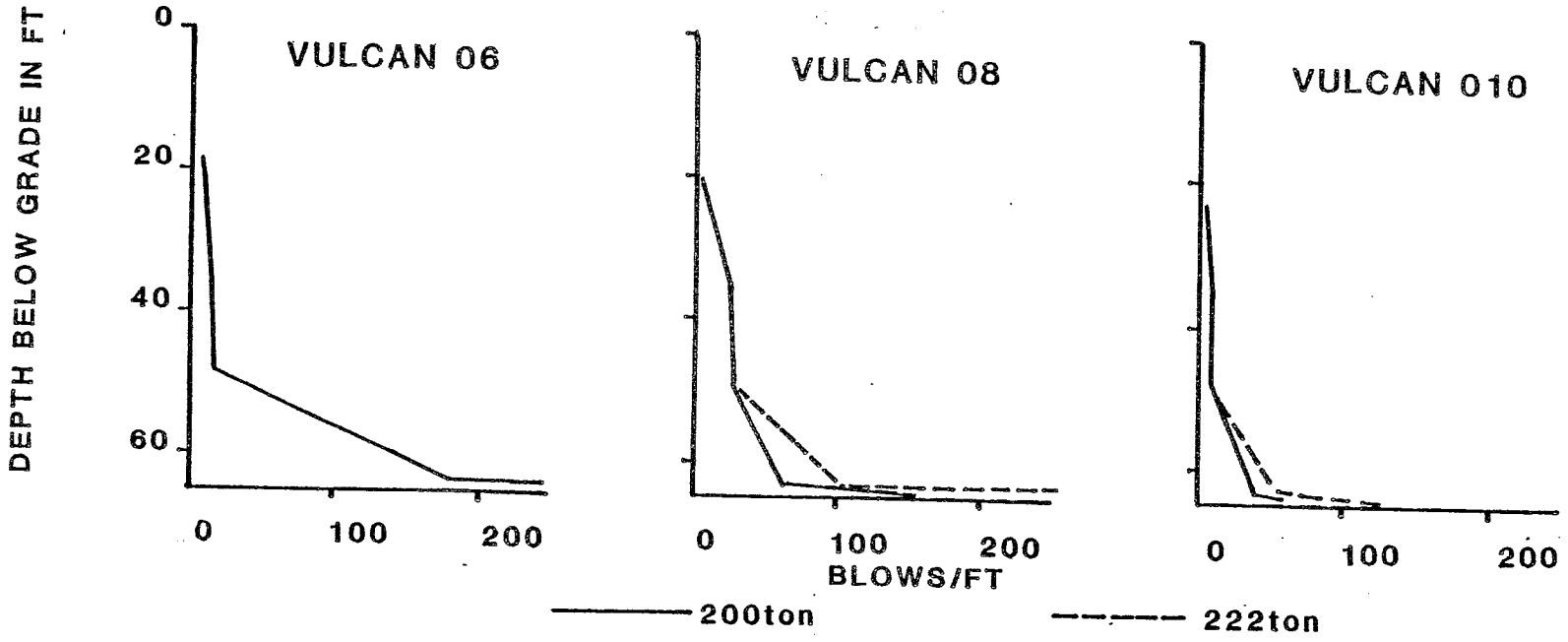

Figure 4.2: Predicted Driving Records for the Air/Steam Hammers

1 ton = 9 KN, 1 ft = .3048 m

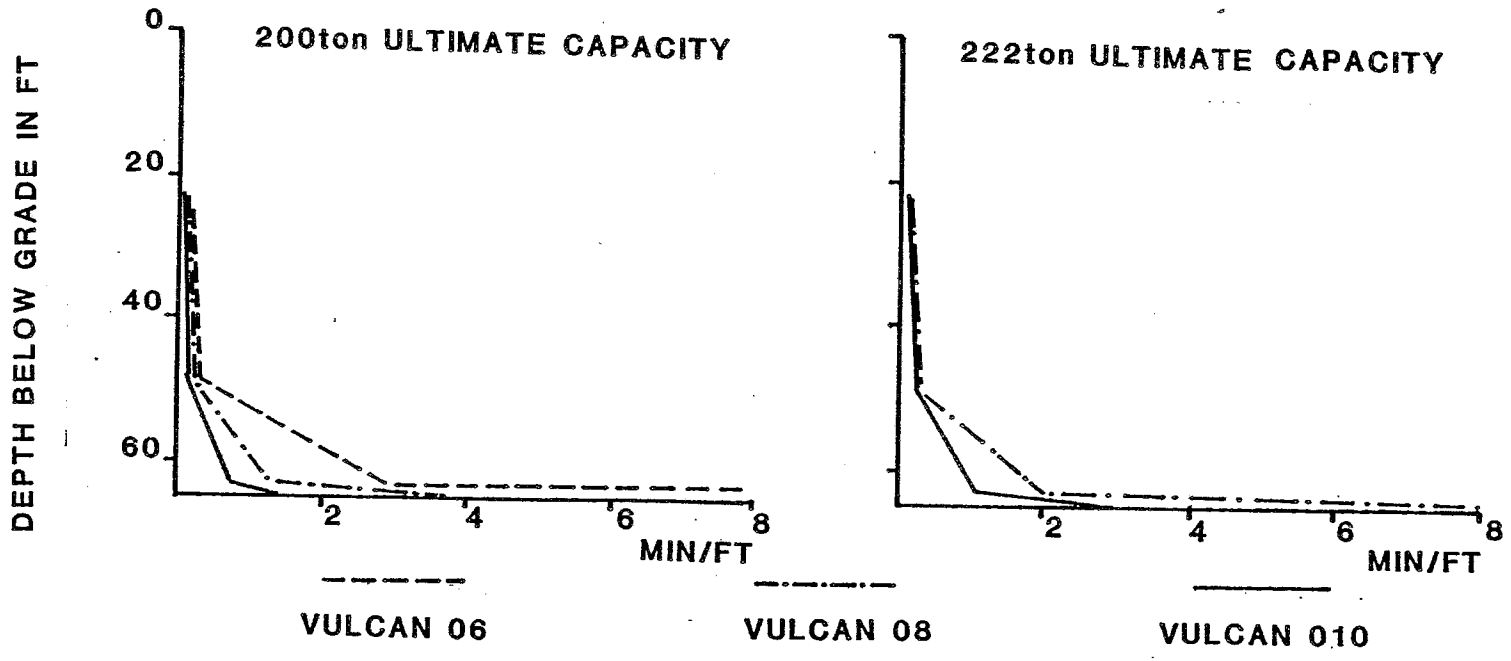

Figure 4.3: Rate of Pile Penetration for Air/Steam Hammers
1 ton = 9 KN, 1 ft = .3048 m

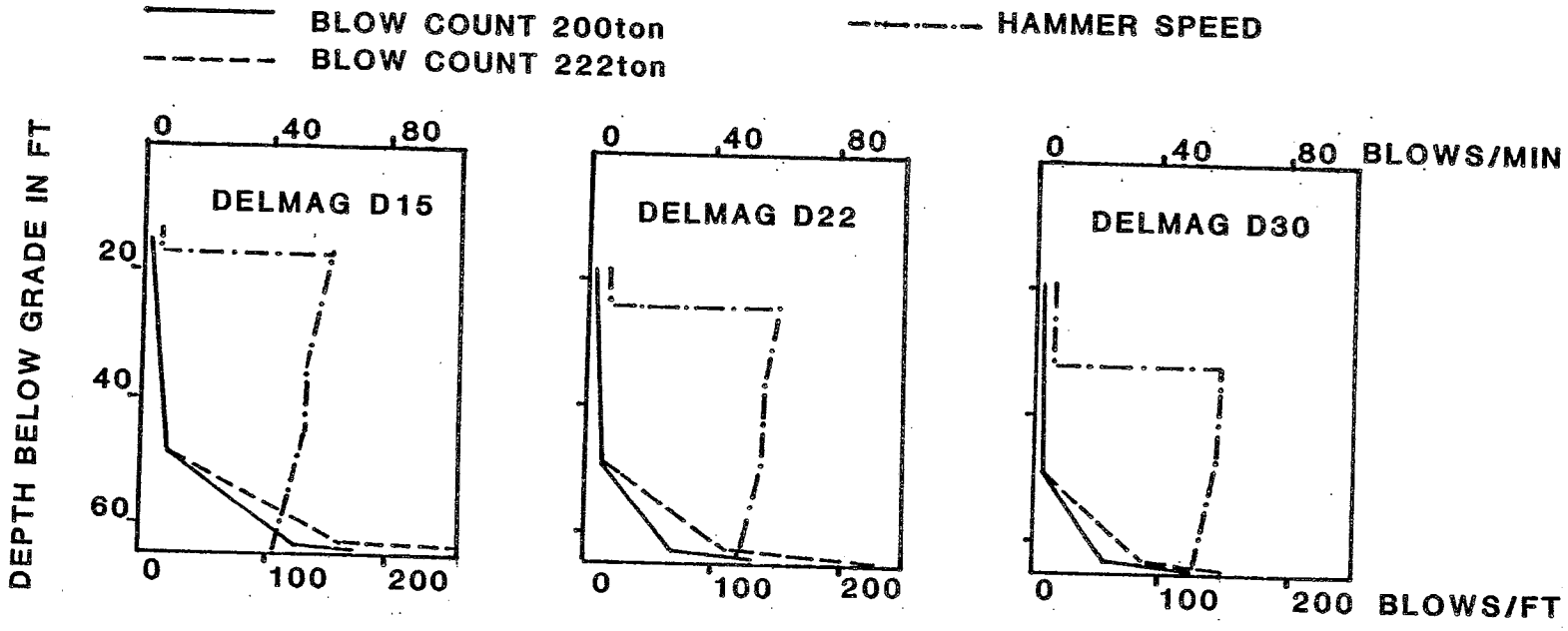

Figure 4.4: Predicted Driving Records for the Diesel Hammer; Hammer Setting - 1 (max) where not indicated.

1 foot = .3048 m
1 ton = 9 KN

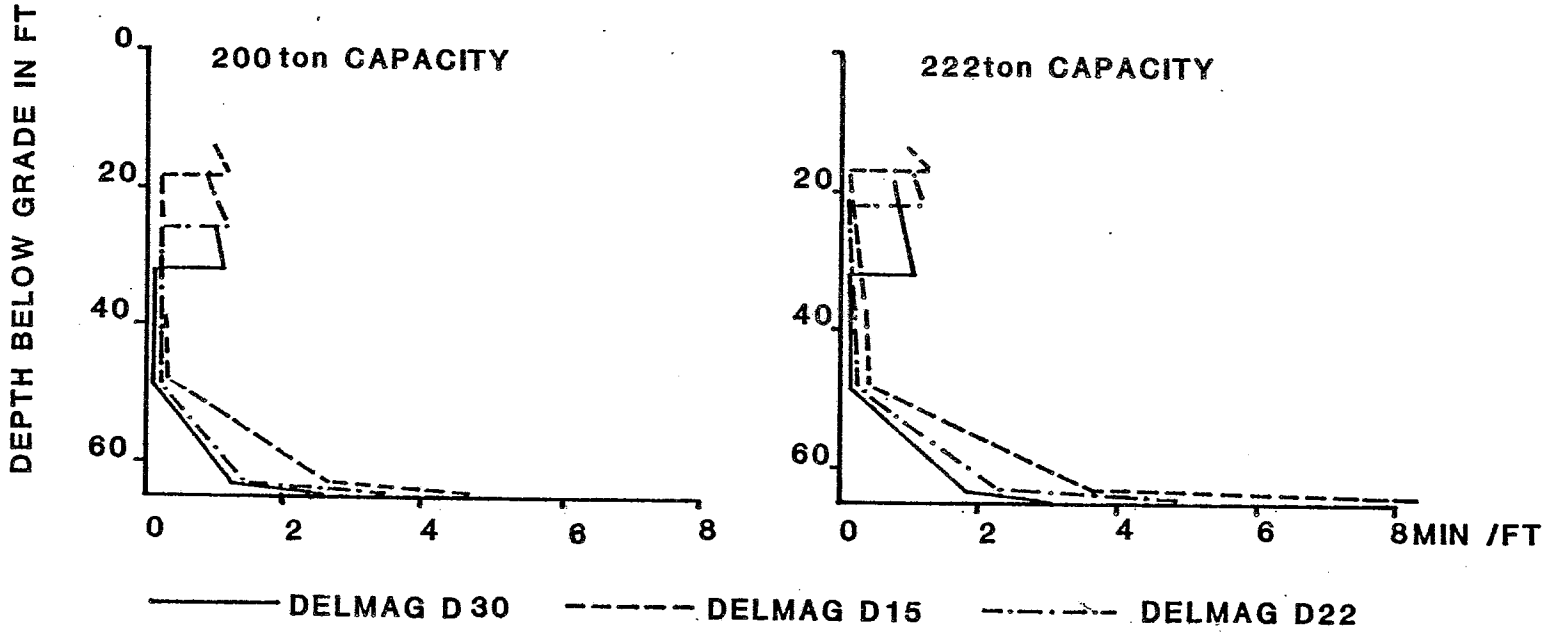

Figure 4.5: Rate of Pile Penetration for Diesel Hammers.

1 foot = .3048 m
1 ton = 9 KN

Below the depth at which the hammer begins to operate, the analysis was identical to the analysis for the air/steam system. The program, however, in addition to determining blow count, determined stroke and operating speed. Stroke and operating speed are inversely related. In general, an increasing resistance produces higher strokes, and therefore, slower operating speeds (Figure 4.4).

Stresses were also checked in each diesel analysis. A stress of 34 ksi was used as the allowable dynamic stress. If this allowable stress was exceeded, the hammer setting was reduced by one setting for the diesel hammers and the analysis was repeated. These are WEAP "hammer settings" which may not correspond to actual fuel pump stops. To obtain rate of penetration, the speed of operation was divided by the blow count, giving a rate of penetration in feet per minute.

Using Figures 4.3 and 4.5, the time required to drive a pile was computed from the areas under each curve. In this way, for each hammer, and for both 200 (1800 kN) and 222 tons (2010 kN) capacities, installation times were obtained and are summarized in Table 4.1. From these installation times, the production rate per day can be determined for each hammer. It should be noted that the Vulcan 06 cannot drive the pile to the 222 ton (2010 kN) capacity according to this analysis, but it can achieve 200 tons (1800 kN) at high blow counts.

Since the start-up time for diesel hammers is not very reliable, and, in fact, experience suggests that, for the soil profile shown, the hammer would start immediately, a productivity assuming immediate start-up was also calculated. These results are also given in Table 4.1.

The cost calculations are summarized in Table 4.2 using the productivity based on the calculated starting times for diesel hammers. If the starting time is not included (since its calculation is questionable), some substantial changes in costs result. Using this assumption, the resulting costs are summarized in Table 4.3. Both tables are based on an effective seven hour day.

Table 4.1: Breakdown of Operating Time in Minutes per Pile

Hammer	Dead Time	200 ton (1800 kN) pile				222 ton (2010 kN) pile			
		Start Time	Driving Time	Total Time w/Startup	Total Time w/o Startup	Start Time	Driving Time	Total Time w/Startup	Total Time w/o Startup
V-06	10	0.0	84.1	94.1	94.1	0.0	inf*	inf*	inf
V-08	10	0.0	21.6	31.6	31.6	0.0	45.0	55.0	55.0
V-10	10	0.0	13.3	23.3	23.3	0.0	18.4	28.4	28.4
D-15	10	3.8	35.5	49.3	45.5	3.3	51.8	65.1	61.8
D-22	10	7.5	19.3	36.8	29.3	5.5	30.0	45.5	40.0
D-30	10	7.1	14.5	31.6	24.5	12.6	22.2	44.8	32.2

*infinite

Table 4.2: Example Problem Cost Summary with Calculated Diesel Start-up Time

Hammer type	Labor Cost Per Day	Crane Rental Cost for Day	Driving System* Rental Cost For Day	Total Cost Per Day	Productivity	Cost Per Pile	Cost Per Foot
	$	$	$	$	Piles/day	$	$
V-06	1600	225	200	2025	4.5 (0)**	450	6.92
V-08	1600	250	282	2132	13.3 (7.6)	160 (280)	2.47 (4.31)
V- 010	1600	275	325	2200	18.0 (14.8)	122 (148)	1.88 (2.29)
D-15	1400	225	223	1848	8.5 (6.5)	217 (284)	3.34 (4.37)
D-22	1400	250	296	1946	11.4 (9.2)	170 (212)	2.63 (3.25)
D-30	1400	250	334	1984	13.3 (9.4)	149 (211)	2.29 (3.25)

* Driving system refers to hammer, helmet, leads and for air/steam hammers to compressor.

** Cost estimates above are based on a 200-ton (1810 kN) pile capacity and numbers in parentheses are based on 222 tons (2010 kN) pile capacity.

Table 4.3: Example Problem Cost Summary Neglecting Diesel Start-Up Time

1 foot = 0.3048 m

Hammers Types	Cost Per Day $	Productivity Piles/Day	Cost Per Pile $	Cost Per Foot $
V-06	2025	4.5 (0)*	450	6.92
V-08	2132	13.3 (7.6)	160 (280)	2.47 (4.31)
V-010	2200	18.0 (14.8)	122 (148)	1.88 (2.29)
D-15	1848	9.2 (6.8)	200 272	3.09 (4.18)
D-22	1946	14.3 (10.5)	136 (185)	2.09 (2.85)
D-30	1984	17.1 (13.0)	116 153	1.79 2.34

* Cost estimates above are based on a 200-ton (1810 kN) pile capacity and numbers in parentheses are based on 222 tons (2010 kN) pile capacity.

Cost calculations in these tables are conveniently divided into two parts: equipment costs and labor costs. Only the most approximate numbers were used for labor costs. A crew was assumed to consist of one foreman, four pile drivers, and one crane operator, with one oiler for diesel hammers, and with two oilers for air/steam hammers. Labor costs were estimated to include the contractor's total labor cost. In particular locations, it is possible to determine labor cost with a high level of accuracy.

Approximate equipment rental costs were obtained from PACO of Seattle, Washington. These costs are the rental rates on a hammer, helmet, 85 feet (26 m) of leads, a crane and a compressor. The required crane size depends on the operating radius and no attempt was made to specify that. Rather, a crane was selected to match typical requirements.

4.4 Discussion and Conclusions

The purpose of this chapter was to describe and illustrate a rational procedure for pile driving equipment selection. While the wave equation sometimes produces inaccurate results, it is surely an improvement over a contractor's guess, unless he has a great deal of experience with very similar sites. The solutions must be used with care, tempered by experience, if available. They depend on a reliable static soil analysis and it can be quite misleading for cases where high blow counts are combined with relatively small errors in the soil analysis. For example, the analysis of the Vulcan 06 indicates that the pile can be driven to depth if it has a 200 ton (1800 kN) ultimate capacity, but if the capacity is only 10 percent higher, the pile cannot be driven.

A weakness of the open-end diesel hammer is illustrated in the difficulty of starting in very easy driving. The analysis presented here is unproven by application to specific examples of field observations, and may be very conservative. A reliable analysis procedure must be developed and proven by field data.

The costs will be very sensitive to required crane radius. Due to the greater weight of the air/steam hammer, they will increase in cost more rapidly with increased working radius than for the diesel hammers.

No overhead was included in the illustrative cost computation. Since it is surely greater on labor than on equipment rental, this will also increase the cost of the air/steam systems relative to the diesel systems.

The purpose of this presentation was to describe a procedure. It must be used and tested if it is to become an effective tool.

5. METHODS OF MEASURING DRIVING SYSTEM PERFORMANCE OR EFFICIENCY

The measurement of hammer performance is relatively new if the very basic visual observation of ram motion is excluded. The accurate determination of hammer performance requires modern measurement techniques.

The objective of driving system performance measurements is to determine the following three parameters:

(a) Ram impact velocity
(b) Energy losses in the driving system
(c) Stiffness of the driving system

For the relatively simple case of ASH hammers, these three quantities are related to the wave equation input parameters: hammer efficiency, cushion coefficient of restitution and capblock stiffness. These three quantities are sufficient to accurately model the performance of a simple hammer and driving system. For diesel hammers, additional thermodynamic parameters like combustion delay and maximum pressure need to be measured.

The ram impact velocity may be measured directly, whereas the driving system parameters can only be deduced from measurements within that system or at the pile top. These measurements are called indirect measurements.

This chapter describes the methods currently employed to calulate hammer efficiency and driving system parameters from indirect measurements. Since many of these methods are proprietary, and were not fully documented in the literature, a strict mathematical derivation or discussion of these methods is not possible. Instead, it is attempted to explain how these methods are actually used. A similar description, but with greater emphasis on the measurement techniques, including direct methods, is given in the Volume II.

5.1 Terminology

Consistent with the current state-of-the-art, the following terminology is often used.

(a) ENTHRU is the maximum energy transferred to the pile top per blow, also called E_t and E_{max} (see also Section 5.2 and Eq. 5.1 following).

(b) Hammer Efficiency, e_h, is defined differently for ASH and diesel hammers. For ASH it is the ratio of kinetic energy just before impact to rated energy (E_r). Thus, for a determination of hammer efficiency, the ram impact velocity must be known. If the hammer efficiency was calculated using an indirectly determined kinetic energy, E_k, (and, therefore, containing either measurement or calculation errors, or both) then the resulting ratio is called e_{kr}, (E_k/E_r). For diesel hammers, e_h denotes efficiencies associated with the ram travel prior to passing the exhaust ports; this is also a wave equation input.

(c) Driving System pertains to all components between the bottom of the ram and the top of the pile. Most commonly the driving system includes a striker plate, a hammer and a cushion. The helmet often includes a pile top adaptor. For concrete piles, a pile top cushion is also part of the driving system.

(d) Driving System Efficiency (or Actual Transfer Efficiency) means the ratio of the energy passed to the pile by the driving system, compared with the energy applied to it by the ram. This ratio may be computed by dividing the transferred energy by the kinetic ram energy just before impact, both calculated from pile top measurements. This ratio is denoted by e_{tk} (E_t/E_k). Determination of this ratio is limited to ASH at present.

(e) Transfer Efficiency (or better Transfer Ratio) is similar to Driving System Efficiency. Two definitions are of interest. The first one divides ENTHRU by the rated hammer energy and is therefore called the

rated transfer efficiency, e_{tr}. It is applicable to any hammer type. The second definition was necessary because of the stroke variability of diesel hammers. Dividing ENTHRU by the product of ram weight and actual stroke, one obtains the actual transfer efficiency, e_{ta}. This latter definition is also useful for ASH hammers that are operated with a reduced stroke.

(f) The term performance does not relate to a physical quantity. It is used to qualify, rather than to quantify, the actual component behavior against the expected behavior.

5.2 Direct Measurement Methods

Various direct or indirect measurement techniques have been or are being developed in an attempt to increase the precision of wave equation predictions.

For ASH hammers, direct measurements of impact velocity have been attempted or are being made by means of:

(a) An optical displacement transducer (MENCK)

(b) The blocking of one or two light beams by the moving ram over a known distance (Case, Fugro)

(c) Radar (McClelland, Pile Dynamics)

(d) Digital displacement transducer (MENCK)

For open-end diesel hammers, Goble Rausche Likins and Associates, Inc. have attempted a direct ram velocity measurement using a rotary potentiometer. Both Delmag and Pile Dynamics have also used radar velocity measurement. Other direct measurement methods are unknown for this hammer type.

Direct measurement of ram impact velocity does not provide information regarding the driving system's efficiency, a very important disadvantage. At present, these methods are primarily experimental attempts to provide for an immediate determination of hammer efficiency. Thus, as opposed to indirect methods, they do not require data analysis. These methods are further discussed in the Volume II.

5.3 Indirect Measurement Methods

Several analytical methods exist that compute ram motion and driving system parameters from indirect measurements. For convenience, measurements are usually taken at the pile top. The analysis often involves a considerable amount of computation and a few restrictive assumptions. The assumptions may reduce the general applicability of the methods, or they may lead to erroneous results.

5.3.1 The Case Method Hammer Performance Computations

This method was developed in the 1960's together with the Case Method of pile bearing capacity determination from dynamic measurements. Appendix B5 shows how the energy transferred into the pile may be calculated as the integral of the product of pile top force and velocity.

$$E(t) = \int_0^t F(\bar{t})v(\bar{t})d\bar{t} \qquad (5.1)$$

The maximum value of the resulting energy vs time curve was called ENTHRU in a similar study performed by the Michigan Highway Commission.

An extension of this method is the momentum approach which integrates the pile top force until the time of zero pile top velocity, t_o.

$$I(t_o) = \int_0^{t_o} F(t)dt \qquad (5.2)$$

The ram impact velocity is then

$$v_{ri} = I(t_o)/m_r \qquad (5.3)$$

This method gives accurate ram impact velocity results for certain hammer and pile types. Recent extensions of the method are presented in Volume III which allow for the direct computation of load deflection characteristics of hammer and pile cushions. Best results are obtained from data on steel piles under ASH hammers. A thorough development of these momentum based concepts is presented in Appendix B5.

5.3.2 The DMS Method

This method is based on the measurement of pile top force. The pile top force record is then analyzed with respect to rise time, maximum pile top force, and the time between the first and second force peaks. Figure 5.1 illustrates the defintion of these three quantities. The DMS Method requires that a family of curves be produced using a wave equation analysis. By matching measured with computed rise times, maximum pile top force, and the peak-to-peak time, the following three quantities are found.

(a) Ram impact velocity
(b) Hammer cushion
(c) Coefficient of restitution of hammer cushion

The method may result in a satisfactory set of answers for hammer efficiency and driving system performance parameters. Obviously, this set of parameters and the process of calculation are appropriate only for air/steam/-hydraulic hammers on steel piles.

A sample case of an ASH hammer on a steel pile was investigated by the DMS Method for this report. Details of the hammer and driving system are given in Appendix C, parts C1 and C2, under ID No. 84. The pile in this case was a 490 feet (149.35 m) long offshore pile, and the mudline was at 270 feet. Because of these circumstances, force and velocity records did not contain

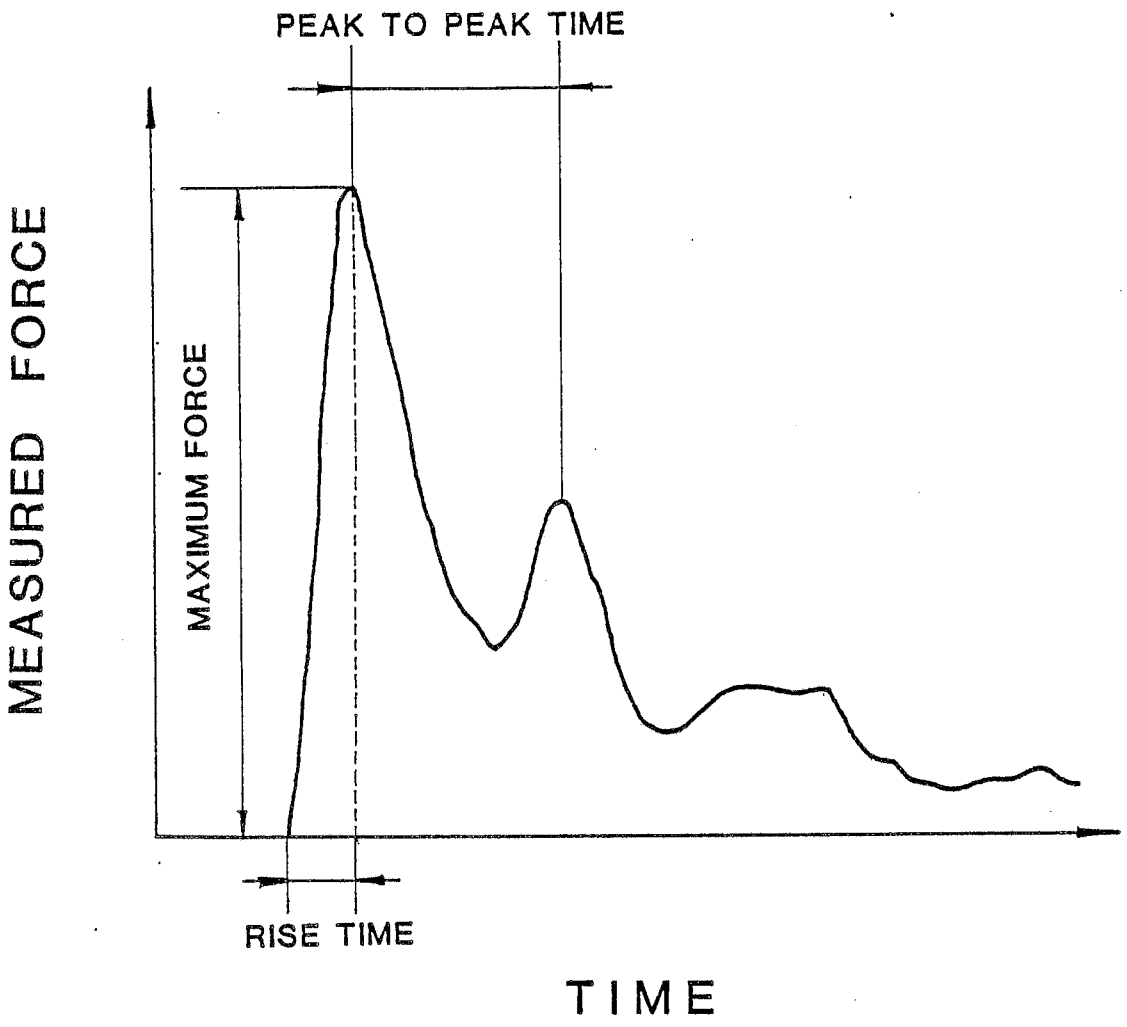

Figure 5.1: Definition of Measurements Used in the DMS Method

resistance reflections until at least 16 milliseconds after impact. Absence of such resistance reflections facilitated application of the DMS method, because unknown soil parameters were not required to simulate the early portions of the record.

To obtain data points required for the DMS method, a series of 51 wave equation simulations were performed. These simulations were run with 4 variations of the hammer cushion stiffness, k, 3 variations of the hammer cushion coefficient of restitution, c, and four or more ram impact velocities representing the hammer efficiency, e_h. Only 12 such wave equations would be required if the assumptions of the DMS method were rigorously applied. The results of these analyses were then used to construct the DMS Method curves. Figures 5.2 and 5.3 present the DMS Method curves obtained for this specific pile/hammer combination.

The curves of Figure 5.2 and 5.3 were used by entering Figure 5.2 with the rise time and peak-to-peak time determined from dynamic measurements. With a measured rise time and peak-to-peak time of 2.0 and 7.0 milliseconds, respectively, an approximate cushion stiffness of 120,000 kip/in and a coefficient of restitution of .6 were deduced. Using these two values in Figure 5.3 indicated that for a hypothetical hammer efficiency of 100 percent, a maximum pile top force, f_{100}, of 5525 kips (24.86 mn) would be expected.

An actual hammer efficiency, e_h, of .72 was then obtained from

$$e_h = (f/f_{100})^2 \tag{5.4}$$

where f is the actual dynamically measured pile top force (4690 kips) or (21.6 mn). If a ten percent uncertainty exists for both the rise time and the peak-to-peak time, then it appears that a 10 percent uncertainty exists for the hammer efficiency. If the measured force is also subject to five percent uncertainty, the net uncertainty in e_h may be as much as 15 percent.

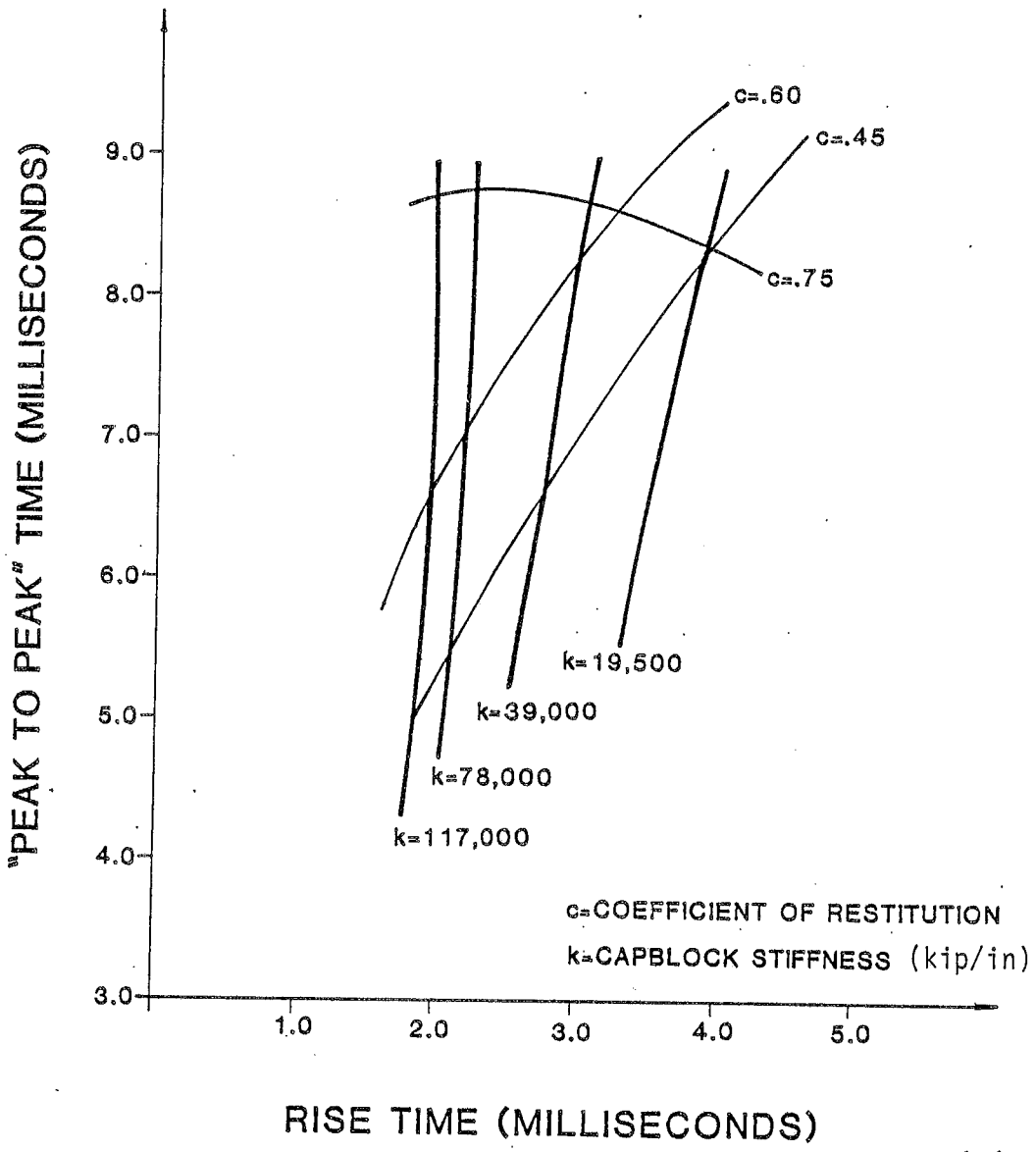

1 inch = 25.4 mm
1 kip = 4.5 KN

Figure 5.2: DMS Method Curve I

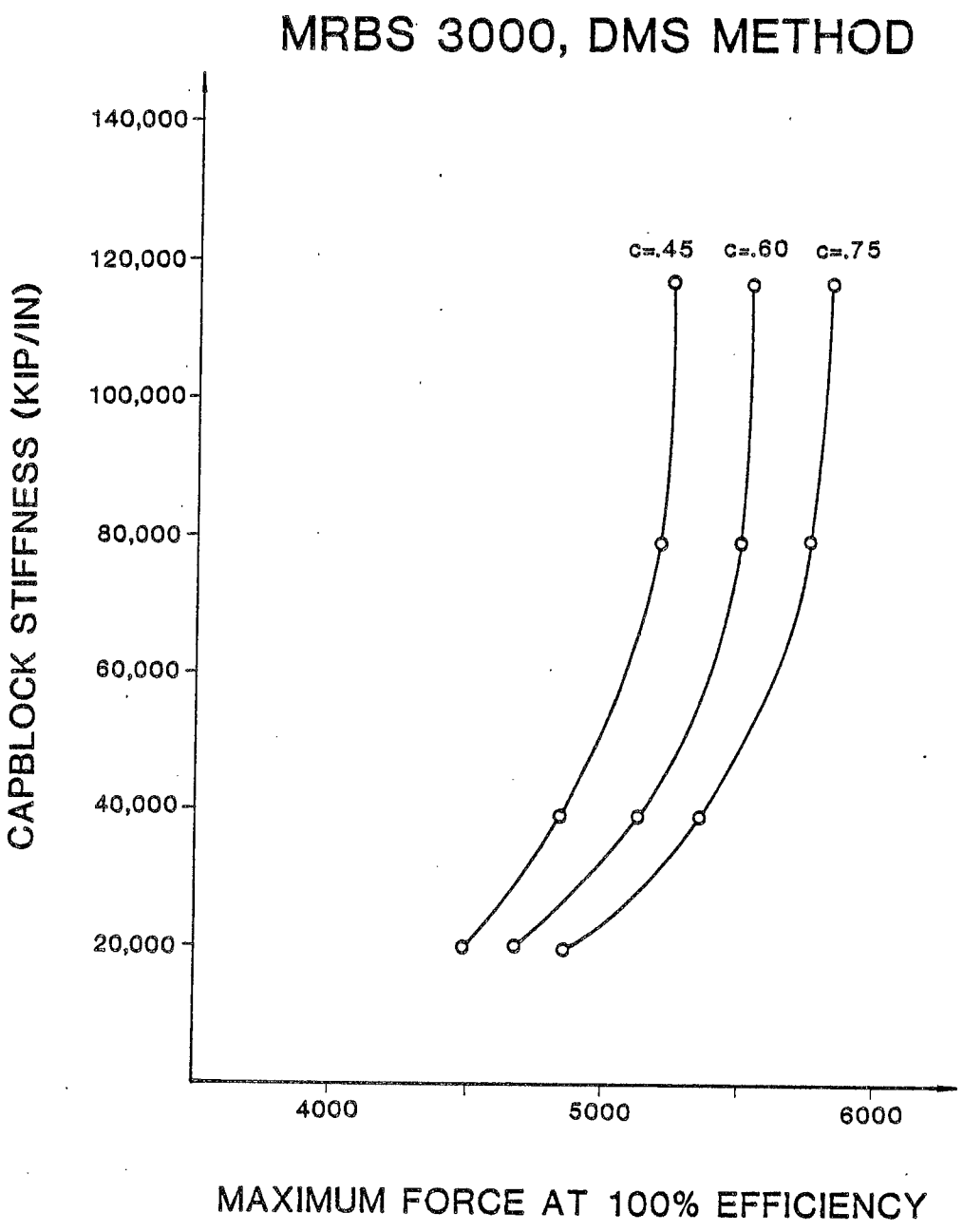

Figure 5.3: DMS Method Curves II

1 inch = 25.4 mm
1 kip = 4.5 KN

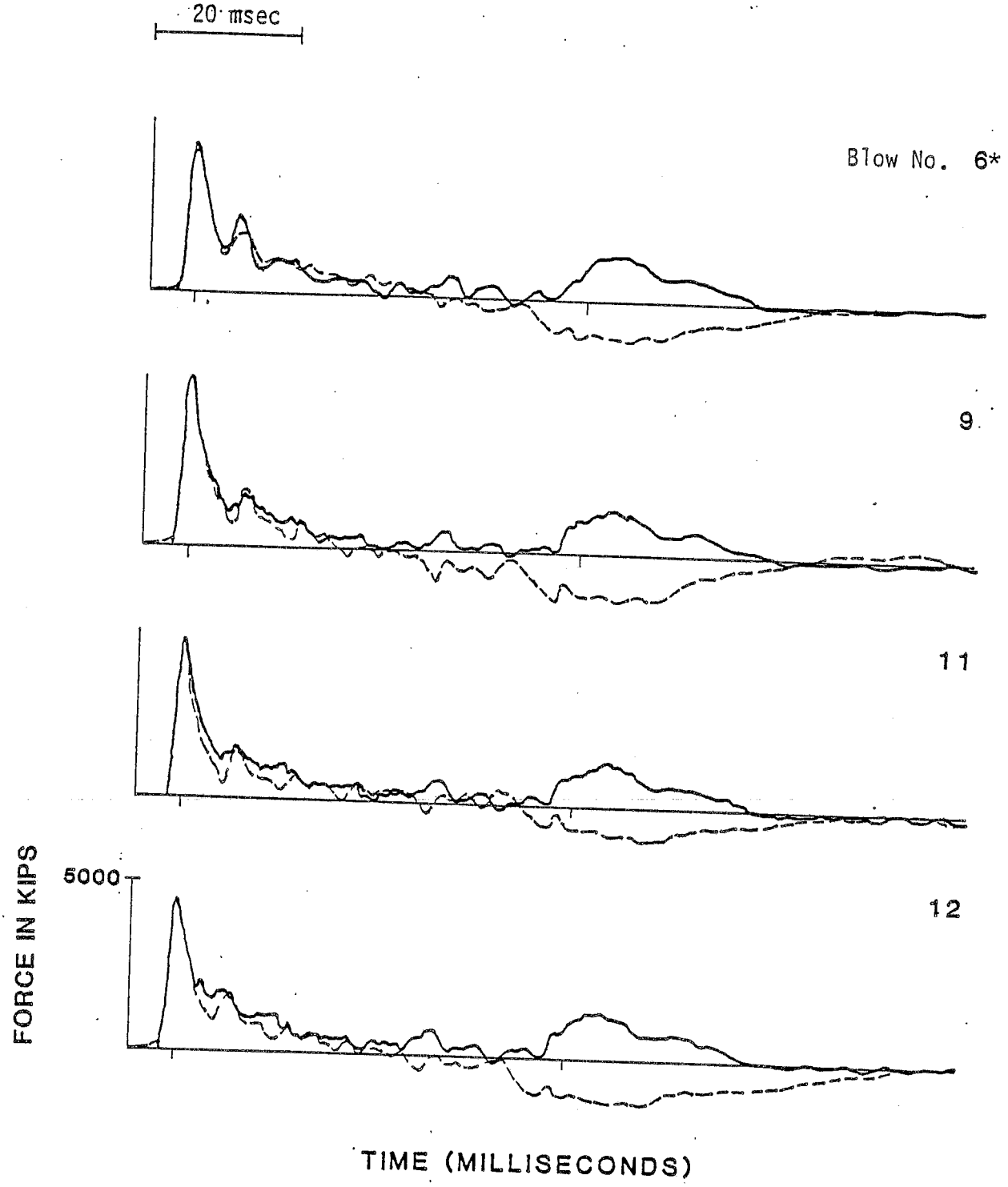

Figure 5.4: Sample Force Records Used For Application of the DMS Method

*Only record suitable for analysis by DMS Method

1 kip = 4.5 KN

Figure 5.4 presents actual measured force records for the above case. The first blow in these records indicates a well defined second force peak seven milliseconds after impact. This peak was selected for measurement of the required peak-to-peak time. The other blows in Figure 5.4 do not contain a second isolated and dominant relative force maxima. The absence of such a readily definable second peak indicated the practical difficulty of determining the peak-to-peak time. The experience of the authors suggests that the difficulty of measuring a peak-to-peak time will pose limitations on use of the DMS Method. On short piles with skin friction this method may not be applicable.

5.3.3 Other Matching Techniques

The QMC approach is very similar to the DMS approach in that it employs force measurements only, and matches these measurements using a wave equation model for the hammer. The difference is QMC's use of a minimization technique for a best fit between the measured and computed force impact pulse. Only the rise of the force and a short time after the force peak are included in the matching process. Thus, DMS includes a longer period of record time, and will possibly give a better simulation of the overall energy transfer of the driving system. On the other hand, the use of an assumed bilinear cushion stiffness and coefficient of restitution seems more reasonable if it is restricted to the time period of first loading and unloading. This period is completed when the pile top force reaches its first major maximum. (The helmet then has a zero acceleration.)

The authors have also undertaken new methods to determine impact velocities for diesel hammers using indirect measurements.

(a) Develop pile, soil and driving system models for wave equation analysis. The soil model should be based on field results using the Case Method, or, preferably, the results of a CAPWAP analysis. The driving system model should be based on the WEAP recommendations.

(b) Investigate the early portions of the force and velocity records and determine if a negative time delay for preignition cases is indicated.

(c) Analyze the system by wave equation, and match the observed hammer stroke by adjusting the maximum pressure value.

(d) Match the measured ENTHRU by adjusting the efficiency value, simultaneously match cushion stiffness and coefficient of restitution to yield a best possible agreement with the impact force value.

This procedure requires extensive computer and engineering time and cannot be recommended for routine application.

5.3.4 The Kuemmel Method

This novel approach is primarily directed towards bearing capacity calculations, but offers a few interesting suggestions regarding the evaluation of hammer performance. The author of this method is a designer of open-end diesel hammers and he concerns himself only with this hammer type. This is not necessarily a disadvantage since most other methods work reliably only for ASH hammers.

As far as hammer performance investigations are concerned, the following observations (Kuemmel, Ref. 8) are of interest:

(a) It is recommended to measure the maximum pile top force, F_{max}.

(b) In absence of measurements and for drop heights in excess of 5 ft (1.5 m), it is claimed that F_{max} is linearly related to stroke. Kuemmel gives a "rated" force value

which corresponds to the rated stroke. Thus, for any other stroke the maximum force value may be computed.

(c) The F_{max} value calculated in (b) may be reduced by a reduction factor, R_f, which depends on the properties of the hammer cushion material. A relatively complete list of R_f values is given by the author.

This approach is contrary to the usual belief that the pile top force is primarily dependent on the pile impedance. For this reason, a correlation study was made using the diesel hammer data presented in Appendix C. Figure 5.5 is a plot of the ratio of measured to rated force against cross sectional area. This plot shows that this ratio is close to one for large cross sectional pile areas, which is not surprising since test stands usually have large cross sectional areas (typically near 100 $inch^2$) (650 cm^2). However, large discrepancies between measured and rated forces are apparent for piles with smaller cross sectional areas.

It appears, therefore, that the Kuemmel approach, which suggests that a given hammer, driving system and pile combination should produce a particular impact force on the pile, may be valid for large piles such as offshore piles. Of course, the basic concept that pile force and hammer performance are related is implied in the DMS and QUC approaches.

Another idea contained in the Kuemmel approach for bearing capacity determination is that the maximum pile top displacement is related to ram impact velocity. The derivation is based on the momentum theorem and on the proportionality of pile top force and velocity:

From Equations 5.2 and 5.3

$$m_r v_{ri} = \int_o^i F(t)\, dt \qquad (5.5)$$

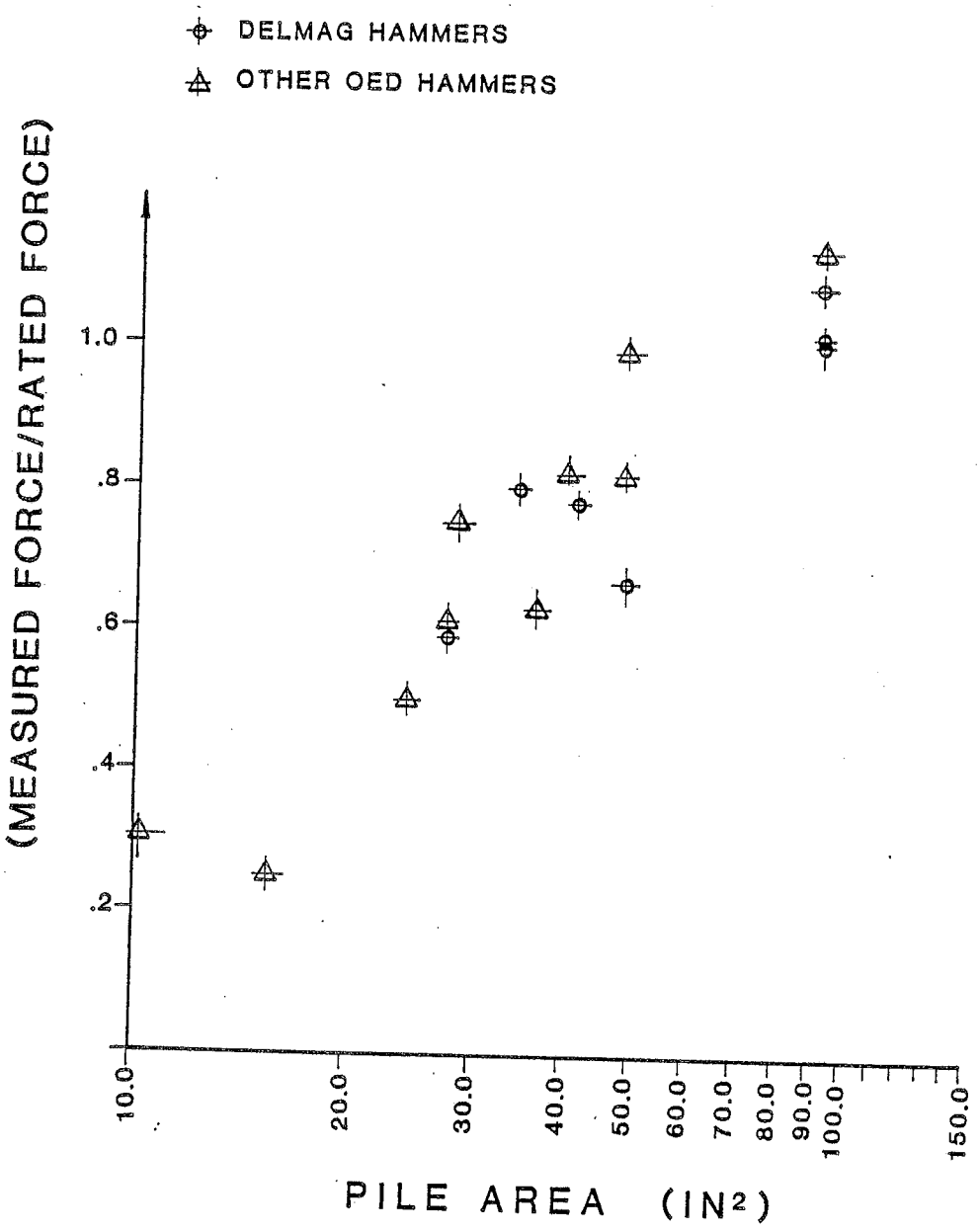

Figure 5.5: Kuemmel Method, Prediction Error vs Pile Crossectional Area

1 inch = 25.4 mm

Now, until force reflections from the soil return to the pile top,

$$F(t) = Z\, v_p(t) \tag{5.6}$$

where Z is the pile impedance, and v_p is the pile top velocity.

The integral of velocity until the time of zero velocity is the maximum pile top displacement, d_{max}. Substituting Eq. 5.6 for F(t) in Eq. 5.5. results in:

$$v_{ri} = Z.d_{max}/(m_r) \tag{5.7}$$

Based on this relationship, it is suggested that the simple measurement of the maximum pile top displacement by the set-rebound technique is sufficient for a determination of the ram impact velocity. Obviously there are limitations to this method, primarily where the velocity is integrated over long periods of time, and for nonuniform piles. In fact, Kuemmel recommends the use of the maximum pile top displacement for ram impact velocity determination only for long piles with small friction over their upper portion, such as are encountered in offshore situations.

5.4 Conclusions

The description of available systems for the investigation of hammer and driving system performance shows that there is, to date, no method available for general use on land pile. For air/steam hammers and steel land piles, the Case Method Momentum approach is useful. For offshore piles driven by ASH hammers, hammer and driving system efficiencies may be obtained from pile top force and/or velocity measurement for which proportionality usually exists.

Further conclusions are:

(a) The applicability of the DMS method may be limited since a meaningful second force maximum does not necessarily occur.

(b) Most methods require a considerable amount of computational effort.

(c) The magnitude of the maximum pile top force is strongly dependent on pile cross sectional area.

(d) The maximum pile top displacement may provide a simple hammer performance check under certain restrictive circumstances.

REFERENCES

1. Michigan State Highway Commission, "A Performance Investigation of Pile Driving Hammers and Piles," Lansing, Michigan, March 1965.

2. Goble, G.G., Scanlan, R.H., and Tomko, J.J., "Dynamic Studies on the Bearing Capacity of Piles," Phase I, Case Institute of Technology, Cleveland, Ohio, July 1967.

3. Goble, G.G., Tomko, J.J., Rausche, F., and Green, P.M., "Dynamic Studies on the Bearing Capacity of Piles," Phase II, Case Western Reserve University, Cleveland, Ohio, July 1968.

4. Goble, G.G., Rausche, F., and Moses, F., "Dynamic Studies on the Bearing Capacity of Piles," Phase III, Case Western Reserve University, Cleveland, Ohio, August 1, 1970.

5. Goble, G.G., Likins, G., and Rausche, F., "Bearing Capacity of Piles from Dynamic Measurements." Final Report, March 1975, Goble & Associates, Inc., Cleveland, Ohio.

6. Goble, G.G., Likins, G.E., Jr. and Teferra, W., "Piles & Pile Driving Hammer Performance for H-Piles Driven to Bedrock," Final Report, for the Ohio Department of Transportation and Federal Highway Administration by the Department of Civil Engineering of Case Western Reserve University, Cleveland, Ohio, November, 1977.

7. Smith, E.A.L., "Pile Driving Analysis by the Wave Equation," Journal of the Soil Mechanics and Foundations Division, Proceedings of the ASCE, Vol. 86, No. EM4, August, 1960.

8. Goble, G.G., and Rausche, F., "Wave Equation Analysis of Pile Driving WEAP Program," Prepared for the U.S. Department of Transportation, Federal Highway Administration, Implementation Division, Office of Research and Development, July 1976.

9. Rempe, D.M. and Davisson, M.T., "Performance of Diesel Pile Hammers," Proceedings of the Ninth International Conference on Soil Mechanics and Foundation Engineering, Tokyo, 1977, Vol. 2, pp. 347-354.

10. Holloway, D.M., Clough, G.W. and Vesic, A.S., "The Effects of Residual Driving Stresses on Pile Performance Under Axial Loads," Presented at the 10th Annual Offshore Technology Conference, Houston, Texas, May 8-11, 1978.

11. Matlock, H., and Foo, S.H.C., "Axial Analysis of Piles Using a Hysteretic and Degrading Soil Model," presented at the 1980 Conference on Numerical Methods in Offshore Piling, Institution of Civil Engineers, pp 127-133, London, 1980.

12. Fischer, H.C., "On Longitudinal Impact II - Elastic Impact of Bars with Cylindrical Sections of Different Diameters and of Bars with Rounded Ends," Appl. Sci. Res., Section A, Vol. 8, 1960, pp. 213-247.

13. Goble, G.G., Rausche, F., and Likins, G.E., Jr., "The Analysis of Pile Driving, A State-of-the-Art," Presented at the Seminar on the Application of Stress-Wave Theory on Piles, Royal Institute of Technology, Stockholm, Sweden, June 1980.

14. Chellis, R.D., "Pile Foundations," McGraw Hill Book Company, New York, New York, 1961.

15. Hirsch, E.J., Carr, L., and Lowery, L.L., "Pile Driving Analysis - Wave Equation Users Manual, TTI Program," Federal Highway Administration, Report No. FHWA-IP-76-13.3, Washington, D.C., April 1976.

16. Likins, G.E., Jr., "Pile Installation Difficulties in High Rebound Soils", presented at the ASCE Conference, Philadelphia, Pennsylvania, May 16-20, 1983.

17. Goble, G.G., and Rausche, F., 1976: "Wave Equation Analysis of Pile Driving, WEAP Program," Vol. 1 - Background, Vol. 2 - User's Manual, Vol. 3 - Program Documentation, U.S. Department of Transportation, FHWA, Office of Research and Development, Implementation Package, 76-14.1, Washington, D.C., 1981.

18. Kuemmel, F. "Wave Equations," Technical Proc. Delmag #ZRE 02014-2, Esslinggen, W. Germany, April 1983

19. Tavenas, F.A. and Audibert, J.M.E., "Application of the Wave Equation Analysis to Friction Piles in Sand", Canadian Geotechnical Journal, Volume 14, 1977, pp. 34-51.

20. Deep Foundations Institute, "A Pile Inspectors Guide to Hammers," The Deep Foundation Institute, P.O. Box 359, Springfield, N.J., 07081, 1979.

21. Hunt, Hal W., "Design & Installation of Driven Pile Foundations," Associated Pile and Fitting Corporation, 1980.

22. Fuller, Frank M., "Engineering of Pile Installation," McGraw-Hill Book Company, 1983.

23. Likins, G.E., Jr., "Evaluating the Performance of Pile Driving Hammers", presented at the PDA Users Day Seminar, Amsterdam, Holland,May 1982.

24. Fischer, H.C., "On Longitudinal Impact I - Fundamental Cases of One-Dimensional Elastic Impact Theories and Experiments," Appl. Sci. Res., Section A, Vol. 8, 1960, pp. 105-139.

APPENDIX A

PART A1: Wave Propagation Theory

PART A2: Stress-Velocity Proportionality

PART A3: Reflections From Ends of Semi-Infinite Rods

PART A4: Application of a Force at a Point along a Rod

PART A5: Impact of a Rigid Mass with an Elastic Rod

APPENDIX A

A1. Wave Propagation Theory

If a disturbance is induced in a slender rod, a stress wave is generated. The normal assumption is that the rod material is linearly elastic with a modulus of elasticity, E, and a mass density, rho. As shown in Figure A1, longitudinal position on the rod is designated by the variable, x, and the displacement of a point on the rod is given as u. One dimensional wave propagation implies that all points on a given cross section displace by the same amount, u(x).

If a free body diagram is taken at a point on the rod as the disturbance is passing, the equation of motion (Newton's Second Law) leads to:

$$E\, u_{xx} = \text{rho}\ a \qquad \text{(A1)}$$

where u_{xx} is the second partial derivative of the displacement u with respect to x and u" the second partial derivative of the displacement with respect to time.

This expression is commonly written as

$$a = c^2\, u_{xx} \qquad \text{(A2)}$$

where $c^2 = E/\text{rho}$.

The solution to this equation is

$$u(x,t) = f(x + ct) + g(x - ct) \qquad \text{(A3)}$$

where f and g are each arbitrary functions.

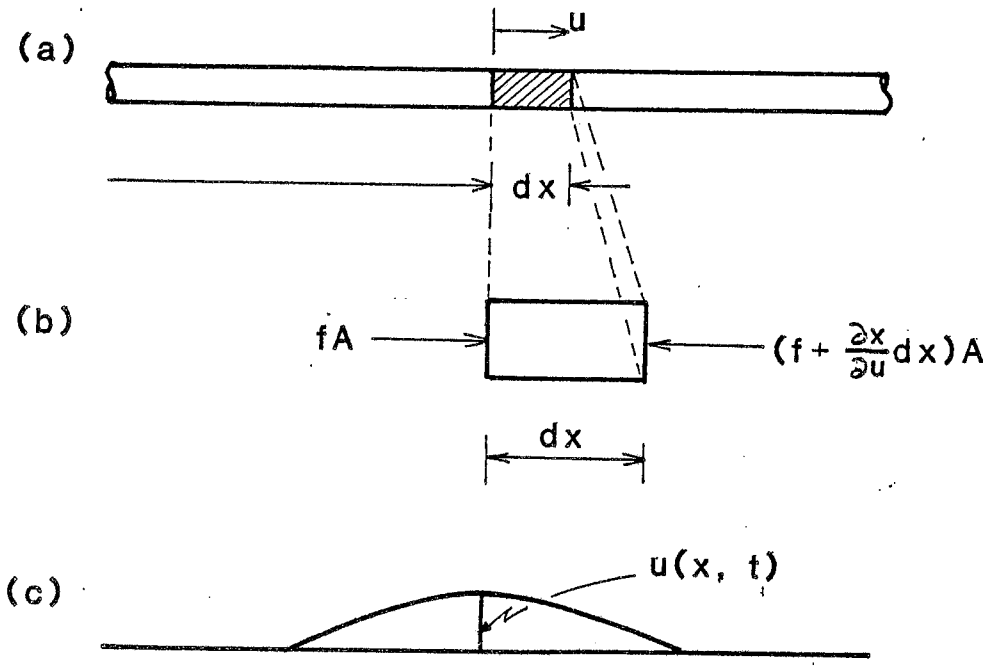

Figure A1: (a) Elastic Rod with Element of Length, dx; (b) Free Body Element During the Passage of a Stress Wave, Subjected to (forces) Stress (f) times Cross Sectional Area, A; (c) Displacement Variation in Rod at a time t_1.

Now examine part of the above solution

$$u = g(x - ct)$$

In Figure A2(a) an assumed function g is shown at a time t_1. The function is shown at a later time t_2 in Figure A2(b). At t_1

$$u(x_1,t_1) = g(x_1 - ct_1)$$

and at t_2

$$u(x_2,t_2) = g(x_2 - ct_2)$$

If at time t_2 the position of the wave is $x_2 = x_1 + c(t_2 - t_1)$ then

$$u(x_2,t_2) = g(x_1 + c(t_2 - t_1) - ct_2)$$

and thus

$$u(x_2,t_2) = g(x_1 - ct_1)$$

Therefore, it can be concluded that the function g(x - ct) represents a wave shape traveling in the x-direction. That the wave is unchanged as it travels along the rod at a speed c equal to $(E/rho)^{1/2}$. The velocity of wave propagation, c is only a material property, and is in no way related to the nature of the impact, within the assumption of elastic material behavior.

The other part of the solution f(x + ct) is a wave traveling in the negative x direction.

A2. Stress-Velocity Proportionality

If a uniform stress is suddenly applied to the end of a semi-infinite rod, a compression wave is induced in the rod. The rod is deformed by the

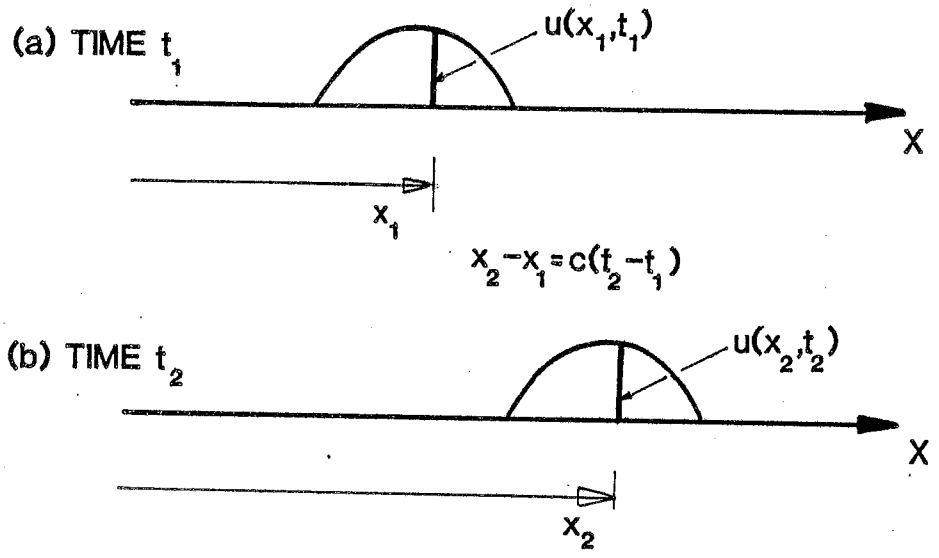

Figure A2: Traveling Displacement Wave at times t_1 and t_2. Wave Moved a Distance $c(t_2 - t_1) = x_2 - x_1$.

compression stresses as illustrated in Figure A3. At time t1 the stress wave has traveled a distance x along the rod, just arriving at point p. A small time, dt, is allowed to elapse during which the wave front travels a distance (c dt), as shown in Figure A3. The stress in this distance (c dt) causes the point p to displace by some amount, du. The velocity of motion of p is

$$du/dt = v$$

The displacement, du, of point p can be computed from the stress f in the rod.

$$du = \frac{f(c\ dt)}{E}$$

Combining the above two expressions yields

$$v = c(f/E)$$

or

$$f = v\ (E/c) \qquad (A4)$$

The associated relationships, in terms of strain (eps)

$$eps = v/c \qquad (A5)$$

and in terms of force (using the cross sectional area, A)

$$F = v\ (EA/c) \qquad (A6)$$

are also frequently used.

These three relationships are very important in pile driving analysis. They show that there is proportionality between force (stress or strain) and

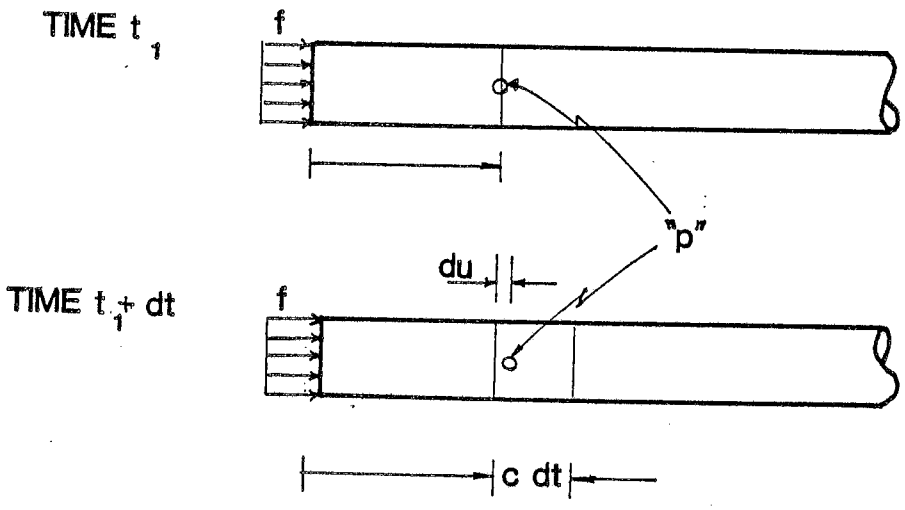

Figure A3: Displacement Increment, du, Caused by Passage of Stress Wave During Time Interval, dt.

velocity during the propagation of a stress wave in one direction in an elastic rod. This condition is of great value in evaluating pile driving measurements.

A3. Reflections From Ends of Semi-Infinite Rods

The influence of the end of a semi-infinite rod can be dealt with by superposition of multiple waves in infinite rods. Consider the case shown in Figure A4(a). In the sign convention, compression stresses and particle velocities to the right are considered to be positive. The arrows indicate the direction of wave propogation. Thus, the two stress waves shown are approaching each other. Since they are compression waves, the particle motion is in the same direction as the wave propagation. Thus, by the sign convention, the rightward traveling wave has both positive stress and velocity. For the leftward traveling wave, the stress is positive, but the velocity is negative.

Since the differential equation governing wave propagation is linear, the waves can be superimposed. The stress and particle velocity state at the instant that the two waves are centered with respect to each other, is shown in Figure A4(b). Finally, after the two waves have passed each other, they continue undisturbed, as shown in Figure A4(c).

Now, consider another case. In Figure A5(a) stress waves with identical magnitude and length approach each other. In Figure A5(b) the two stress waves are exactly superimposed. At this instant the stresses in the rod are equal to twice the magnitude of the individual stress waves. Likewise, the particle velocity superimposes and in this case sums to zero. The stresses have doubled, but all motion has ceased! As before, the two stress waves then travel apart unchanged.

This case is identical with a fixed ended rod. A stress wave arriving at the fixed end will reflect back on itself with the same sign while motion stops (thus satisfying the boundary condition). The stress wave then reflects

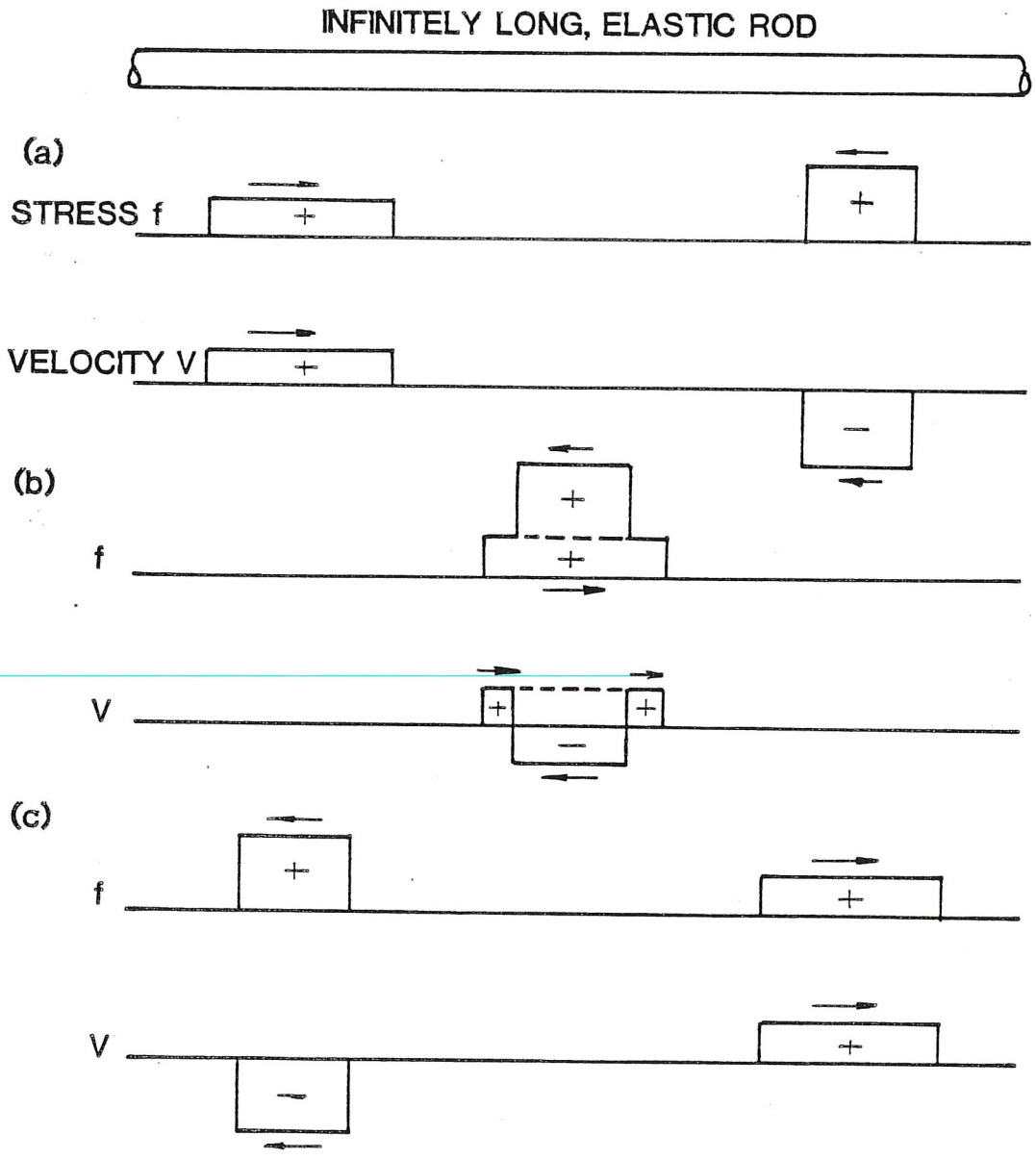

Figure A4: (a) Stress Waves Traveling in Opposite Directions along an Elastic Rod; (b) as Waves Meet, Compressive Stresses (Velocities) Add (Subtract); (c) Waves Continue to Travel Unchanged in Shape or Magnitude.

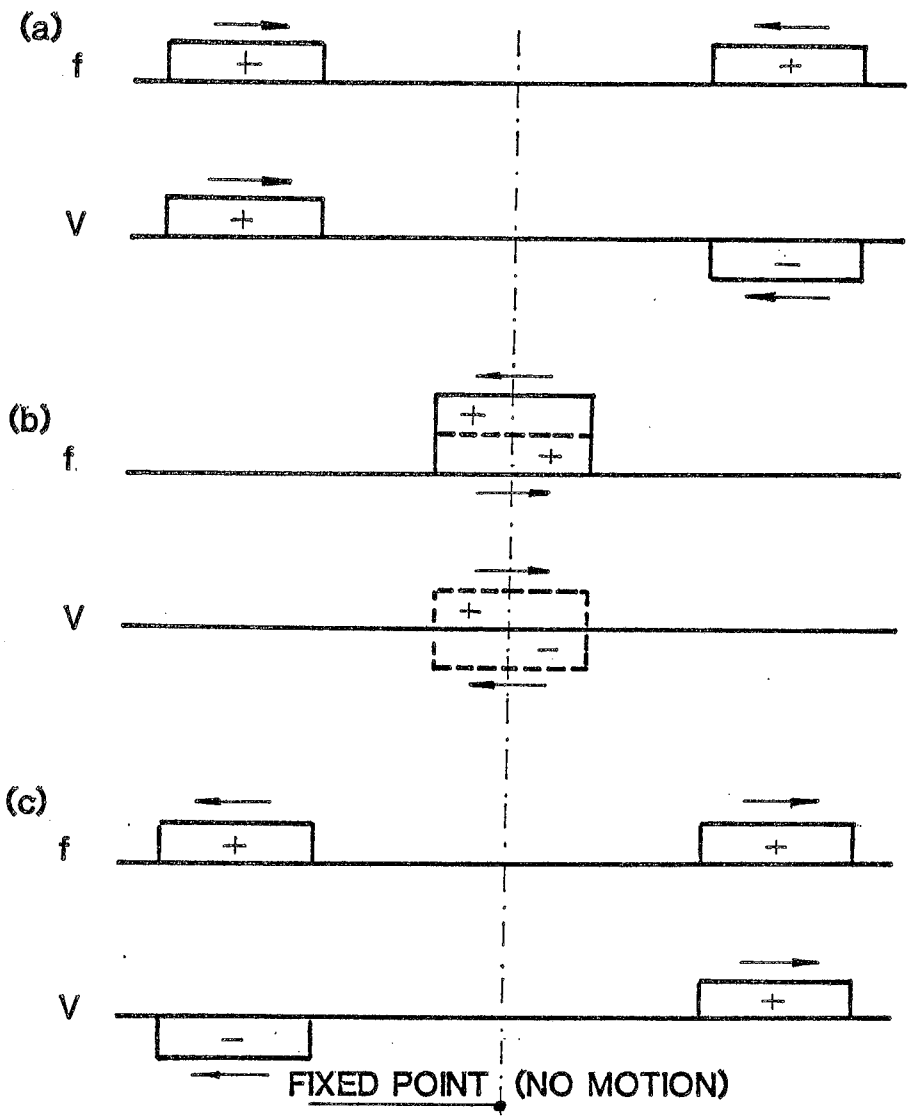

Figure A5: Superposition of Two Identical Compression Waves Traveling in Opposite Directions. (a) Waves Approach Each Other; (b) Waves Superimpose: Stresses Double, Velocities Cancel; (c) Waves Continue Undisturbed. Considering the Left Part a Real and the Right One an Imaginary Rod, a Fixed Condition for the Left Rod is Modeled at its Right End.

away from the fixed end with the same sign as the arriving wave, but with a velocity of opposite direction.

Another special case is shown in Figure A6. In this case, two stress waves of identical magnitude, but opposite sign, approach each other. It should be noted that the tension stress wave causes particle motion in the direction opposite to the direction of wave propagation.

In this case, when the two waves meet, the stresses of opposite sign cancel, producing a condition of zero stress. At the same instant the velocities add to double the velocity. This satisfies the boundary condition of a free end. In the final condition, Figure A6(c), the two stress waves travel apart, again unchanged.

This case is equivalent to the case of a compressive wave reflecting from a free end. The induced stress wave is reflected from a free end with the same magnitude but opposite sign as the incoming wave. The velocity of the reflected wave has the same magnitude and sign as the velocity of the incoming wave.

A4. Application of a Force at a Point along a Rod

It is interesting to examine the solution given by Eq. A3 for the special case of a suddenly applied force acting at some point along an infinite rod. At the time t=0, a displacement $u^*(x)$ is suddenly induced in the previously at-rest rod. For these conditions, from Eq. A3

$$u(x,0) = f(x) + g(x) \qquad (A7)$$

and

$$v(x,0) = c[f'(x) - g'(x)] \qquad (A8)$$

If the initial velocity along the rod is zero and the initial displace-

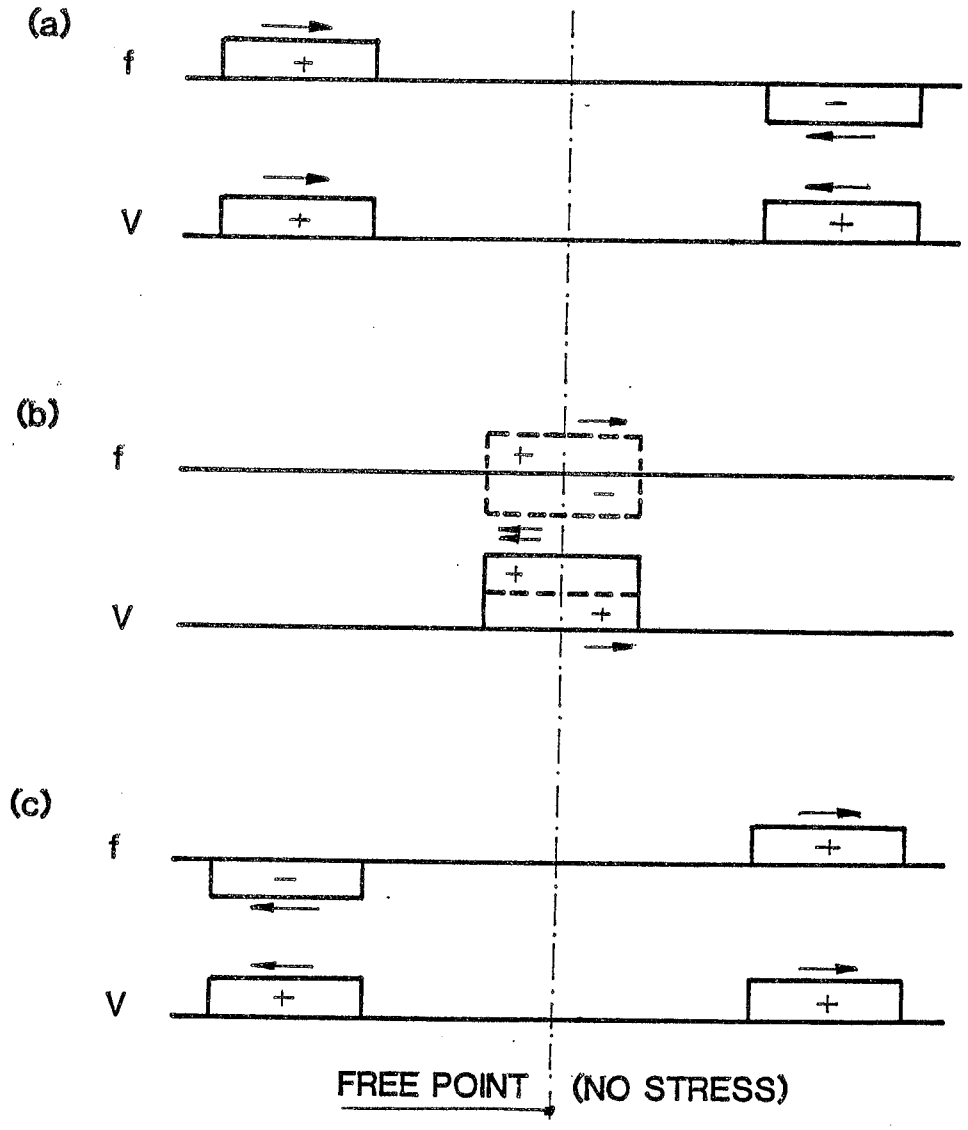

Figure A6: Superposition of Two Waves with Equal Magnitudes but with Opposite Signs Traveling in Opposite Directions. (a) Waves Approach Each Other; (b) Waves Superimpose: Stress Cancels, Velocity Doubles; (c) Waves Continue Traveling Undisturbed. Considering the Left Part a Real and the Right Part an Imaginary Rod, a Free End Condition is Modeled for the Left Rod at its Right End.

ment is $u^*(x)$ then from Eq. A7

$$f(cx)+g(x) = u^*(x) \qquad \text{(A9)}$$

and from Eq. A8

$$f'(x) - g'(x) = 0 \qquad \text{(A10)}$$

Eq. A9 and A10 are satisfied by the solution:

$$f(x) = g(x) = 1/2u^*(x)$$

Therefore, if a displacement is suddenly applied at a point on an infinite rod, two stress waves, each equal to one-half of the disturbing force, propagate away from the point of disturbance in opposite directions.

A5. Impact of a Rigid Mass with an Elastic Rod

Consider the case shown in Figure A7(a). A rigid mass of magnitude m_r impacts the end of an elastic rod. The rod is of uniform cross section with an elastic modulus E, a wave speed c and a cross sectional area A. An ideal impact is assumed; at the instant the mass contacts the rod, every particle at the end of the rod assumes the velocity of the mass. A free body diagram of the impacting mass is shown in Figure A7(b) for any time when it is still in contact with the end of the rod. A force F in the rod impedes the motion of the ram. Newton's Second Law can be applied to the free body (a denotes the acceleration)

$$m_r a + F = 0 \qquad \text{(A11a)}$$

If the stress-velocity proportionality is considered (Eq. A6), then

$$a = (c/E)(df/dt) \qquad \text{(A11b)}$$

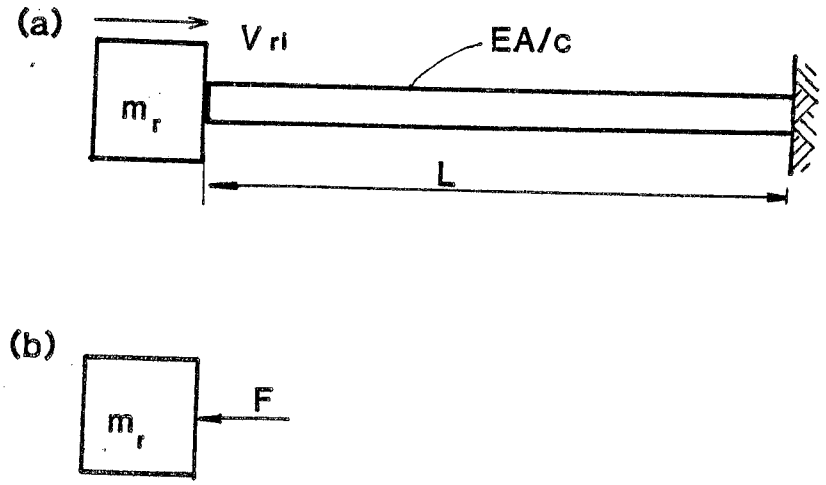

Figure A7: Mass, m_r, Impacting a Uniform Elastic Rod of Impedance, EA/c, and Length, L.

Substituting into Eq. A11(a) and converting the force F to stress f, the following relationship is obtained (f' is the time derivative of f)

$$m_r f' + (EA/c) f = 0 \qquad \text{(A12)}$$

This differential equation of the stress at the impacted end of the rod as a function of time holds so long as the force-velocity relationship holds (i.e. until time that the reflections arrive back at the impacted end).

The solution of Eq. A12(b) is

$$f = f_o e^{-(m_r c/EA)t} \qquad \text{(A13)}$$

from Eq. A4, f_o is the stress induced at initial impact ($f_o = E v_{ri}/c$). This solution shows that the maximum stress is a function of the initial stress, which is governed by the impact velocity of the ram. The decay rate of the stress wave is controlled by the mass of the ram and the pile impedance EA/c. If the ram mass is increased, the decay rate is reduced while an increase in the pile impedance increases the rate of stress wave decay.

APPENDIX B

DETAILS OF THE ANALYSIS OF PILE DRIVING

TABLE OF CONTENTS

APPENDIX B1

HAMMERS, DRIVING SYSTEMS, PILES AND SOILS

B1.1 Hammers

Impact pile driving hammers of the commonly used types can be conveniently divided into two groups, external and internal combustion hammers. In the first case, the power source is external to the hammer and power comes to the hammer through a fluid under pressure or through wire rope in the case of a drop hammer. For internal combustion systems, the power source is the burning of fuel inside the hammer.

B1.1.1 External Combustion Hammers

External power media are usually compressed air, steam or hydraulic fluid (thus, ASH hammers). Drop hammers may also be included in this category; their power medium is usually a winch. Because of their simplicity, drop hammers are not specifically discussed in this section. External combustion hammers can be subdivided into three categories: single-acting, double-acting and other, more exotic types.

(A) Single-Acting Hammers

In the operation of a single-acting external combustion hammer, the

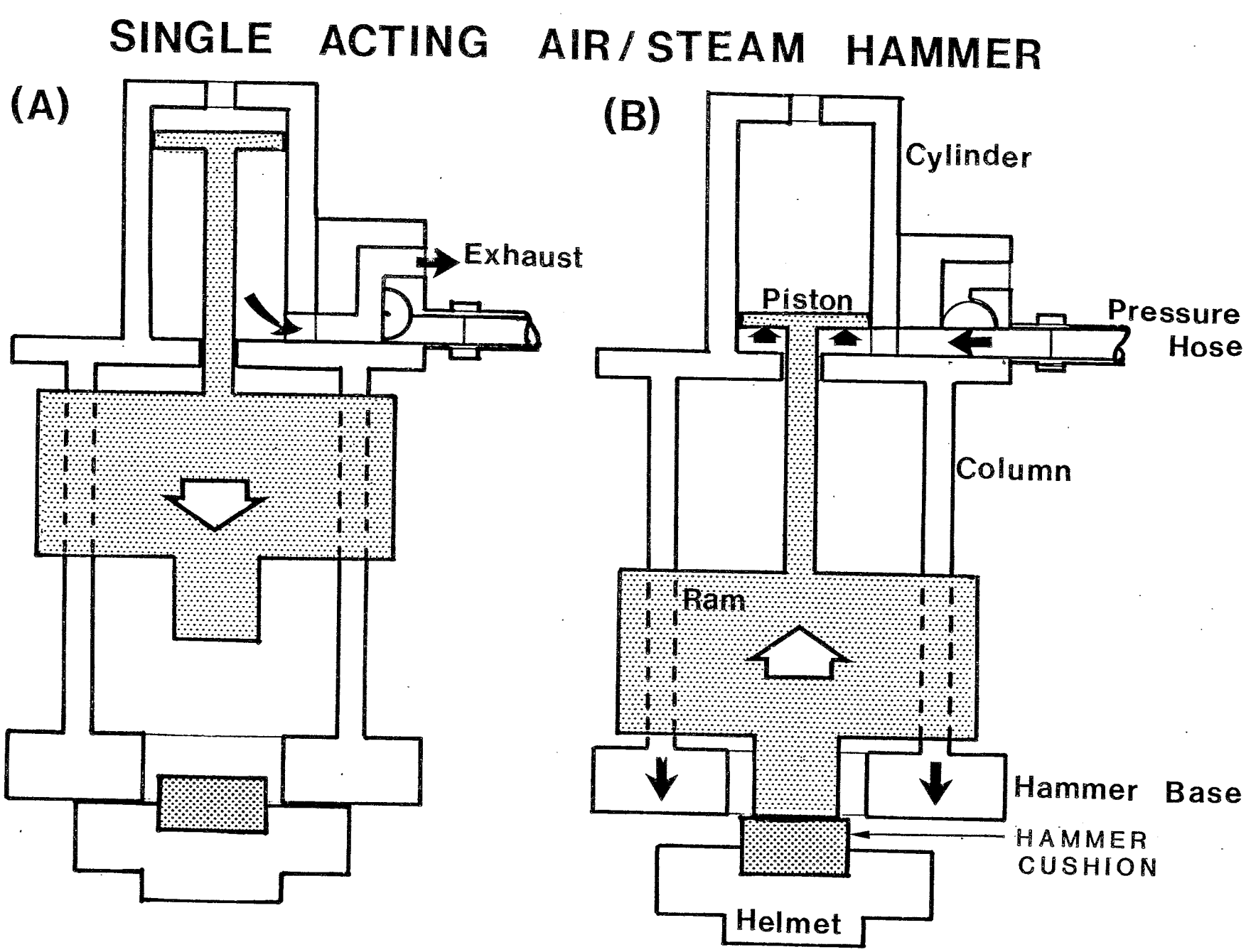

Figure B1.1: Working Principle of a Single-Acting Air/Steam Hammer

ram is usually a short, stocky block which is lifted by the power medium and allowed to fall freely. It impacts a striker plate and/or cushion which, in turn, delivers the energy to the pile top (Figure B1.1). The single-acting air/steam hammer is a well-developed piece of equipment which has been used for many years in pile driving.

In the process of construction control, only one variable need be considered, and that variable is ram stroke. However, the ram stroke will be to some extent dependent on the driving resistance which the pile experiences. If the pile meets only light resistance, then there will be little rebound energy returned to the ram and, consequently, all of the work required to raise the ram for the next blow must come from the external power source. In this case, the ram arrives at the point where the exhaust valve opens at a relatively low velocity, and consequently the total stroke will be less than for the case of hard driving where substantial rebound occurs, delivering some of the energy from the previous blow back to the ram. In extreme cases, if the ram does not overshoot the point where the valve opens, a counteracting pressure will be present during the early part of the ram fall. The resulting total energy output will be even smaller. Note that insufficient pressure can sometimes cause similar effects.

(B) Double-Acting Hammers

Double-acting external combustion hammers come under a variety of titles, including compound and differential. The Deep Foundations Institute, 1979, gives a good summary of their basic differences. All of these machines, however, have the same general characteristics. The stroke is shorter than for the single-acting hammer, and some mode of power is applied during the downward part of the stroke. This means that often the ram will be enclosed and not be visible for external examination. Because of the shortened stroke and the downward applied pressure, a double-acting hammer impacts at approximately twice the rate of single-acting hammers.

The ram starts its upward stroke by receiving a thrust from the power source, in addition to any rebound energy which has been delivered to it by the pile. The ram continues upward to the top of the stroke, at which point the thrust is applied in a downward direction. The initial upward thrust must be reacted by the hammer assembly weight, and if it is too great, the hammer assembly will lift off. This is generally quite undesirable, because the assembly impact can produce an erratic and uneven blow. Operating pressures should be limited so that the assembly does not lift off the helmet. A double-acting hammer of the differential type is shown in Figure B1.2, both in the upward and downward motion.

(C) Other Hammer Types with External Power Units

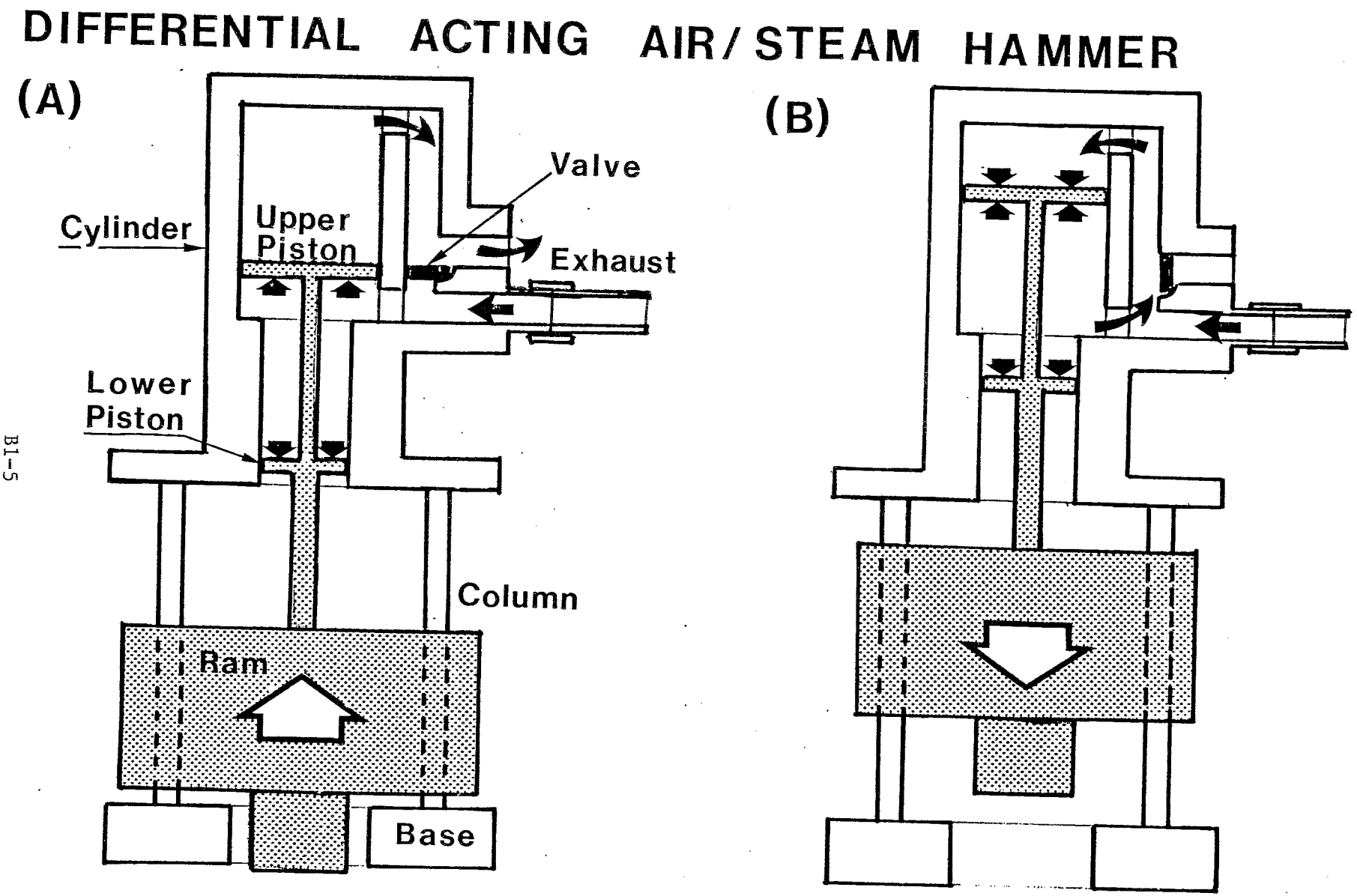

Figure B1.2: Working Principle of a Double-Acting (Differential type) Air/Steam Hammer

Occasionally new hammer types appear on construction sites that do not fit in the above categories. Among these are the HBM (Hydroblock) and the Bolt units. HBM utilizes a compressed nitrogen cushion to transfer the ram energy, while the Bolt unit works through compressed air.

B1.1.2 Internal Combustion Hammers

Internal combustion hammers exclusively derive their power from burning diesel fuel. They are, therefore, also called diesel hammers. Like external combustion hammers, internal combustion hammers can be divided into two groups, single-acting and double-acting.

(A) Single-Acting Diesel Hammers

The single-acting, or open-end diesel hammer, is simply a two cycle diesel engine with a free floating piston. While its operation is very simple, the operational mechanisms are viewed differently by different manufacturers.

Figure B1.3 shows four stages of open-end diesel hammer operation. The hammer is started by raising the ram with a lifting mechanism. At the upper end of its travel, the lifting mechanism is tripped, and the ram is released and descends by gravity. At the time the ram bottom passes the exhaust ports, a certain volume of air, called the Initial Volume, is trapped and compressed (Figure B1.3(a)). Usually, shortly after the time of exhaust port closure, a certain amount of fuel is squirted into the cylinder. Some hammers inject highly pressurized fuel (atomized fuel injection) for combustion later in the cycle when the combustion chamber pressure increases.

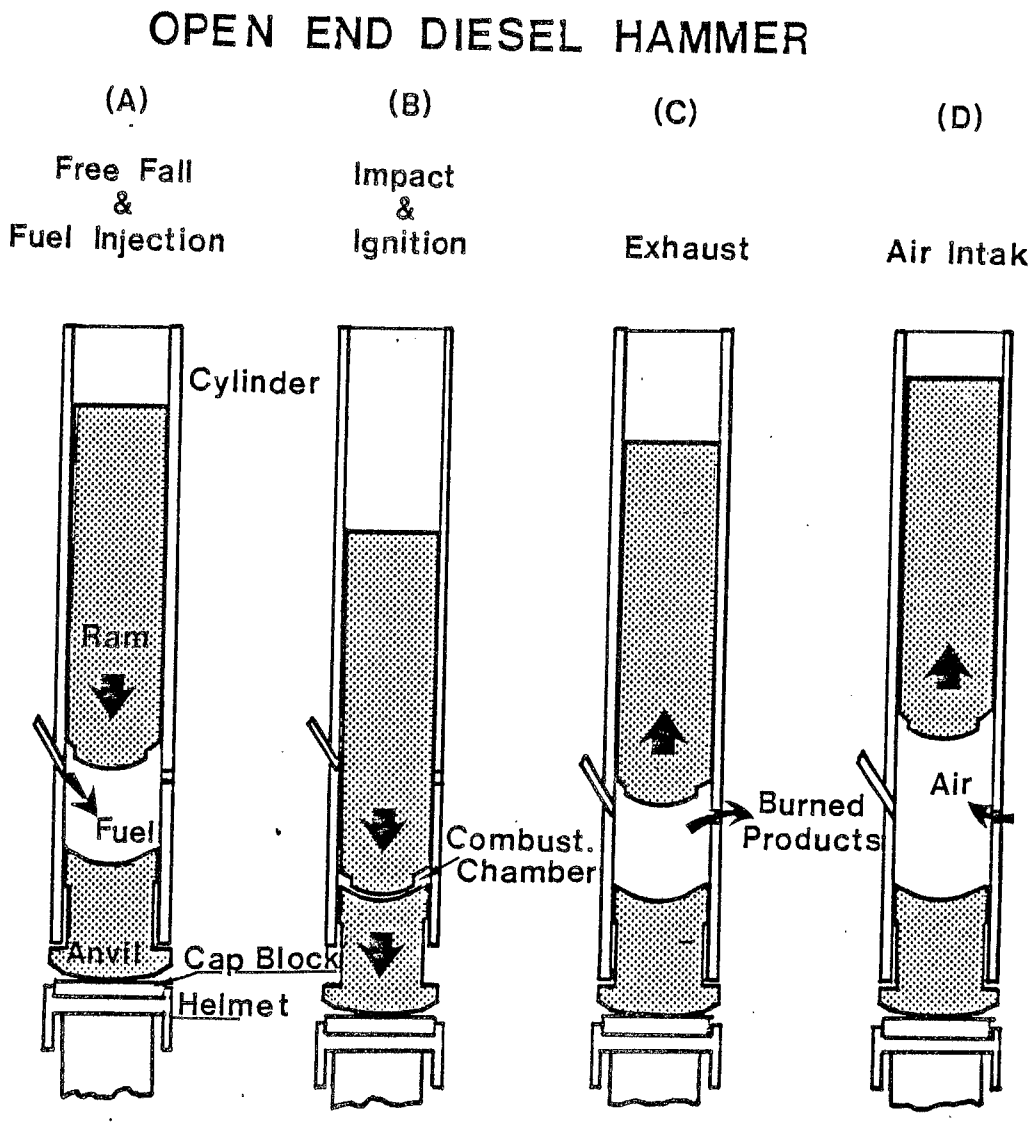

Figure B1.3: Working Principle of an Open End Diesel Hammer

When the ram impacts against the impact block (also called anvil), the air is compressed to a final volume (combustion chamber volume). The previously injected fuel is splattered by the impact into this final volume (if fuel atomization was not used) after which combustion occurs. This ignition retardation is referred to as the combustion delay. The combustion delay is caused by the fuel requiring a finite time to mix with the hot compressed air, and to ignite. More volatile fuels in general have a shorter combustion delay than heavier ones. Combustion occurring before impact is called preignition and can be caused by the wrong fuel type or an overheated hammer. Atomized, fuel injection hammers are sometimes designed so during easy driving when the ram descends slowly that preignition occurs , allowing easier starting with low soil resistance.

During impact, the impact block, cushions, and pile top are rapidly driven downward (Figure B1.3(b)., leaving the cylinder with no support. The cylinder then starts to descend by gravity. Pile rebound and combustion pressure push the ram upwards.

When the exhaust ports are cleared, some of the combustion products are exhausted, leaving a volume (equal to the inital volume) of burned gases at ambient pressure in the cylinder (Figure B1.3(c). As the ram continues upward, fresh air is drawn in through the exhaust ports and mixes with the remaining burned gases (Figure B1.3(d).

Depending on the reaction of the pile and the energy provided by combustion, the ram will rise to some height (stroke). It then descends again by gravity to start a new cycle.

Regarding hammer control, it is usually suggested that diesel hammer performance can be evaluated by multiplying the ram weight with the observed stroke. Thus, the engineer should always be in a position to determine, with reasonable accuracy, the performance level of the hammer by measuring the blow rate, which is directly related to stroke. Alternatively, he may visually observe the stroke, although this method is far less accurate than conversion from blows per minute.

(B) Double-Acting Diesel Hammers

Double-acting operation of diesel hammers is achieved by the use of a passive gas rather than an active gas, as is the case in the external combustion hammer. On the up stroke, the upper portion of the ram rises into a closed chamber, compressing the air which is initially at atmospheric pressure. Figure B1.4 shows schematically the principles of operation of two closed-end hammer types.

As the ram rises, the pressure in the upper or bounce chamber increases inducing a downward force on the ram, storing some energy in the gas and thereby reducing the time required for the ram to resume its

CLOSED END DIESEL HAMMERS

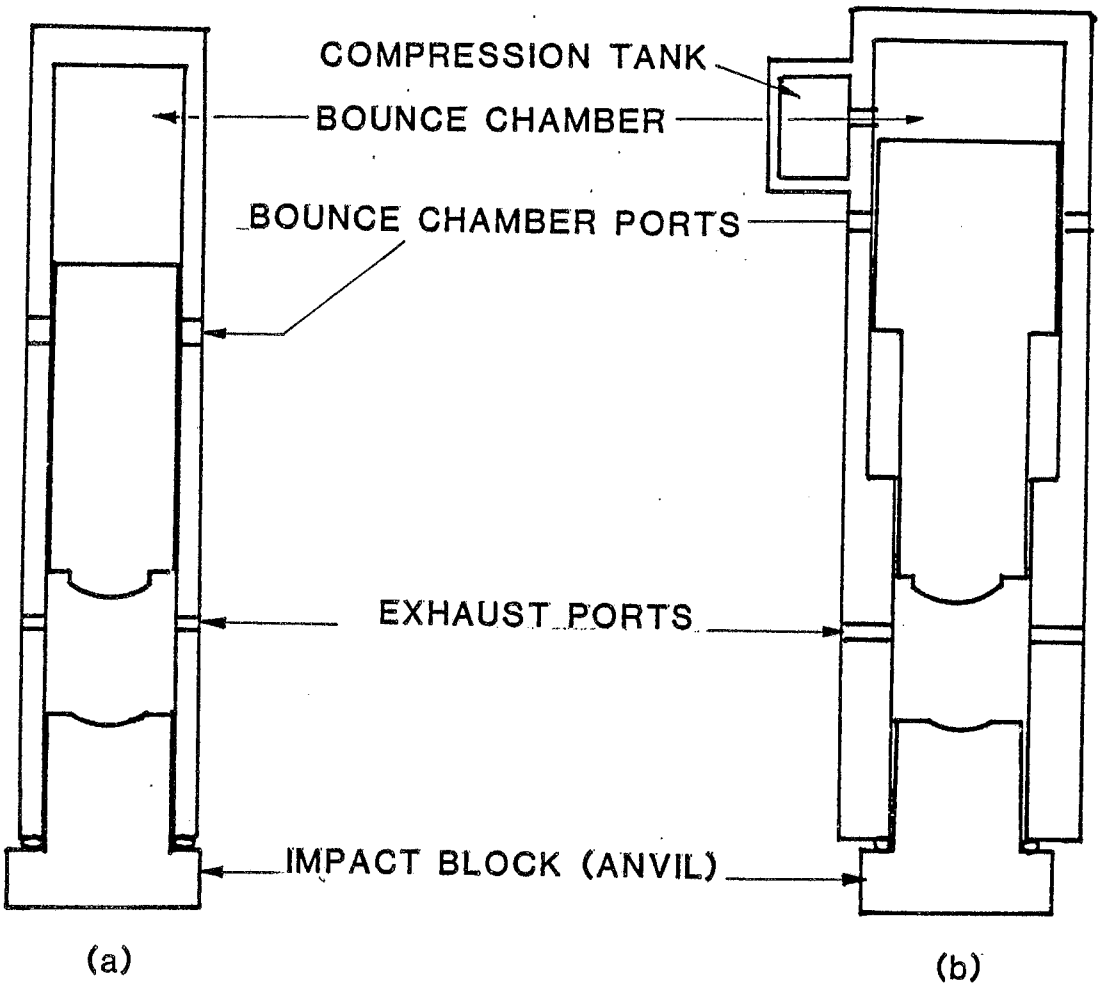

Figure B1.4: Schematics of two types of Closed-End Diesel Hammer. (a) MKT type, (b) ICE type with compression tank and sometimes non-uniform ram.

downward motion. In this way the ram stroke is shortened substantially, and faster operation is achieved.

If the ram rises too high, then the gas pressure acting on the hammer cylinder weight and the hammer assembly will lift off the pile top. This type of behavior is undesirable just as for double-acting external combustion hammers, although in this case, lift off is less critical since the bounce chamber pressure is reduced as soon as the ram begins to descend. If the casing does not lift too high, it will have time to settle back down on the pile top prior to the impact of the ram.

The hammer is equipped with a continously adjustable fuel pump, and is usually operated at full output. If the cylinder lifts off, the amount of fuel delivered should be reduced until lift off is just imminent.

The operation of double-acting diesel hammers can be observed by measuring the pressure in the bounce chamber. The bounce chamber pressure is related to the equivalent ram stroke which would be experienced by a single-acting diesel. Most hammers of the double-acting type incorporate a simple bounce chamber pressure gage.

A second type of double-acting diesel hammer is different from conventional double-acting diesel hammers only in that the downward acting force which is used to shorten the cycle time comes from a vacuum chamber

beside the ram. Since this hammer type is extremely rare no further discussion is included here.

B1.2 Driving System

B1.2.1 Introduction

The system for holding the hammer and the pile during driving is of an important part of the driving system. The hammer and pile must be held in accurate alignment during the driving operation. For poor alignment of hammer and pile, considerable loss of energy can be expected, and the potential for pile top damage is greatly increased.

B1.2.2 Leaders (Leads)

Pile driving leads for land work come in three different categories: fixed, semi-fixed and swinging (Figures B1.5 and B1.6). Particular applications require certain lead types.

The alignment of hammer and pile is primarily ensured by fitting both hammer and helmet with guides which slide along the lead rails. However, alignment is also assisted by provision of a loosely fitting enclosure called a gate around the pile near the bottom of the lead. Offshore leads are quite different, (Figure B1.6). They are inserted over the pile top for a distance sufficient to maintain alignment. Thus, the offshore lead is guided by the pile, which therefore needs additional guides such as a template.

(A) The fixed lead is attached at some point near its top, with a pin con-

nection to a crane's boom tip. Near its bottom, it is tied to a point near the base of the boom by a kicker brace. The kicker brace can be powered to extend and shorten, thus achieving a batter of the leads.

A disadvantage of many fixed lead systems is if the pile tries to deflect from the initial alignment, it is not easy to maintain the alignment with the pile. Therefore, if fixed leads are being used, careful observation during the driving operation must be made to insure that the hammer and the pile remain in alignment.

(B) Swinging leads consist of a set of leads which simply hang from a line on the crane. Thus, the lead is free to swing or rotate about its own axis. The leads should be long enough to accommodate the pile and the hammer at the beginning of driving, and the base of the leads should be set firmly on the ground.

Swinging leads should come equipped with spikes which settle into the ground as the leads are lowered. A gate is also closed around the pile. The pile is thus held firmly in position at the beginning of driving. If the pile moves from this position during the driving, the gate will cause the leads to follow the pile and maintain the hammer-pile alignment. This is very important and an advantage of the swinging lead system.

A disadvantage of this system is that the swinging leads change their angle as the center of gravity of the hammer-lead-pile system changes.

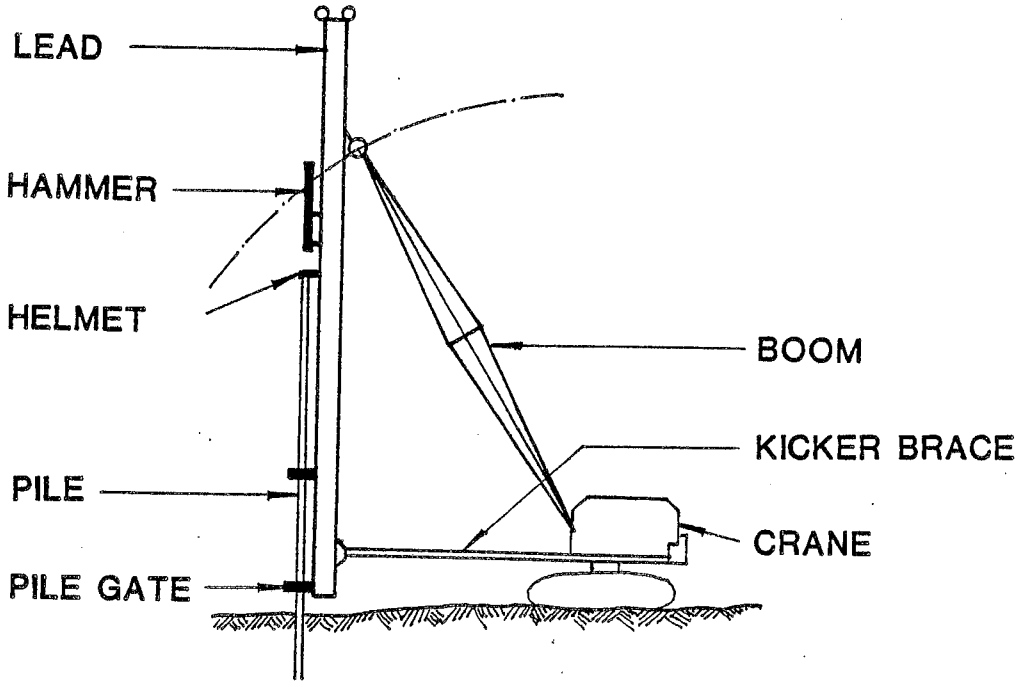

(a) FIXED LEAD

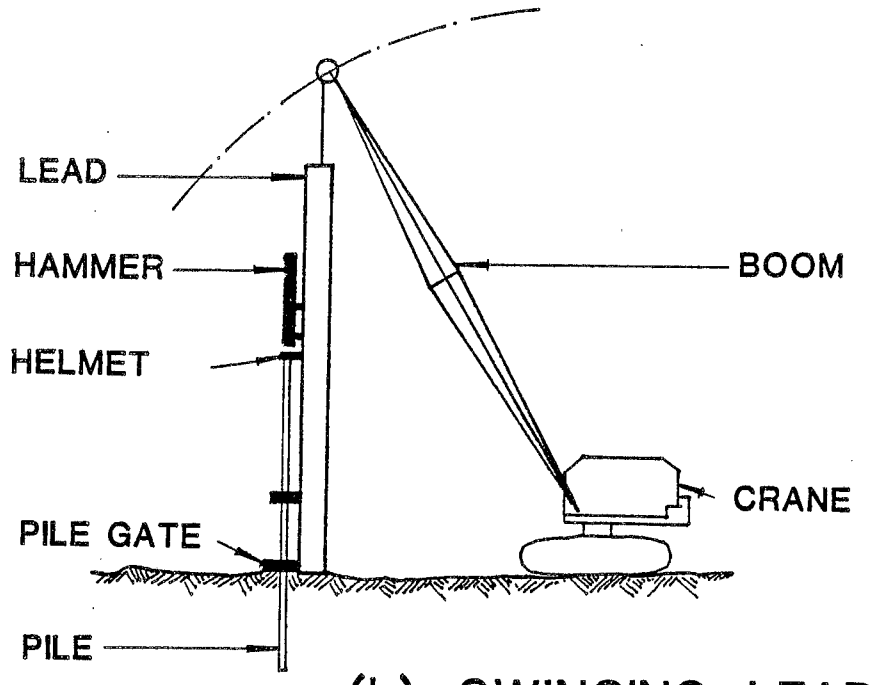

(b) SWINGING LEAD

Figure B1.5: Four types of Pile Driving Leads

For example, if the pile has a large batter, it is difficult to maintain the batter as the crane hoist raises the ram to start a diesel hammer. This action pulls the leads from their prescribed proper batter. If the batter is not too great, batter piles can be driven with this system.

(C) The semi-fixed lead system is similar in appearance to the fixed lead, except the lead is free to slide axially at the kicker brace connection. Thus, the base of the lead can be set on the ground.

(D) Offshore leads can only be used with a guided pile. The offshore lead aligns hammer and pile. In a batter situation, the pile's section modulus has to be sufficient to avoid overstressing by bending due to the hammer weight.

B1.3 Helmet, Hammer, and Pile Cusions

The combination of these components is usually referred to as "the driving system. The helmet consists of a steel box or container which fits over the end of the pile, and holds the pile in alignment on its under side. The helmet is guided by the leads. On the top of the helmet is a built-in container for an insert known as the hammer cushion (also called capblock).

Cushions can be any flexible material. They are used between helmet and hammer and helmet and pile. The cushion material must have sufficient flexibility to protect the hammer during the driving operation. Micarta and other synthetic materials have largely replaced hardwood as a cushioning material because of their greater constancy of mechanical performance. In general, as the constancy of mechanical performance is increased, energy losses are decreased. The engineering properties of commonly encountered materials are summarized in Table B1.1.

Pile cushions are not normally used for the driving of steel or timber piles. However, pile cushions are required for concrete piles in order to distribute the driving force uniformly over the pile top surface. The cushion material used for concrete piles varies widely in different parts of the world. Increasing the stiffness as much as possible will reduce the considerable amounts of energy absorbed in this element. More pile top damage is due to poor alignment than to the application of uniform and excessive driving

stresses. Therefore, stiffer cushions than are currently being used might be satisfactory if the material adapts to the pile top surface under the first blows, and if correct hammer-pile alignment is carefully maintained.

Pile cushions also control tension cracking of the pile in easy driving. With little resistance, the compression input wave is reflected from the bottom as tension. Larger compression inputs result in larger tension reflections. The cushion serves to smoothen the impact force so that tension reflection waves become sufficiently small. In this case, soft energy absorbing cushions cannot be avoided unless the hammer energy is reduced by short stroking (ASH) or reduced fuel injection (diesels). Such methods are often more effective control measures than the use of thick cushions.

B1.4 Piles

Even piles can be of considerable complexity. There are many types available and it would exceed the scope of this report to include a complete discussion. Details of the particular advantages, applications and load ranges of given pile types can be found in the appropriate references (e.g., Chellis, Ref. 14, Hunt, Ref. 21, and Fuller, Ref. 22).

The most common types of impact driven piles are:

(A) Steel piles including top driven pipes - both closed and open-ended, fluted and/or tapered pipes, and H-piles - both with and without toe

protection,

(B) Mandrel driven shell piles using either step tapered or expandable mandrels for continuous mandrel - shell interaction. Bottom driving mandrels are also encountered which practically "pull" a pipe into the ground.

(C) Timber piles, commonly made of spruce, fir or pine. Their length may be as much as 60 ft (20m) and they may have both top and bottom protection in the form of steel bands or tips.

(D) Concrete piles which may consist of prestressed square, octagonal, triangular, or large diameter pipe sections. Reinforced, non-prestressed, square concrete piles are frequently encountered in countries other than the United States.

Prestressed concrete piles longer than 100 ft, and nonprestressed piles longer than 40 ft are usually jointed. Many patented splicing systems are available.

(E) Composite piles, which usually combine prestressed square concrete piles with H-profiles for tip protection or for penetration into stiff layers. These "H-tips" may be up to 30 ft long. There are also rare combinations of steel and timber or timber and concrete materials.

"Cast-in-Situ Piles" may be formed by top driven pipes or mandrel driven shells which are filled with concrete after installation. Dynamic analysis of these piles is valid. However, there are a number of proprietary systems which may be called "semidriven." For example, the Franki approach is to drive a plugged pipe and then to withdraw the pipe while continuously forcing concrete into the voids near the pile bottom and along the shaft. A similar process is used for the Interpile. For both systems, the pile driving resistance may only be a lower bound of the actual pile bearing capacity and a "blow count" record may only give qualitative results about the soil resistance.

Splicing of pile sections may have some effect on the results of dynamic analyses. Welded or epoxied connections which fully transfer tensile and compressive forces do not affect the analysis. However, so-called "can" splices (full compressive, zero tension transfer) have significant effects on stress wave transfer, and must be modeled accordingly. Mechanical splices for concrete piles (Herkules, Hard-Drive, etc.) have some tolerance and may cause both tensile and compressive slacks. Attempts to model these effects do not always increase the precision of the dynamic analysis.

Table B1.1: Selected Cushion Materials

Trade Name	Material	Elastic Modulus E ksi	Coefficient of Restitution C_c
Ascon	Asbestos	45	0.50
Conbest	Micarta	450/560	0.80
Forbon	Vulcanized Fiber	800	0.85
N/A	Urethane	350	0.72
N/A	Nylon	350	0.92
	Oak (Load Parallel Grain)	1500±	0.5
	Plywood (Load Across Grain)	50±	0.5
	Bongossi (Load Parallel Grain)	280	0.7
Hamortex	Paper/Aluminum	90	0.5
Force 10	Knitted Metal	200	0.5
	Aluminum	10000	1.0

Note: The engineering properties were taken from various publications and may not have been obtained by standard methods.

1 kip = 4.5 kn 1 ft. = .3048 m 1 in. = 25.4 mm

APPENDIX B2

WAVE EQUATIONS

B2.1 Introduction

During recent years pile driving analysis "by the wave equation" has become a frequently used tool in design and construction control. Engineers have either worked with "canned programs" such as WEAP or TTI or they have retained the services of a consulting firm to analyze their particular pile-soil systems.

All users should familiarize themselves with the background of this analysis to avoid misinterpretation. The program manuals (Goble and Rausche, 1976 and Hirsch et al, 1976) are therefore a highly recommended source of information. In addition, this report provides a summary of wave equation details. Chapter 3 describes the general concepts of dynamic pile analysis. This appendix summarizes the mathematical and physical details.

B2.2 The Wave Equation Pile Model

Figure B2.1 shows a real pile and its model. For a wave equation analysis to be applicable, the real pile should be a long, slender (at least ten times longer than wide) rod of elastic material. The piles may consist of different materials.

Figure B2.1 shows a lumped mass pile model in its most general form (another type of pile model - the continuous one - is not frequently used, but is briefly discussed later). The pile is segmented and average properties - A (cross sectional area), E (Young's Modulus) and rho (mass density) of each segment of length l_p (usually 5 ft (1.5m)) - are assigned to each segment, which consists of a mass, spring and, sometimes, a dashpot.

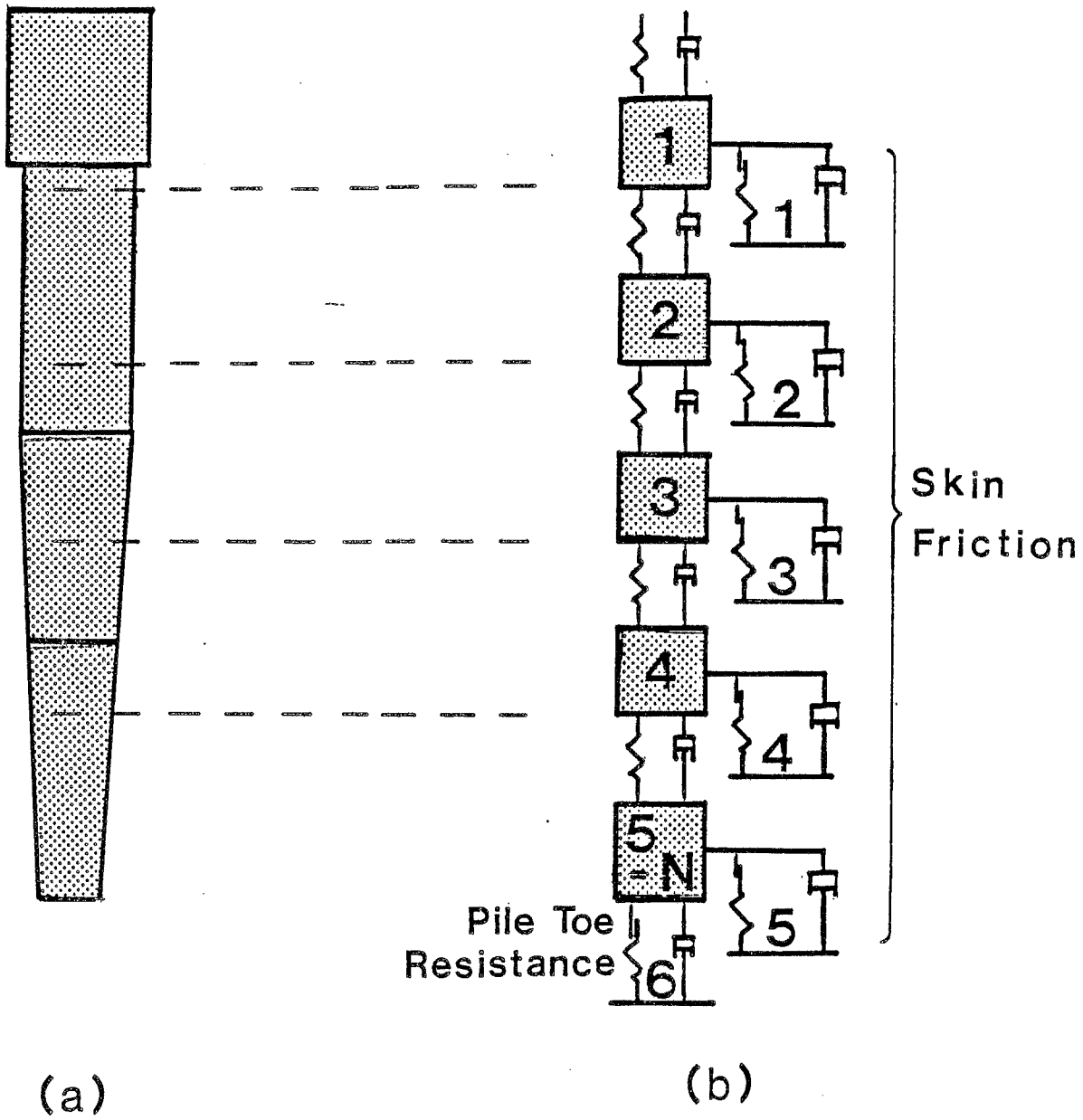

Figure B2.1: (a) Real, Nonuniform Pile and (b) Corresponding Lumped Mass Pile Model and Soil Model after Smith.

The spring is fully described by a stiffness value k_p.

$$k_p = AE/l_p \tag{B2.1}$$

The segment's mass is defined as

$$m_p = A(rho)l_p \tag{B2.2}$$

and the daspot constant may be expressed as a small percentage (say 1%), p_p, of the pile's impedance Z. Thus with

$$Z = EA/c = (k_p m_p)^{1/2} \tag{B2.3}$$

the dashpot constant is

$$c_{dp} = p_p Z. \tag{B2.4}$$

These quantities completely describe the pile's dynamic behavior unless slacks are present. Slacks allow for deformations between pile segments with reduced or zero forces. For example, a tension slack allows for a zero tension force separation between two segments. This separation may be unlimited as is the case with can splices. Compressive slacks may occur in mechanical splices. These devices may have a slight separation before hammer impact. This separation needs to be compressed before normal wave transmission can take place. Since such devices absorb some wave energy, it is advisable to use bilinear or nonlinear properties for springs with slacks. For further details on this relatively infrequent situation, the wave equation manuals should be consulted.

B2.3 The Wave Equation Hammer Model

Major hammer model components are shown in Figure B2.2(a) and B2.2(b). ASH hammers consist primarily of a stocky mass, m_r, which impacts against a striker plate and cusion. This mass is easily modeled by m_r itself. If the

(a) ASH HAMMERS

(a1) RAM

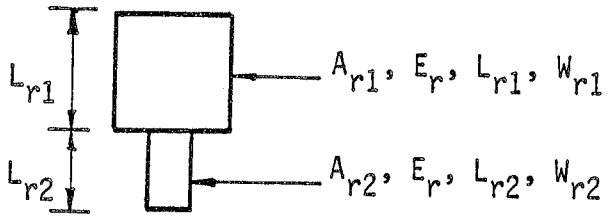

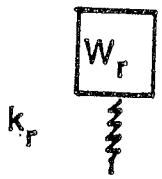

$$k_{r1} = \frac{A_{r1}\, E_r}{L_{r1}}$$

$$k_{r2} = \frac{A_{r2}\, E_2}{L_{r2}}$$

$$K_r = \frac{k_{r1}\, k_{r2}}{k_{r1} + k_{r2}}$$

$$W_r = W_{r1} + W_{r2}$$

(a2) ASSEMBLY

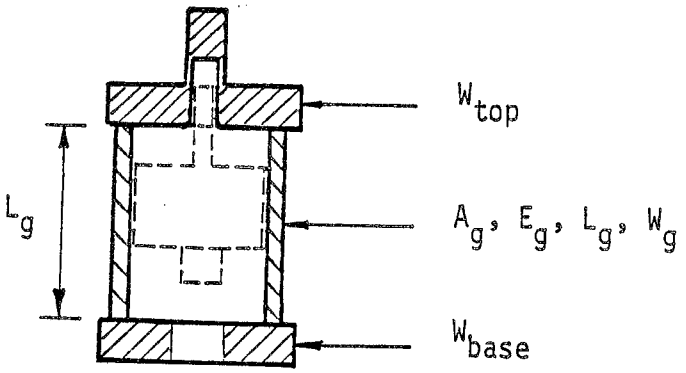

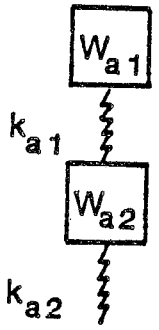

$$W_{a1} = W_{top} + W_g/2$$

$$W_{a2} = W_{base} + W_g/2$$

$$k_{a1} = k_{a2} = 2\,\frac{A_g\, E_g}{L_g}$$

Figure B2.2: (a) ASH Hammer Model

cushion is not a soft material it may be necessary to represent the ram's flexibilty with a spring of stiffness k_r. The computation of this spring stiffness is not always easy, since the ram has a nonuniform shape. On the other hand, it is unnecessary to use great accuracy in these computations. If a ram stiffness has been computed and a soft cushion material is present then these two stiffnesses may be combined to a single one using Kirchhoff's Law (see Eq. B2.5a).

For diesel hammers, which have relatively slender rams, the ram should be divided into a number of segments of length l_r. Three segments are usually recommended. The ram segment stiffnesses and masses are then computed.

Diesel hammers include an impact block between ram and cushion. The corresponding mass, m_a, and stiffness, k_a, are easily computed from average cross sectional area, mass density and Young's Modulus. For the diesel hammer, it is advisable to combine the bottom ram spring with the anvil spring using Kirchhoff's law. Thus, the combined spring stiffness is

$$k_{ra} = (k_a k_r)/(k_a + k_r). \qquad \text{(B2.5a)}$$

The combined coefficient of restitution may be calculated from

$$c_{c,ra} = (k_a c_{c,r} + k_r c_{c,a})/(k_a + k_r) \qquad \text{(B2.5b)}$$

Masses and springs are the major components of a hammer model. Sometimes the elastic behavior of the hammer springs cannot be described by an ideal elastic behavior. In those cases, coefficients of restitution and round-out deformations may be needed. Such extensions to the basic hammer model will be described in the section on driving system modeling.

(b) DIESEL HAMMERS

(b1) RAM

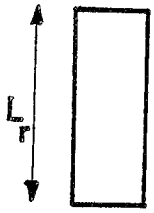

A_r, E_r, L_r, W_{rt}

$$k_r = 3 \frac{A_r E_r}{L_r}$$

$$W_r = W_{rt}/3$$

(Note: Nonuniformities may be considered by calculating variable k_r and W_r values)

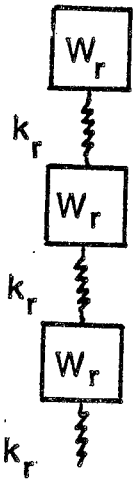

(b2) IMPACT BLOCK

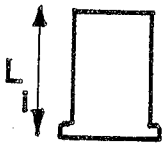

A_i, E_i, L_i, W_i

$$k_i = \frac{A_i E_i}{L_i}$$

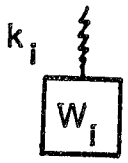

Note: Usually bottom ram and impact block spring are combined to single spring with stiffness

$$k_{ri} = \frac{k_r k_i}{k_r + k_i}$$

Figure B2.2(b): Diesel Hammer Mechanical Model

B2.4 The Thermodynamic Model of Diesel Hammers

Depending on the particular wave equation program used, thermodynamic modeling may be more or less complex. For example, the TTI program uses only a preprogrammed force versus time function. The only parameters needed to model the thermodynamic cycle for the TTI program is the explosive force, i. e., the maximum combustion pressure times the cross sectional area of the ram.

The WEAP program completely models three separate phases according to thermodynamic laws (see Figure B2.2c):

(a) Compression
(b) Ignition and
(c) Expansion

WEAP requires the input of the Gas Law's compression exponent, the compressive stroke, the cross sectional area of the ram, the combustion chamber volume at impact, the combustion delay time (positive - or negative to model preignition), the duration of ignition and the maximum combustion pressure. Further details on diesel hammer models can be found in Goble and Rausche, Ref. 17; Rempe, Ref. 9 and Likins, Ref. 23.

B2.5 The Wave Equation Model of Driving Systems

The wave equation represents the cushion, helmet and pile cushion as a spring-mass-spring system (see Figure B2.2e). Sometimes, a dashpot is also included. The model only requires the hammer cushion stiffness, k_c (see Chapter 3), the helmet mass, m_h, and the pile cushion stiffness, k_{cu}. The following extensions are made.

B2.5.1 Bilinear Springs

All wave equation programs require the input of a coefficient of restitution. They may be denoted c_c for the hammer cushion and c_{cu} for the cushion

(c) DIESEL HAMMER THERMODYNAMICS

(c1) GEOMETRY

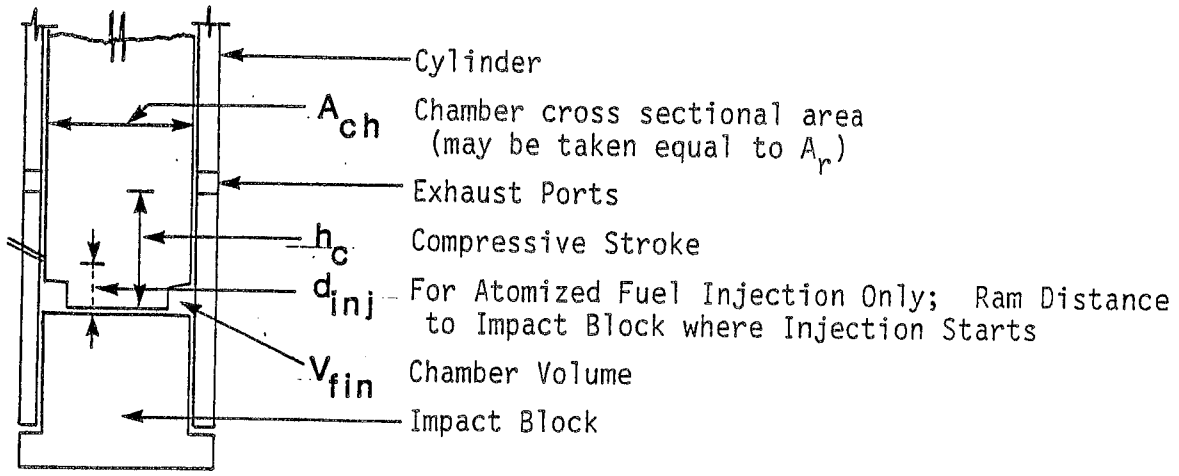

(c2) TIMING, PRESSURE

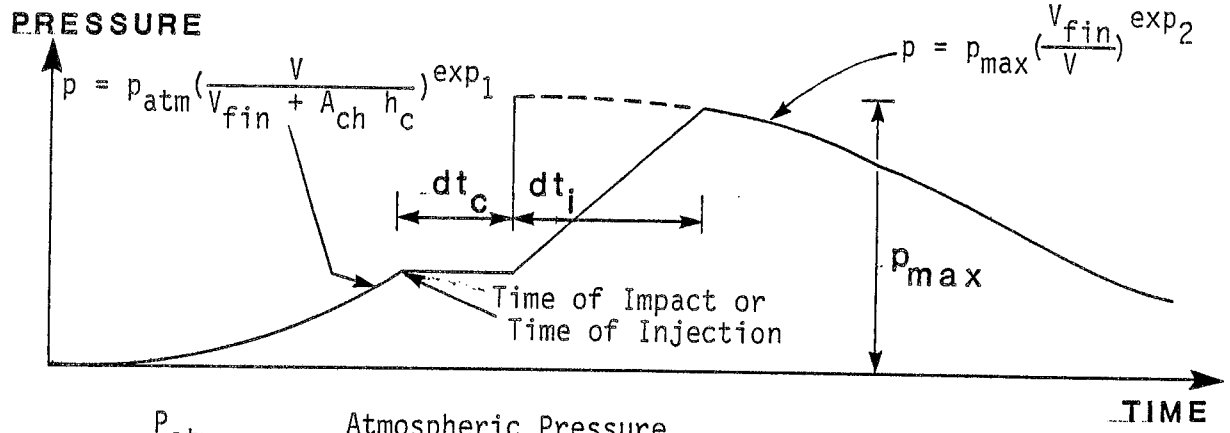

	P_{atm}	Atmospheric Pressure
	P_{max}	Maximum Combustion Pressure
Note:	$P_{max}\ A_{ch}$	Explosive Force
	dt_c	Combustion Delay
exp_1	Compression	dt_i Ignition Duration
exp_2	Exponent	Expansion Exponent

Figure B2.2(c): Diesel Hammer Thermodynamic Model

(d) IMPACT VELOCITY CALCULATION

(d1) SA ASH HAMMERS

h.... rated stroke; e_h.... hammer efficiency

$$V_{ri} = (2gh\ e_h)^{1/2}$$

V_{ri} ....impact velocity

g .... grav. acc (32.18 ft/gL)

(d2) DA ASH HAMMERS

h.... rated stroke, p_r.... rated pressure,
p.... actual pressure, e_h.... hammer efficiency

$$V_{ri} = (2gh\ (1 + p/p_r)e_h)^{1/2}$$

Note: $E_r = h(W_r + p_r\ A_{eff})$, i.e., energy of free fall plus the work done by the rated pressure. A_{eff} is the effective area over which pressure acts.

(d3) DIESEL

h.... actual hammer stroke, h_c.... compressive stroke,
e_h... hammer efficiency

$$V_{rp} = (2g(h-h_c)e_h)^{1/2}$$

Velocity at impact to be computed from thermodynamics

Figure B2.2(d): Data Required for Computation of Impact Velocity

(e) DRIVING SYSTEM

Components

Striker Plate: W_s

Capblock: A_c, E_c, L_c, W_c, c_c

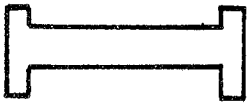

Helmet: W_H
(incl. inserts)

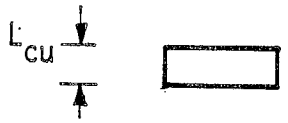

Cushion: A_{cu}, E_{cu}, L_{cu}, W_{cu}, c_{cu}

$$W_c = W_c + W_H + W_{cu}$$

$$k_c = \frac{A_c E_c}{L_c}, \qquad c_c$$

$$k_{cu} = \frac{A_{cu} E_{cu}}{L_{cu}}, \qquad c_{cu}$$

Figure B2.2(e): Components and Model of Driving System. Required Data:
W_{cap}... Weight of all components between hammer and pile
k_c....capblock stiffness, c_c...capblock coeff. of restitution
k_{cu}... cushion stiffness, c_{cu}...cushion coeff. of restitution

spring. As shown in Figure 3.4(a), the coefficient of restitution increases the stiffness during the expansion of a spring. In that manner, energy is dissipated by the spring. The spring expansion stiffness for the capblock is

$$k_{c,e} = k_c / c_c^2. \tag{B2.6}$$

B2.5.2 Nonlinear Springs

WEAP uses partially nonlinear springs for the curvilinear force deformation relationship at the onset of impact. Figure 3.4(b) shows the force nonlinearity modeled by a linearly variable stiffness within the range of a specified "round-out deformation". This concept is particularly useful for the modeling of soft cushions.

B2.5.3 Dashpots

From experience, improved agreement between computed and measured forces and motions can be achieved if the wave equation includes a dashpot in parallel with the hammer cushion spring. The dashpot constant is computed using a small percentage p_h of the impedance of the ram-cushion system. Thus,

$$c_{dc} = p_h (m_r k_c)^{1/2} \tag{B2.7}$$

This dashpot parameter cannot be derived from basic material properties.

B2.6 The Soil Model

The wave equation soil model relates the soil resistance forces to the pile motion. For example, the static soil resistance at segment i, is denoted by R_{si} and is related to the segment displacement u_i. The dynamic resistance, Rd_i, is directly related to the segment velocity, v_i'. It is assumed that the soil does not move.

For the static resistance, a soil compression value, q_i, is introduced and called quake. Usually, the engineer assigns one quake value for all pile skin segments and one for the toe. The quake is that deformation at which the elastoplastic soil resistance becomes plastic. R_{si} then reaches the ultimate resistance value, R_{ui} (see Figure 3.5(a)). Thus,

$$R_{si} = u_i(R_{ui}/q_i) \tag{B2.8}$$

The bracketed term is the soil stiffness. The static resistance can never become greater than the ultimate resistance, or

$$R_{si} \leq R_{ui} \tag{B2.9a}$$

When the pile rebounds, R_{si} decreases according to its stiffness, R_{ui}/q_i. Denoting a negative resistance bound by R_{ei}, the static resistance must obey

$$R_{si} \geq -R_{ei} \tag{B2.9b}$$

For end bearing,

$$R_{ei} = 0 \tag{B2.9c}$$

and for skin friction,

$$R_{ei} = -R_{ui} \tag{B2.9d}$$

Further extensions to the static soil resistance law are discussed in the CAPWAP section. However, for typical wave equation analyses, the above rules are sufficient.

A skin friction percentage, r_f, is introduced. The total skin friction, R_{uf}, therefore, becomes

$$R_{uf} = r_f R_{ut}/100 \tag{B2.10}$$

where R_{ut} is the total ultimate pile capacity being analyzed. The end bearing is, of course

$$R_{ue} = (100 - r_f)R_{ut}/100 \tag{B2.11}$$

R_{uf} is assigned to the individual pile segments according to static formula considerations. Thus, with the exception of the toe resistance, the R_{ui} values sum to R_{uf}; they may be distributed by the operator in any reasonable manner.

Soil damping (Figure 3.5(b)) is modeled by a dashpot for each soil element. The relationship governing this resistance is:

$$Rd_i = j_{vi}v_i \tag{B2.12}$$

where j_{vi} is the so-called viscous damping factor. The viscous damping factor may be different for each pile segment. To simplify the selection of dashpot coefficients, Smith introduced a damping coefficient, j_{si}.

$$Rd_i = j_{si}R_{si}v_i. \tag{B2.13}$$

In other words, the viscous damping factor is non-dimensionalized by the static resistance at the same segment. If there is no static resistance acting against the motion of a pile segment, then the dynamic resistance will also be zero. For most cases only a skin and a toe damping factor are chosen.

B2.7 Force Balance at a Hammer or Pile Segment

Consider the segment shown in Figure B2.3. The segment is subjected to forces, F_{ti} and F_{bi}, from neighboring springs and dashpots. These forces can be computed if the displacements and velocities of the top and bottom neighbor segments (i-1 and i+1, respectively) are known.

$$F_{ti} = k_i(u_{i-1} - u_i) + c_{di}(v_{i-1} - v_i). \tag{B2.14}$$

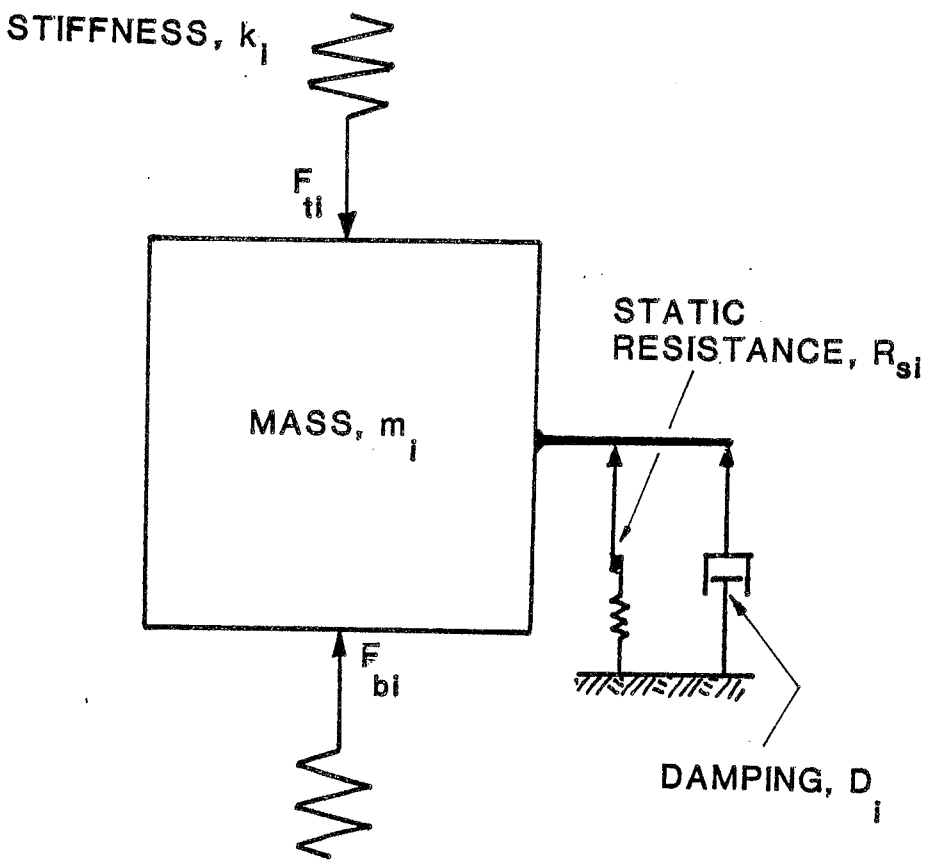

Figure B2.3: Pile Segment with Soil Model

The stiffness, k_i, and the dashpot coefficient, c_{di}, represent either a hammer, a pile, or a driving system spring or dashpot, respectively. They act on the top of the segment mass, m_i. Similarly one finds

$$F_{bi} = k_{i+1}(u_i - u_{i+1}) + c_{di+1}(v_i - v_{i+1}). \qquad \text{(B2.15)}$$

The total soil resistance R_i, if present, acts on segment i.

$$R_i = R_{si} + Rd_i. \qquad \text{(B2.16)}$$

From Newton's Second Law, the acceleration u_i'' of segment i can be computed.

$$a_i = g + (F_{ti} - F_{bi} - R_i)/m_i \qquad \text{(B2.17)}$$

where g is the earth gravitational acceleration (32.17 ft/s^2 or 9.81 m/s^2). For the helmet and all pile segments, g is usually set to zero, which implies that the soil resistance forces necessary to support both pile and helmet weight are not included in the dynamic analysis. Therefore, the bearing capacity dynamically determined does not include the pile weight.

B2.8 Integration

For integration, a time increment, t_d, must be determined. This increment has to be small enough so that no numerical instability occurs during the computational process. On the other hand, it has to be large enough so that the accumulated round-off errors are small and that the total computational time is kept relatively small. Experience shows that sufficiently accurate results may be obtained if

$$t_d = (1/phi)(Min(m_i/k_i))^{1/2} \qquad \text{(B2.18)}$$

The square-rooted expression is the minimum mass to stiffness ratio of any neighboring mass-spring combination, and actually represents the shortest

wave travel time in any one segment of the total system. This is called the critical time. The factor, phi, is a "safety factor" against numerical instability; it must be greater than one (1).

After the acceleration of a segment is determined, integration begins. Both velocity and displacement are computed from the integration of acceleration. In the beginning of the analysis, the ram has an initial velocity; helmet and pile masses are at rest. Denoting the known velocity and displacement values by v_{oi} and u_{oi}, respectively (the subscript "o" stands for "original"), and the values after a time increment has passed (denoted u'_{ni} and u_{ni}, for "new"), can be computed as

$$v_{ni} = v_{oi} + a_i t_d \tag{B2.19}$$

and

$$u_{ni} = u_{oi} + v_{oi} t_d \tag{B2.20}$$

This is a simple Euler integration; the displacement is computed by assuming that the velocity stays constant during the time increment. An improved method of calculation is

$$v_{ni} = v_{oi} + (a_{oi} + a_{ni}) t_d/2 \tag{B2.21}$$

and

$$u_{ni} = u_{oi} + v_{oi} t_d + (2a_{oi} + a_{ni}) t_d^2/6 \tag{B2.22}$$

These equations assume the acceleration is linearly variable between two consecutive computation times. Both approaches are used. For the more complicated computation, a somewhat larger time increment is admissible and computational effort may be reduced.

B2.9 Computational Procedure

The initial conditions imposed on the model are zero displacements for all but the ram segments which may be placed slightly above (negative) the anvil or hammer cushion spring. The ram segments are the only segments not at rest. They are given an initial velocity which is computed from rated hammer energy, E_r, and efficiency e_h (Figure B2.2d).

$$v_{ri} = (2E_r e_h M_r)^{1/2} \qquad \text{(B2.23)}$$

For the second time increment, integration leads to displacement of the ram which brings the ram into contact with the hammer cushion spring. These displacements induce spring forces which cause accelerations and hence velocities for the total pile string.

A complication exists where at the time the force balance is evaluated, the displacements and thus the forces are not known for the new time increment. It must be assumed, for force calculations only, that displacements have not changed. This assumption leads to errors which are lower when time increments are very small. Because of the practical limit of both with computational effort and accumulated round-off error, a prediction-correction type analysis has proven advantageous.

Using the previous velocities, new displacements are predicted by Euler integration. After forces, accelerations and velocities are computed, the new velocities are compared with the previous ones. If they do not meet a convergence criterion, a new cycle of computation is started within the same time increment using the new forces and displacements for an improved set of velocity values.

All wave equation analyses contain at least some type of prediction-correction scheme, but they generally do not include more than a few cycles of iteration.

Once the pile displacements decrease due to the action of resistance forces, a maximum pile toe displacement is computed. The blow count is usually calculated by subtracting the toe quake from this maximum toe penetration. This approach assumes that the pile rebounds as much as the toe quake. Considerable errors may be introduced by this definition of blow count when skin and toe quakes differ substantially.

APPENDIX B3

CASE METHOD

The "Case Method" refers to the Methods developed at Case Institute of Technology beginning in the 1960's. The objective of that research effort was calculation of pile bearing capacity from pile top force and acceleration measurements. Today, the term "Case Method" refers to both measurement techniques and interpretations of soil effects, pile stresses, pile integrity and hammer performance. Related techniques are CAPWAP (see Appendix B4) and the Momentum Method (Appendix B5).

B3.1 Case Method Derivation

The following derivations are based on wave propagation. This concept is also used in Appendix B4, Section B4.4. For a pile with impedance, Z, the force $F_i(t)$, at time t and location i, and the velocity $v_i(t)$ may be used to determine upward and downward traveling wave magnitudes ($F_{ui}(t)$ and $F_{di}(t)$)

$$Fa_i(t) = (F_i(t) - Zv_i(t))/2 \qquad \text{(B3.1a)}$$

$$F_{di}(t) = (F_i(t) + Zv_i(t))/2 \qquad \text{(B3.1b)}$$

If measured forces and velocities at time j are denoted by F_{Mj} and v_{Mj}, respectively, then the two waves at the point of measurement are:

$$F_{uMj} = (F_{Mj} - Zv_{Mj})/2 \qquad \text{(B3.2a)}$$

$$F_{dMj} = (F_{Mj} + Zv_{Mj})/2 \qquad \text{(B3.2b)}$$

If a resistance force begins at time $t = t_1 + x/c$ at some intermediate point, x, along the pile (caused by an impact at time $t = t_1$ at the pile top),

then two waves are created, each having a magnitude of $R_x/2$ (Figure B3.1). To satisfy equilibrium and continuity, the upward wave is in compression and the downward wave in tension. The upward compressive resistance wave reaches the top at time $t_x = t_1 + 2x/c$. The tensile resistance wave reaches first the pile bottom at time $t_L = t_1 + L/c$ where it is reflected in compression. It then travels upwards and arrives at the top at time $t_2 = t_1 + 2L/c$.

If a resistance force, R_b, begins at time $t_L = t_1 + L/c$ at the pile bottom, then it will create a compressive upward traveling wave of magnitude R_b, which also arrives at the pile top at time $t_2 = t_1 + 2L/c$.

If all resistance forces are constant throughout the time $t_1 + x/c < t < t_1 + 2(L-x)/c$, then at time $t_2 = t_1+2L/c$, the force and velocity records contain the effects of

(A) the upward traveling tension wave due to reflection at the pile bottom of the initial downward moving compression input at a time 2L/c earlier, $[-F_{dM}(t_1)]$

(B) the summation of all upward traveling compression resistance waves $[R_x/2]$

(C) the initially downward traveling tension resistance waves now traveling upward in compression after reflection at the bottom $[R_x/2]$ and the upward wave from the tip resistance $[R_b]$, both arriving at the pile top together with (A)

(D) all downward traveling waves, $[F_{dM}t_2]$.

Wave (B) and wave (C) have a total magnitude, R ($R = R_x + R_b$) since they contain both half waves of skin friction and the full end bearing. Thus, the combination of all upward traveling waves contains the resistance and the bottom reflected (negative) impact wave of time t_1.

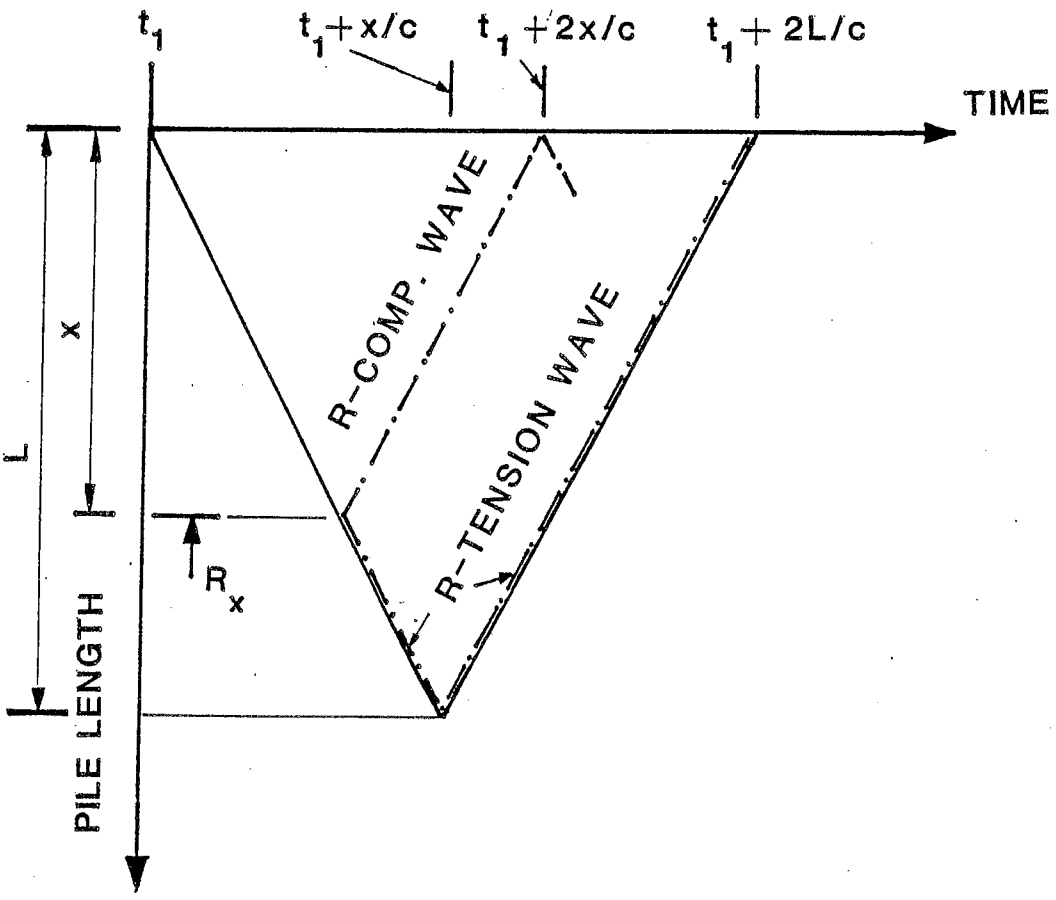

Figure B3.1: Waves caused by a Resistance R_x, at Location x Below the Pile Top, Generated by an Impact Wave which Started to Move Down the Pile at Time t_1.

$$F_u(t2) = R - F_d(t1)$$

or

$$(F_{M2} - Zv_{M2})/2 = R - (F_{M1} + Zv_{M1})/2$$

Rearranging, we can now solve for the total resistance

$$R = (F_{M1} + Zv_{M1} + F_{M2} - Zv_{M2})/2 \qquad \text{(B3.3)}$$

where the indices 1 and 2 refer to times t_1 and $t_2 = t_1 + 2L/c$.

B3.2 Static Capacity

In Eq. B3.3, R is the total resistance encountered during a complete passage of the wave (during a time period of 2L/c). This total resistance is the sum of the static resistance of the pile and dynamic resistance. In order to determine the static resistance R_s the following modifcations are necessary:

(A) Elimination of soil damping

(B) Proper choice of time t_1 such that R is already at full magnitude when F_M and v_M samples are taken

(C) Correction for an R_s that decreases during 2L/c because of early pile rebound (negative velocity before 2L/c)

(D) Time dependent soil strength changes (setup or relaxation). Since the dynamic methods give the resistance at the time of testing, it is always recommended to test piles at the end of driving for the strength of the remolded soil, or by restrike after a wait period for the long-term service load, or at both times to determine strength changes. The capacity at the end

of driving may not be equal to the service capacity after a waiting period due to reconsolidation, dissipation of excess pore pressures, etc. Static test correlations should not, in general, be made with end of driving data but rather with data from restrike.

(E) The pile must experience permanent set during the blow. If no permanent penetration (or only a very small one) is achieved, then the computed capacity indicates only that portion of the resistance that was mobilized. This is roughly analogous to a static proof test not run to failure, but rather terminated in the elastic range (we then know only that the pile has <u>at least</u> the tested capacity.

Consideration D contains soil mechanics considerations which do not affect the Case Method computations. Consideration E is self-explanatory. The first three considerations will now be investigated in more detail.

Damping is associated with velocity. The toe velocity can be obtained from the top measurements as follows:

$$v_b(t) = F_d(t-L/c)/Z - F_u(t+L/c)/Z = (F_{M1} + Zv_{M1} - R)/Z \qquad (B3.4)$$

By defining the damping force $R_d = J_c Z v_b$ (J_c is the dimensionless Case damping constant), we can also solve for the damping. Since the <u>total</u> resistance is the sum of the static and damping forces, the static resistance can be obtained from

$$R_s = R - R_d = R - J_c(F_{M1} + Zv_{M1} - R) \qquad (B3.5)$$

or expanding into terms of only F_M and v_M,

$$R_s = (1-J_c)[F_{M1} + Zv_{M1}]/2 + (1+J_c)[F_{M2} - Zv_{M2}]/2 \qquad (B3.6)$$

The damping constant has been found to be related to the soil grain size near the pile tip, or can be computed directly from this R_s equation if dynamic measurements have been taken, and the failure load from a static load test or the total static resistance from CAPWAP is known, since J_c is then the only unknown in the equation.

The static resistance is a function of pile displacement. Assuming that the usual assumptions of elasto-plastic resistance are valid, a resistance increases to a maximum at some specified displacement (called the "quake") and then remains constant (plastic) until rebound starts. Typical quakes are 0.1 inch (2.5 mm), although values up to 1.0 inch (25mm) have been observed.

For each time t_1, a resistance R_s may be determined from Eq. B3.6. Usually, the first major velocity peak defines time t_1. In most cases, the velocity integral (i.e. displacement) at the first arrival of the peak input at any point along the pile is larger than the soil quake, assuring that the full resistance is mobilized. In some cases, it may be necessary to delay time t_1 until either a second major peak or a maximum resistance R_{max} is found. If a second major velocity peak occurs when force and velocity are still proportional, this second peak should always be chosen for t_1. Alternatively, if a large quake soil condition exists requiring a considerable compression of the soil before its ultimate capacity is reached, then the maximum R_s (called R_{max}) should be found by variation of t_1. Large quakes are most often observed for displacement piles with large diameters or in saturated soils. The R_{max} method may also be necessary if the velocity integral is small at the intital peak due to a low energy input or a sharp rise time.

If the pile toe velocity in Eq. B3.5 is set to zero, the toe damping is also zero. Thus, any resistance present at that time is static and, therefore, independent of the damping constant. This solution can be seen graphically in Figure B3.2, at the point where the curves for R(t) and $R_s(t)$, are equal for the first time after time t_1. for piles with very little or zero skin friction, the R_{auto} Method is a perfect solution.

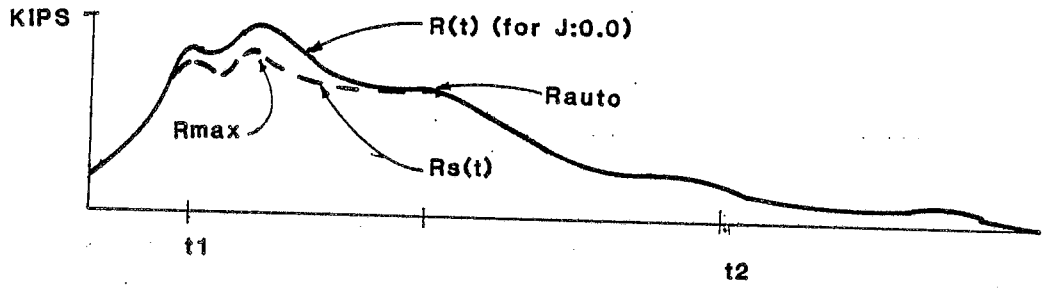

1 kip = 4.5KN

Figure B3.2: Typical Resistance vs Time Plot for a Pile Showing the Total Resistance R(t), the Static Resistance Rs(t), and other Selected Resistance Values.

For piles with little skin friction, the pile toe force, velocity and displacement may also be computed directly from the pile top measurements and one dimensional wave theory. Using the subscript "b" for pile bottom (toe), the pile toe force (or resistance) is

$$F_b(t) = F_{Md}(t-L/c) + F_{Mu}(t+L/c) \qquad \text{(B3.7a)}$$

Similarly, the velocity is

$$v_b = [F_{Md}(t-L/c) - F_{Mu}(t+L/c)]/Z \qquad \text{(B3.7b)}$$

and the displacement becomes

$$u_b = \int v_b dt \qquad \text{(B3.7c)}$$

A static toe resistance force-displacement graph may be obtained by reducing F_b by the damping resistance $J_c Z v_b$ and plotting this force for each time increment against the toe displacement. (This procedure is referred to as PEBWAP, Pile End Bearing Wave Analysis Program.

Correction (C) is necessary because the Case Method computes the simultaneously acting soil resistance. For long piles having significant shaft resistance, the Case Method may underpredict capacity; specifically, when the pile top velocity becomes negative before time 2L/c, the pile top is moving upward and some skin friction is beginning to unload. The basic Case Method can be "corrected" for this situation by adding the resistance in this upper portion of the pile that has unloaded. The dynamic component is then subtracted.

B3.3 Pile Driving Stresses

Pile damage is usually the result of either poor hammer alignment (high local contact stresses) or high driving stresses. High compression stresses are of concern. For friction piles, the maximum compression force occurs at

the pile top, whereas for end bearing piles, the pile toe resistance may be critical.

For concrete piles, tension stresses are important. From the upward wave, one can easily investigate whether tension is present. For a small resistance, the impact compression stress wave will be reflected from the pile toe at time L/c as an upward tension wave and will arrive at the pile top at time 2L/c. This upward tension force has been transmitted along the entire pile shaft, but is not necessarily the net tension at any location since the continuing downward waves must be superimposed. The maximum net tension (F_{tn}) occurs when the downward compression stress is a minimum and can be found mathematically by

$$F_{tn} = F_u(t_2) + F_d(t_3) \tag{B3.8}$$

where t_3 is the time when the downward wave is minimum before time 2L/c.

B3.4 Pile Damage Detection

For a uniform pile, an upward traveling tension wave should be observed only after reflection from the pile tip and should, therefore, be detected at time 2L/c after impact. If an upward tension wave is observed prior to 2L/c, it must be due to a change in impedance (reduced section area, modulus reduction or damage). Consider the equilibrium conditions for the downward waves F_d^1 and F_d^2 and the upward reflection wave F_u^1 at a cross section change with impedances Z_1 and Z_2, respectively. Since there is no upward traveling wave in Section 2

$$F_d^1 + F_u^1 = F_d^2 \tag{B3.9a}$$

And from velocity continuity considerations:

$$(F_d^1 - F_u^1)/Z_1 = F_d^2/Z_2 \tag{B3.9b}$$

Solving for the input wave reflection, one obtains for the relative cross sectional change $B = Z_2/Z_1$

$$B = (F_d^1 + F_u^1)/(F_d^1 - F_u^1) \qquad \text{(B3.10)}$$

The wave force F_d can be found from the superposition of the initial downward wave with the downward resistance tension waves. (R_x is the sum of all resistance above the location of cross sectional change).

$$F_d^1 = F_{dM1} - R_x/2 \qquad \text{(B3.11)}$$

The upward wave at time $t_1 + 2x/c = t_4$ is the sum of the resistance effects above location x and the cross section change effect (negative if $Z_2 < Z_1$)

$$F_{uM4} = R_x/2 + F_u^1 \qquad \text{(B3.12)}$$

or, rearranging, $F_u^1 = Fum4 - Rx/2$

We can then solve

$$B = [(F_{dM1} - R_x + F_{uM4})/(F_{dM1} - F_{uM4}) \qquad \text{(B3.13)}$$

The time t_4 should be chosen when the upward wave at the pile top, F_{uM}, has a temporary minimum after a peak $R_x/2$ compression increase (Figure B3.3). For a uniform pile, F_{uM4} will monotonically increase to a value of $R_x/2$. Then B will be equal to 1.0. If a uniform pile should indicate a B less than 1.0 prior to $t_1 + 2L/c$, the pile is damaged at location $x = ct_4/2$ and the cross section reduction can be calculated. The following classification scale has been proposed:

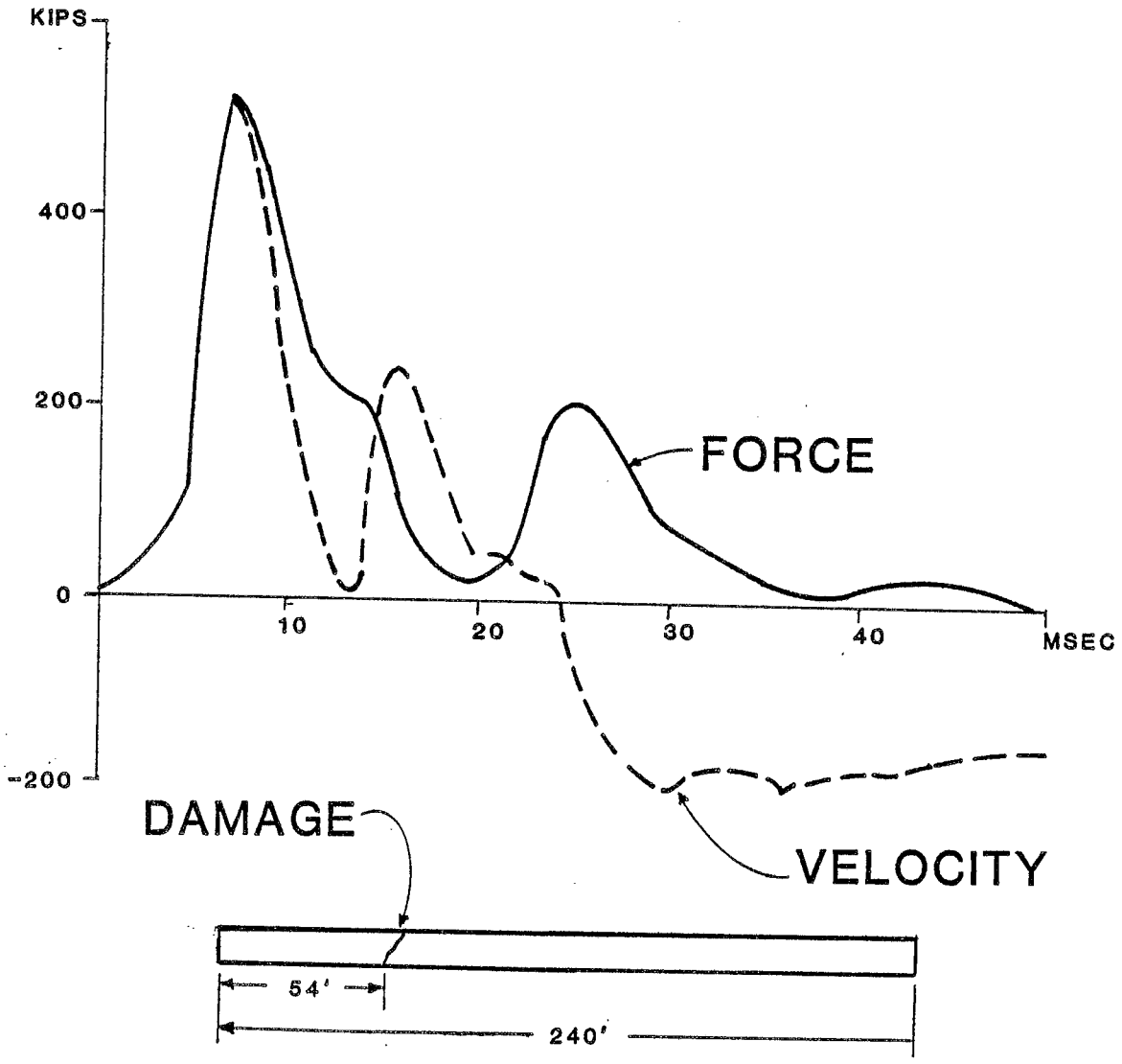

Figure B3.3: Typical Plots of Pile Top Force and Velocity of a Damage Pile

1 kip = 4.5 KN
1 foot = .3048 m

B =	1.0	uniform pile
	0.8-1.0	pile with slight damage
	0.6-0.8	damaged pile
	below 0.6	broken pile

APPENDIX B4

CAPWAP

B4.1 Computational Details

(CAse Pile Wave Analyses Program) combines measured data with wave equation analysis. Its objective is the interpretation of measured force and velocity records to obtain the soil resistance effects acting on the pile.

Since actual force and velocity measurements are input into the program, it is unnecessary to model the hammer and the driving system. Thus, with the lumped mass pile model of the wave equation, either the force or the velocity of the top element may be prescribed as the input excitation.

If the pile top force is prescribed, then an acceleration and therefore velocity can be computed, which may be compared with the measured velocity.

The acceleration at the pile top is

$$a_1(F_m - F_{b1} - R_1)/m_1 \qquad \text{(B4.1)}$$

using the notation of Appendix B2 (Section B2.7). F_m represents the measured force. Of course, the reverse approach (acceleration input) leads to

$$F_1 = F_{b1} + R_1 + am \qquad \text{(B4.2)}$$

From this point on, computation proceeds as in the wave equation.

B4.2 Soil Model Extensions

There are a few extensions to the soil model which were necessary in order to achieve agreement between computed and measured pile top quantities. These are as follows:

(A) In CAPWAP, the lower static skin friction bound is

$$R_i = -U_n(R_{si}) \tag{B4.3}$$

with

$$0 \leq U_n \leq 1$$

Thus, the negative skin friction limit is variable in CAPWAP. For end bearing, U_n is always zero.

(B) The soil stiffness is given by

$$k_{si} = R_{ui} / q_{im} \tag{B4.4}$$

with q_{im} being the modified quake at segment i. With a positive segment velocity ($u_i' > 0$), q_{im} is given by

$$q_{im} = q_i \tag{B4.5}$$

For negative segment velocity ($v_i < 0$), q_{im} is given by

$$q_{im} = q_i(e_s) \tag{B4.6}$$

The factor e_s may be different for skin and toe and is limited to a range of 0.01 and 1.0. Thus, for negative velocities, the quake may be smaller, and soil stiffness higher, than during loading. In fact, e_s is the square of the soil's coefficient of restitution. In CAPWAP, therefore, the "loading quake" and "unloading quake" are not necessarily equal.

Another difference between the wave equation and CAPWAP soil model is in the use of damping parameters. It is convenient in CAPWAP to use the viscous coefficients rather than the Smith values since they can be assigned independent of the static resistance. A recomputation of Smith damping factors from viscous ones is approximately possible using

$$j_{si} = j_{vi}/R_{ui} \tag{B4.7}$$

In order to avoid referring to individual skin damping parameters, the Case skin damping factoris defined as the nondimensionalized sum of the viscous damping factors.

$$J_s = \text{Sum}(j_{vi})/Z \tag{B4.8}$$

where Z is the average pile impedance. Similarly, for the pile toe, one obtains the Case toe damping factor

$$J_t = j_{sn+1}/Z \tag{B4.9}$$

where "n+1" refers to the toe element, n being the total number of pile segments.

B4.3 Computational Procedure

A pile model is created. In most cases the pile properties are well known. Next, an assumption is made regarding the total resistance and its distribution, the damping constants and the quakes. CAPWAP can use either force or velocity as the input to the first segment, and performs the computations for the complete record of the dynamic event, in time increment steps similar to those used for wave equation analysis. The record length analyzed extends at least till 20 ms after 2L/c time (L is pile length below measuring gages, c is the stress wave speed).

Comparison of the computed with the measured pile top response is then investigated as follows:

(a) from the time period between impact and time 2L/c after impact, differences require changes in the resistance distribution.

(b) from the time period immediately following the first return of the stress wave from the pile toe, damping effects are separated from static soil resistance.

(c) from the later record portion, loading and unloading quakes are estimated.

Improvements in the soil parameters may be done in a rather formal manner, and an automated routine had been written in the early 1970s which worked well for piles less than 100 feet (30.48 m) in length. Today the necessary steps are done interactively by an engineer who uses a micro/minicomputer for calculations, together with his experience with wave mechanics for input decisions. This semi-automated procedure avoids problems with excessive computer storage and/or time requirements.

B4.4 CAPWAP/C (CAPWAP Analysis Using Continuous pile segments)

CAPWAP/C is a modification of CAPWAP, that uses continuous and uniform segments, rather than masses and springs for pile modeling. Research work was originally done by Fischer (Ref. 24). The pile is again divided in a number, say N_p, segments. Each segment is of uniform cross section, but the segments may be different from each other. Denoting a segment number by i, it has a defined length, dL_i, such that its wave travel time, dt_i, equals the analysis time increment, dt.

Using wave mechanics, it is known that the force in the downward traveling wave, F_{di}, may be computed from the measured force at point i, $F_i(t)$, and the product of velocity (downward positive), $v_i(t)$, times segment

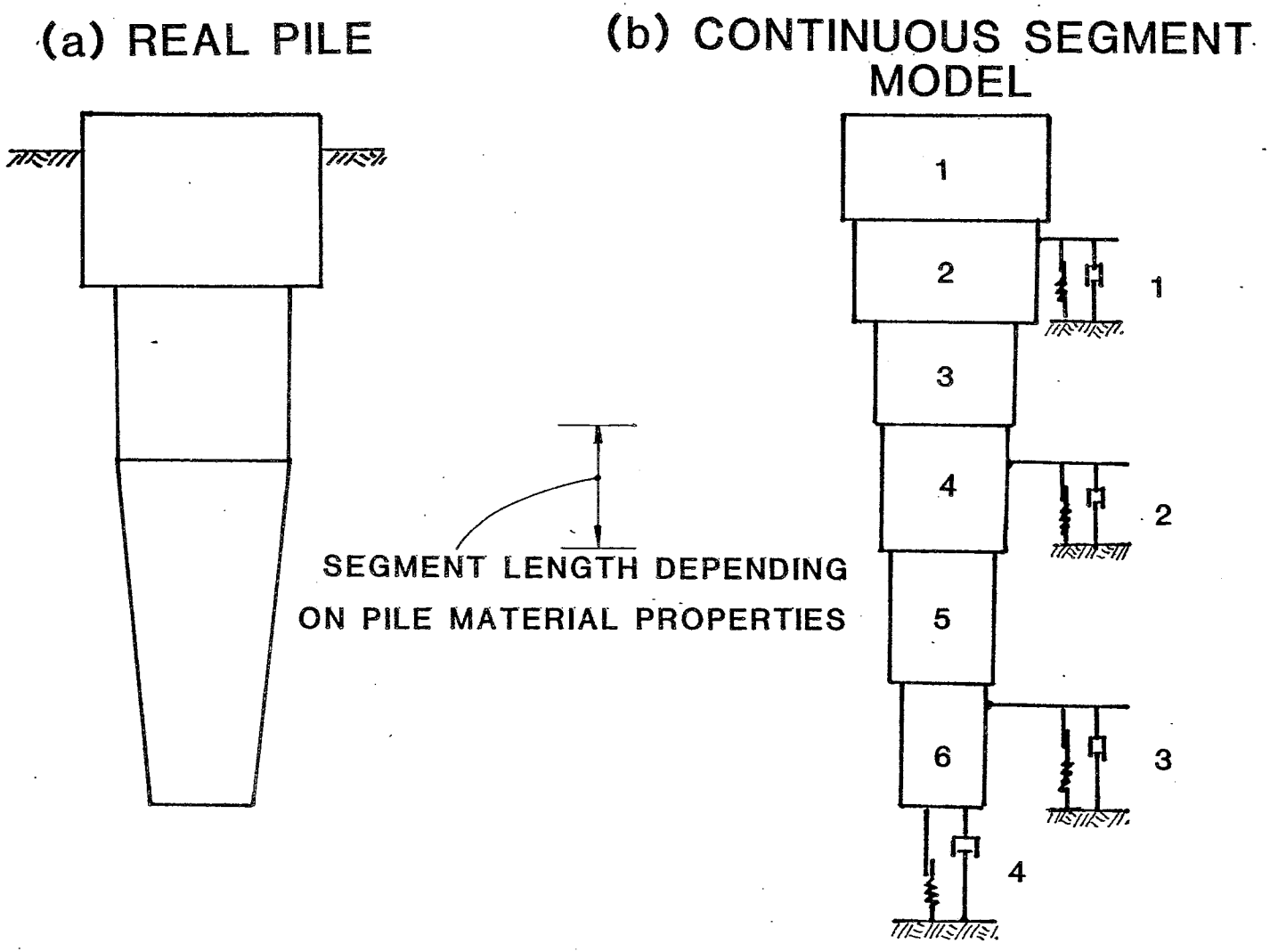

Figure B4.1: Continuous Model of a Pile with Smith Soil Model

impedance, Z_i, from

$$F_{di} = (F_i(t) + Z_i\ v_i(t))/2 \qquad \text{(B4.10)}$$

Similarly, for the upwards traveling wave,

$$F_{ui} = (F_i(t) - Z_i\ v_i(t))/2 \qquad \text{(B4.11)}$$

Thus, if the upwards and downwards traveling waves are known at the bottom and top of a continuous segment, at time t, then the corresponding wave values can be determined as they arrive at the top and bottom at time t + dt.

For variable pile properties E_i, rho_i (elastic modulus, mass density), the wave speed of a segment is

$$c_i = (E_i\ /rho_i)^{\ 1/2} \qquad \text{(B4.12)}$$

where c_i, E_i and rho_i, are average properties over a segment's length. For a constant time increment, the individual segment lengths are variable if the pile material changes.

$$dL_i = (dt)c_i \qquad \text{(B4.13)}$$

Soil resistances may act at each pile segment i. However, above the pile point a constant number of soil segments may be skipped. Thus, N_p, the number of pile segments, may be different from N_s, which is the number of soil resistances. Figure B4.1 shows a general model.

At any time, t_j, both upwards and downwards traveling waves, $F_{u,i,j}$ and $F_{d,i,j}$, respectively, are present in segment, i. For two neighboring segments of equal properties

$$F_{u,i,j+1} = F_{u,i+1,j} \qquad \text{(B4.14)}$$

and

$$F_{d,i,j+1} = F_{d,i-1,j} \tag{B4.15}$$

If the cross sectional properties change between i and i+1 then the pile impedance, Z_i, has to be considered for reflections.

$$Z_i = E_i A_i / c_i \tag{B4.16}$$

where A_i is the cross sectional area of segment i, and Z_i is the impedance. Defining,

$$Z_{r,i} = Z_i / (Z_i + Z_{i+1}) \tag{B4.17}$$

and

$$Z_{s,i-1} = Z_i / (Z_i + Z_{i-1}) \tag{B4.18}$$

the new waves may be determined from

$$F_{u,i,j+1} = Z_{r,i}[2F_{u,i+1,j} - F_{d,i,j} + R_i] + Z_{s,i+1} F_{d,i,j} \tag{B4.19}$$

$$F_{d,i,j+1} = Z_{s,i}[2F_{d,i-1,j} - F_{u,i,j} - R_i] + Z_{r,i-1} F_{u,i,j} \tag{B4.20}$$

Internal damping may be added (although unnecessary for reasons of numerical stability) by computing the change of a wave and reducing the new wave by a specified fraction, P_p. Thus,

$$F_u^*{}_{,i,j} = F_{u,i,j} - P_p (F_{u,i,j} - F_{u,i,j-1}) \tag{B4.21}$$

$$F_d^*{}_{,i,j} = F_{d,i,j} - P_p (F_{d,i,j} - F_{d,i,j-1}) \tag{B4.22}$$

The * indicates the dampened wave value; P_p is usually less than 0.02.

At the pile top, either force, $F_{m,j}$, or velocity, $v_{m,j}$, are prescribed (m stands for "measured" and j for a time increment). Then the complementary

quantity is either

$$F_{c,j} = Z_1 v_{m,j} + 2F_{u,1,j-1} \tag{B4.23}$$

or

$$v_{c,j} = [F_{m,j} - 2F_{u,1,j-1}]/Z_1 \tag{B4.24}$$

At the pile toe

$$F_{u,Np,j} = - F_{d,Np,j-1} + R_{Ns} + R_{Ns+1} \tag{B4.25}$$

with R_{Ns+1} denoting the toe resistance.

The force at segment i is

$$F_{i,j} = F_{u,i,j} + F_{d,i,j-1} \tag{B4.26}$$

and the velocity

$$v_{i,j} = [F_{d,i,j-1} - F_{u,i,j}]/Z_i \tag{B4.27}$$

thus displacements become

$$u_{i,j} = u_{i,j-1} + (1/2)(v_{i,j-1}+v_{i,j})dt \tag{B4.28}$$

Since no double integration is involved (acceleration may only be obtained from velocity by differentiation), such a simple integration is sufficiently accurate. This completes the computational description. Note that the computation is direct and that no predictor-corrector approach is needed.

The continuous segment analysis has the advantage of shorter computation times than the lumped mass analysis. It also more accurately follows the wave propagation; by definition the wave generated at the pile top arrives unchanged at the pile bottom while the lumped mass analysis tends to smoothen a wave. On the other hand, it is difficult to model any pile material non-

linearities, slacks or complicated hammers. Thus, the continuous approach is more applicable to CAPWAP than to wave equation work, and is not as easily applied to piles containing slacks or concentrated masses.

APPENDIX B5

CASE METHOD HAMMER PERFORMANCE COMPUTATIONS

Given Case Method measurements of pile top force and acceleration, hammer and driving system performance parameters can be calculated. They are described in this separate section because of their particular importance to the present research work.

B5.1 Energy Considerations

Current comparisons of hammers are usually based on rated energy. Hammers have a potential energy, E_p, which may be computed from ram weight, W, and fall height (stroke), h.

$$E_p = Wh \tag{B5.1}$$

This is a simple calculation for single acting hammers. For doubleacting units, an equivalent stroke must be entered in Eq. B5.1 such that E_p is the theoretically available potential energy. E_p is usually denoted by E_r, the "rated" hammer energy.

The potential energy does not install the pile. It first must be transferred into kinetic energy E_k immediately preceding impact.

$$E_k = 1/2\ m_r\ (v_{ri})^2 \tag{B5.2}$$

where m_r is the ram mass and v_{ri} is the ram impact velocity which may be computed from

$$v_{ri} = [2e_h(E_p/m_r)]^{1/2} \tag{B5.3}$$

where e_h is the hammer efficiency (a number between 0 and 1) which accounts for all hammer energy losses. This formulation is valid for all hammer types except diesel hammers. The evaluation of energy losses in diesel hammers is complicated by the presence of precompression. In this case, the ram velocity is often determined at the exhaust ports using Eqs. B5.1 and B5.3 and an "h" that neglects the compressive stroke.

The only useful energy is that energy which is actually transferred to the pile. This energy was named ENTHRU in a report by the Michigan State Highway Commission of 1965. The same quantity is denoted in this report by E_t. The difference between the energy transferred to the pile and the available kinetic energy is stored or consumed by the other driving system components in the form of kinetic or strain energies (i.e. the anvil, hammer cushion, helmet, pile top cushion for concrete piles, inelastic collisions as represented by coefficients of restitution and in the compression of gases for diesel hammers). Since these components can be varied and affect the actual transmitted energy, each hammer system is best judged from E_t.

The energy transferred to the pile top can be computed from the time functions of pile top force, F, and velocity, v.

$$E_t(t) = \int_0^t F(\bar{t})\, v(\bar{t})\, d\bar{t} \qquad \text{(B5.4)}$$

Two values of the E_t time curve are important: the maximum value E_t is the energy available to do work on pile and soil. The final value E_{tf} is the residual in the pile/soil system which actually did the work. The difference, $E_t - E_{tf}$, is a rebound energy which is returned to the driving system.

The force and velocity are proportional by the pile impedance, $Z = EA/c$, if the pile is uniform and no reflections occur from soil resistance or the pile end.

$$F = (EA/c)v \qquad \text{(B5.5)}$$

The downward and upward traveling force waves can be computed from

$$F_d = (F + Zv)/2 \qquad \text{(B5.6)}$$

and

$$F_u = (F - Zv)/2 \qquad \text{(B5.7)}$$

The corresponding wave velocities, v_d and v_u, may be calculated from the wave forces by division with the impedance, Z. The energies in the downward and upward traveling waves are computed from

$$E_d = \int F_d \, v_d \, dt \qquad \text{(B5.8a)}$$

$$E_u = \int F_u \, v_u \, dt \qquad \text{(B5.8b)}$$

However, the energy at any time remaining below the location of measurement is the difference between the downward and upward energy which reduces to Eq. B5.4 if B5.6 and B5.7 are substituted in B5.8. It should be noted that the energy in the downward traveling wave may contain the contributions from previously upwards traveling waves which were reflected at the pile top. For this reason the E_d value is not a measure of true hammer performance.

Other transferred energy definitions have been proposed, for example,

$$E_f = 1/Z \int F^2(t) \, dt \qquad \text{(B5.9a)}$$

or

$$E_v = Z \int [v(t)]^2 \, dt \qquad \text{(B5.9b)}$$

which combine B5.4 and B5.5, but are incorrect except in the case of infinitely long, uniform piles with no friction or damping forces; these cases obviously have little practical importance, especially for typical land piles.

The available kinetic energy is an important parameter; however, the impact velocity cannot be easily measured for all hammer types. Obtaining the maximum kinetic energy of the ram requires that either the potential energy and losses must be known, or E_t must be calculated from pile top measurements and added to the energy stored or lost in the other hammer components. Unfortunately, measurement or computation of energy losses or stored energy is not practical or accurate.

B5.2 Conservation of Momentum and Ram Impact Velocity

Newton, in his famous "Principia", expressed the Second Law of motion in terms of the momemtum, p. For the ram

$$p_r = m_r v_r \tag{B5.10}$$

Newton expressed this law as: "The rate of change of momentum of a body is proportional to the resultant force acting on the body and is in the direction of that force". More importantly, if the resultant external force acting on a system is zero, then there is no momentum change. This general result, the conservation of linear momentum, is applicable to all pile driving since even the combustion of diesel hammers is an internal force and cancels because of Newton's Third Law. The only external force is gravity and since the time during impact is very small, momentum changes due to gravity are negligible but could be easily calculated.

The momentum of each hammer element is computed using Eq. B5.10. However, the entire system includes the pile and soil. The concept of impulse can be used to find the difference between the momenta, p_o and p_1, at times, t_o and t_1, respectively.

$$p_1 - p_o = \int_o^1 F(t)\, dt \tag{B5.11}$$

The total impulse is equal to the time integral of the measured force over the entire hammer blow. Thus, the momentum of the ram at the time of impact t_o could be calculated if the final rebound momentum were known. Unfortunately, rams usually rebound with an appreciable but unknown velocity.

Consider Figure B5.1 which shows the pile top velocity and ram velocity as a function of time. These curves were obtained from a wave equation analysis of an ASH hammer on a steel pile. The ram and pile-top velocities can be seen to "track" each other and are zero at approximately the same time. This was found to be true in a large number of parameter studies, (Likins, Ref. 23) except in very easy driving. Thus, the ram, helmet, and pile top velocities are similar for air/steam hammers from a time shortly after impact until the time when the pile top velocity is a minimum. When the hammer component velocities are zero, the momentum has been completely transferred to the pile. Therefore, considering time t_1 as the time of pile-top zero velocity, Eq. B5.10 and B5.11 can be combined to yield

$$\int_{}^{t_1} F(t)\, dt = m_r(v_{ri}) \qquad \text{(B5.12a)}$$

since p_1 is zero at the time of zero velocity. Thus,

$$v_{r_i} = 1/mr \int_{}^{t_1} F(t)dt \qquad \text{(B5.12b)}$$

The validity of Eq. B5.12b was checked by wave equation parameter studies, and indicated reasonably accurate results. However, the times of ram and pile top zero velocity are not always exactly identical. The often relatively large force at this time means results are good but can be sensitive to small changes in the time of zero pile top velocity.

The difference between pile top and ram velocities becomes even larger when soft capblocks and/or cushions separate the hammer from the pile.

The impulse can also be computed from Eq. B5.5 thru B5.7 as follows.

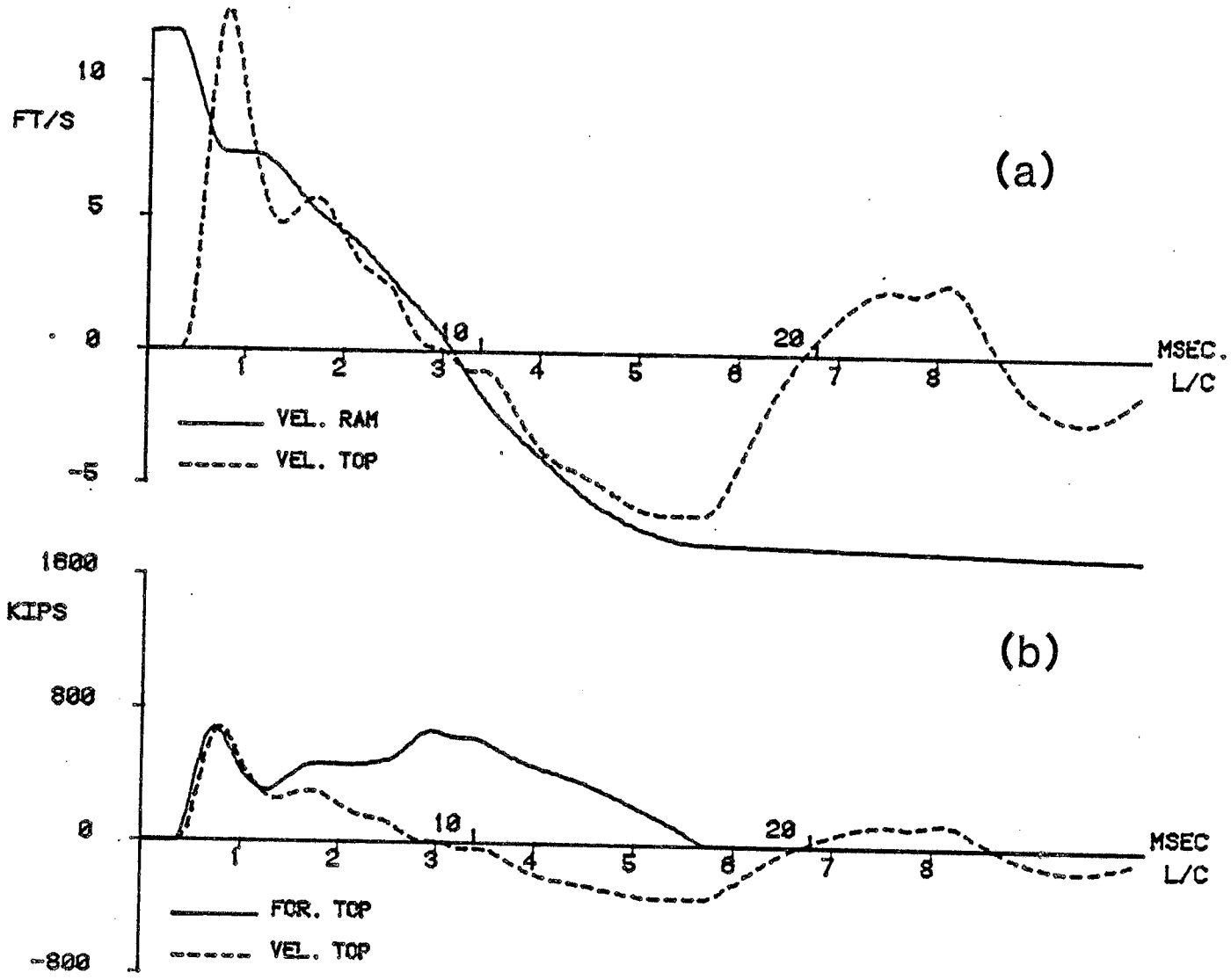

Figure B5.1: Example of (a) pile (A=30 in^2, Steel, L= 50 ft) top and ram (Vulcan 010) velocity and (b) pile top force and velocity from a wave equation air/steam hammer simulation. 1 kip = 4.5 kN; 1 ft = .3048 m; 1 in = 25.4 mm.

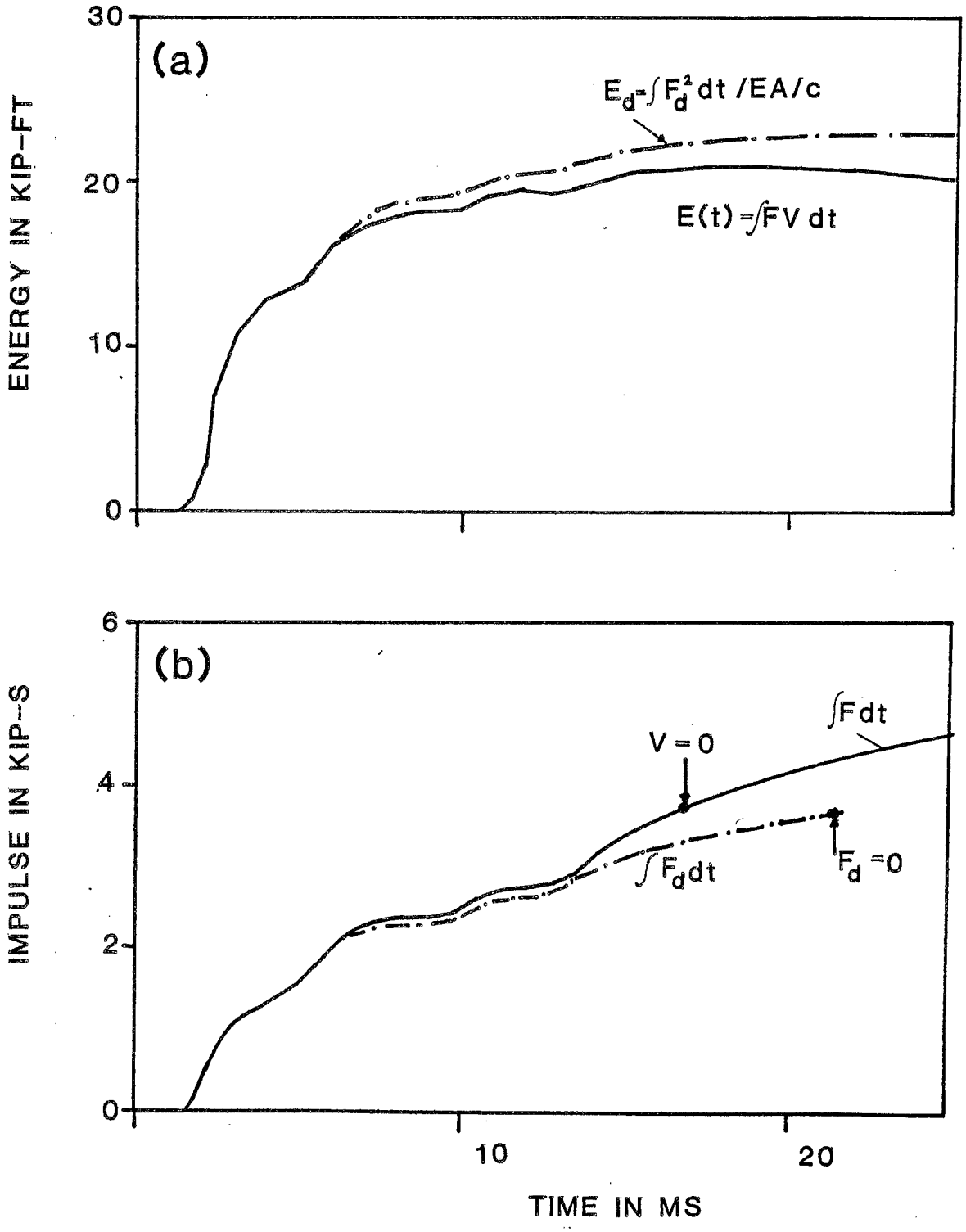

Figure B5.2: (a) Energy and (b) Momentum Transfer from a Vulcan 010 to a Steel Pile (A = 10 in2, L = 50 ft) from Air/Steam Analysis.
1 kip ft = 1.381 kN-m and 1 kip-s = 4.53 kN-s.

$$dp = \int F_d \, dt + \int F_u \, dt \qquad \text{(B5.13)}$$

In other words, the force impulse was split into impulses of the downward and upward travelling waves. As long as the downward wave, F_d, is positive and F_u is relatively small, the pile is receiving input from the hammer. When F_d becomes zero for the first time, the initial hammer momentum has been transferred to the pile (an exception is during easy driving). Calculation of the impact momentum is then made from the momentum of the downward wave until the time when the downward wave becomes zero, the time of separation. Again, comparison with wave equation simulations have shown that very good results can be expected.

The wave equation simulations used to check the momentum approach, were conducted with two different coefficients of restitution for the capblock. The computed impact velocity results were insensitive to this assumption.

In summary, it is concluded that the ram impact velocity of an air/steam or drop hammer may be calculated from pile top force and velocity records. If the hammer is fitted with a hard capblock, and no pile cushion exists, then the resulting impact velocity should be within five percent of the real one. Low blow counts may cause greater errors. The impact velocity can then be used for a direct calculation of the kinetic energy.

B5.3 Special Considerations for Diesel Hammers

A similar study was performed for a diesel hammer using the WEAP program with both normal combustion and with preignition. Sample force and velocity time relations are given in Figure B5.3 for a normally operating hammer. The curves show that the time of ram and pile top zero velocity are not similar. Thus Eq. B5.12 cannot not be used for diesels. However, the maximum ram velocity may be obtained from Eq. B5.14. Due to the compression of the gases, the maximum ram velocity is not much larger than the velocity at the exhaust ports from Eq. B5.3. Of course, this implies that the friction losses occur-

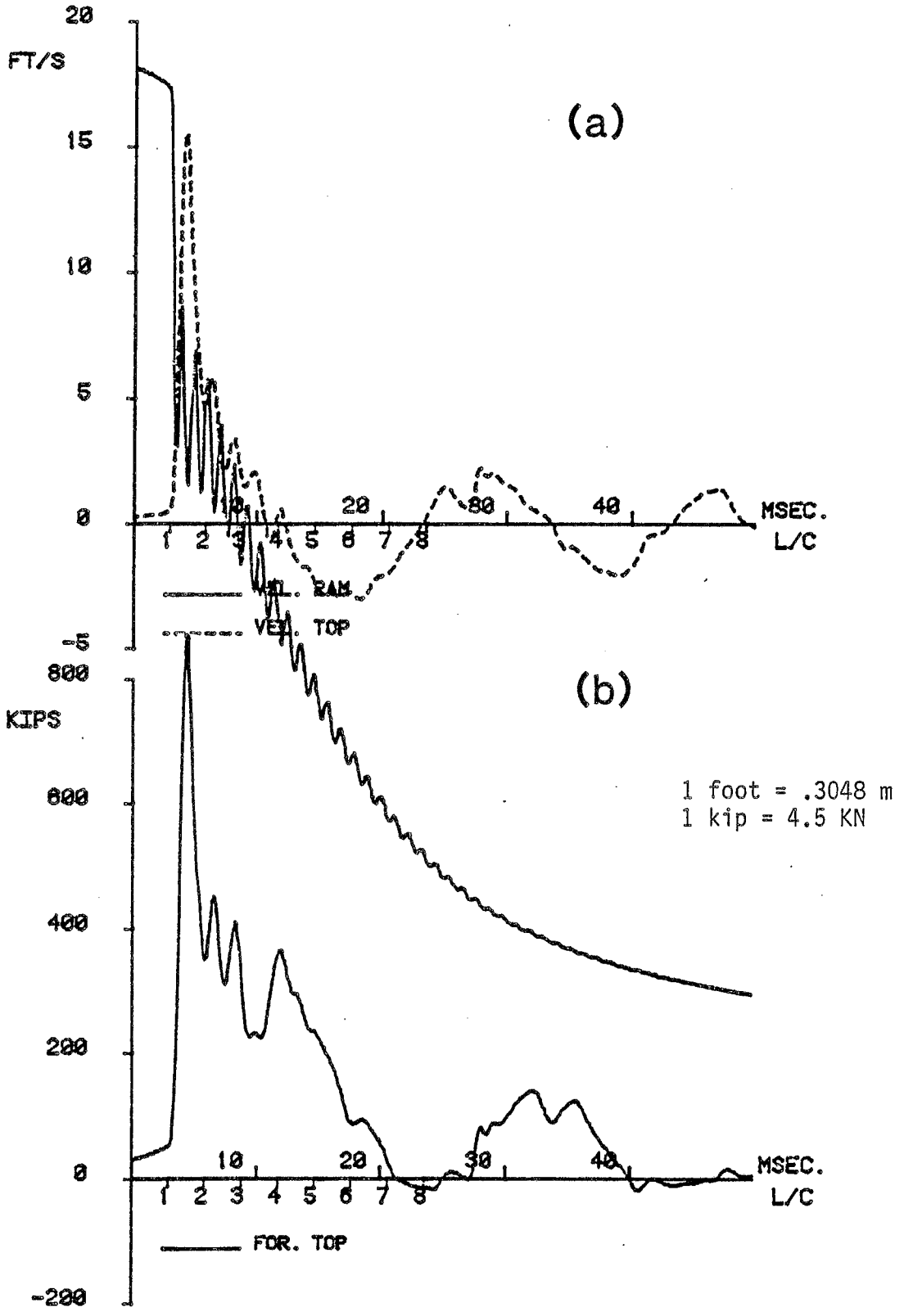

Figure B5.3: Example of (a) Ram (Delmag D-22) and Pile (A= 30 in, Steel, L = 50 ft) Top Velocity and (b) Pile Top Force from a Wave Equation Simulation Diesel Hammer Simulation.

ring during the ram descent, above the exhaust ports, and therefore e_h, are known.

For a given velocity at the exhaust ports, the ram impact velocity may be calculated by integrating the pile top force minus the ram weight until the time of impact. This impulse, when subtracted from the ram momentum at the ports, yields the ram impact momentum and therefore the ram impact velocity.

Measurements, field experience, and wave equation simulations have shown that similar strokes can be obtained for several combinations of combustion pressure, ignition time and soil resistance. At the same time, transferred energies, and blow counts show large differences. Thus, the stroke or the potential energy of a diesel hammer may be misleading, and better hammer performance indicators, such as E_t or the impact velocity should be used.

Preignition can be easily observed in the measured pile top force record (Figure B5.4). Normally the force rises slowly and can be computed from the Gas Law (Goble and Rausche, Ref. 8) and hammer dimensions. At impact, the force rises steeply to a much higher value; the time where the steep rise begins can be used to define the time of impact. If preignition is present, the force before impact rises at a faster rate and to a higher level. Since the actual impact velocity is less, the peak force is reduced and so is the pile top velocity, making the overall transferred energy much lower than during normal operation.

A diagram of the energy in the various system elements is shown in Figures B5.5 and B5.6 for a normal and a preignition case, respectively. It can be seen that the gases store energy which is later recovered by the ram prior to exhaust. In these examples, the energy in the gas prior to impact increases and the transferred energy decreases dramatically in the preignition case. The energy lost due to inelastic collisions (I.C.) or temporarily stored in the anvil Helmet (cap) (A/C) system are also reduced.

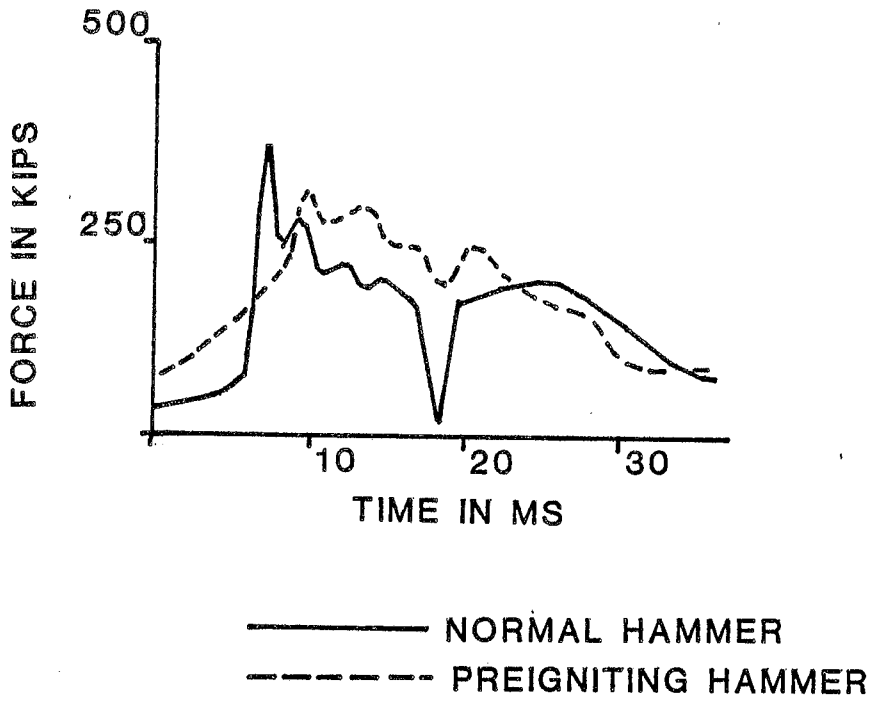

Figure B5.4: Example of Pile Top Forces Records from the same hammers (Delmag D-30) and Pile Type (Steel, A = 11 in2, L = 85 ft) With and Without Preignition. Although Impulses Look Similar, Transferred Energies were Different by 50% Because of Very Low Pile Top Velocities.

1 kip = 4.5 KN

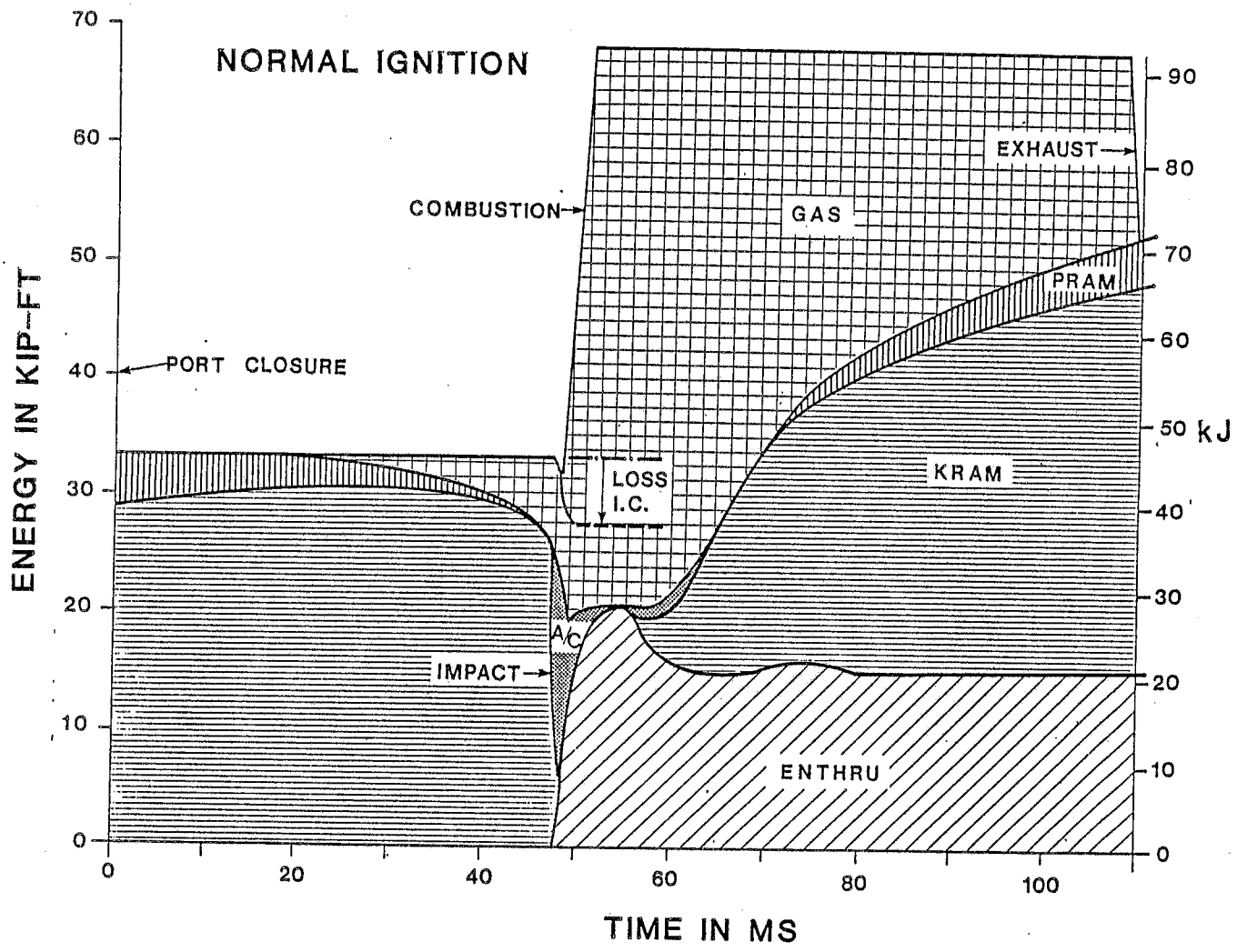

Figure B5.5: Example of Energy Transfer vs. Time from a Delmag D-22 with Normal Ignition to a Steel Pile Through Impact Block and Helmet. I.C.= Inelastic Collision Loss, KRAM = Ram Kinetic Energy, PRAM = Ram Potential Energy, A/C = Total Anvil (Impact Block), Hammer Cushion, Helmet Energy.

1 foot = .3048 m
1 kip = 4.5 KN

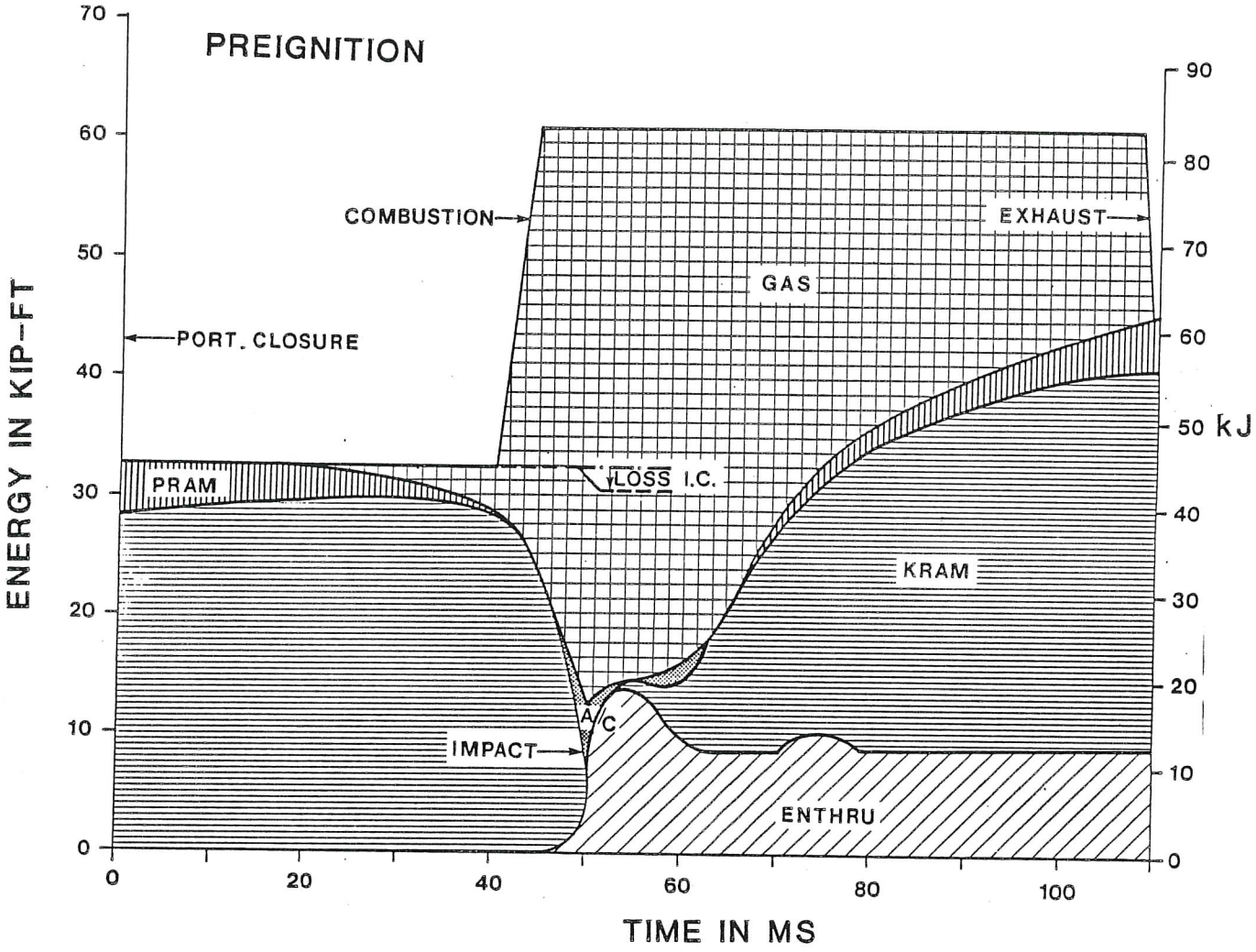

Figure B5.6: Example of Energy Transfer vs. Time from a Delmag D-22 with Preignition (Ignition Start 8 Ms Before Impact) to a Steel Pile Through Impact Block and Helmet. For Explanation of Symbols See Figure B5.5.

1 foot = .3048 m
1 kip = 4.5 KN